

**Electrochemically controlled polyelectrolyte complex hydrogel and its applications for  
antibacterial wound dressings**

by

Prakriti Dhungana

Submitted in Partial Fulfillment of the Requirements

for the Degree of  
Master of Science

in

Chemical Engineering

YOUNGSTOWN STATE UNIVERSITY

May 2023

Electrochemically controlled polyelectrolyte complex hydrogel and its applications for  
antibacterial wound dressings

Prakriti Dhungana

I hereby release this thesis to the public. I understand that this thesis will be made available from the OhioLINK ETD Center and the Maag Library Circulation Desk for public access. I also authorize the University or other individuals to make copies of this thesis as needed for scholarly research.

Signature:

---

*Prakriti Dhungana*, Student

Date

Approvals:

---

*Dr. Byung-Wook Park*, Thesis Advisor

Date

---

*Dr. Holly Martin*, Committee Member

Date

---

*Dr. Jonathan Caguiat*, Committee Member

Date

---

*Dr. Salvatore A. Sanders*, Dean of Graduate Studies

Date

## Abstract

The main goal of this research is to address the urgent need for a new treatment for chronic wounds. These types of wounds, which have difficulty healing in a timely manner, can result in significant economic loss, a need for organ replacement, and psychological complications. Our proposed solution involves the development of a cost-effective wound healing material called hydrogel that can release drugs through an electrochemical process. In this research, an electrochemically active polyelectrolyte (E-PEC) hydrogel was developed by crosslinking ferrocene (Fc) with chitosan (CHI) and alginate (ALG). Various tests were conducted to evaluate the properties of the hydrogel, including ninhydrin, turbidity, viscosity, FTIR spectroscopy, EDS/SEM imaging, swelling ratio, and gel content tests. The addition of Fc improved the hydrogel's electro-responsiveness, resulting in enhanced drug and water molecule movement towards the anodic terminal. The release of the drug was controlled by an electric stimulus, and the Fc-CHI/ALG hydrogel's responsiveness increased with increasing Fc content. The release of low molecular weight drugs, fluorescein isothiocyanate (FITC) was expedited up to two times with the addition of 54  $\mu\text{g}$  of Fc, and the release became electro-responsive when an electric stimulus of 2 V and 1.5 A current was applied, shortening the release time by one-third. Fc also helped in the release of larger drug molecules, such as fluorescein isothiocyanate Dextran (FITC-Dextran) and fluorescein isothiocyanate Bovine Serum Albumin (FITC-BSA), improving the release time by 20% and 25% times faster, respectively. 30 seconds ON and 30 seconds OFF cyclic voltage application demonstrated the hydrogel's responsiveness to electric fields as the release pattern shows the clear rise in release while ON and steady while OFF. The hydrogel system was effective in controlling the release of antibiotics and eliminating bacterial biofilms, making it practical for real-world applications. The release of ciprofloxacin (CIP) from the E-PEC hydrogel with an

electric field eradicated the *S. aureus* biofilm and reduced the colony formation unit (CFU) from 140 to 41. The release was higher with the electric field, resulting in greater inhibition of bacteria compared to release without the electric field.

Overall, this study demonstrates the successful development of an E-PEC that can be used for controlled drug release and the elimination of bacterial biofilms. The addition of Fc improves the hydrogel's electro-responsiveness, making it more effective in releasing both low and high molecular weight drugs with the application of an electric stimulus. This research presents a promising approach for developing practical and effective hydrogels for hemostasis and inflammatory stages of wound healing.

## **Acknowledgments**

I would like to take this opportunity to express my gratitude to those who have supported and guided me throughout my journey in completing this thesis. Firstly, I extend my sincere thanks to my thesis advisor, Dr. Byung-Wook Park, for his valuable guidance, support, and encouragement. Without his unwavering support and patience, this research work would not have been possible. I am grateful for inspiring me to complete this project within a short time frame. This extensive work would have required much more time and effort, but your constant guidance made it easier to achieve the desired level of perfection in a shorter time.

I am also thankful to Dr. Jonathan Caguiat and Dr. Holly Martin for serving as committee members for my defense. Thank you for taking the time to review this thesis book. I would like to express my gratitude to Dr. Jonathan Caguiat for his valuable insights, feedback, and suggestions during the course of this research work. His inputs have been immensely helpful in shaping the direction of this research. Although I did not have time to work with Dr. Holly Martin, I appreciate her knowledge and contribution to the class.

I would also like to acknowledge Dr. Pedro Cortes, Ray Hoff, and Dr. Virgil Solomon for their help in accessing the necessary research materials and resources. A warm thanks to Dr. Pedro Cortes for his direct and indirect support in this research. Special thanks to my colleagues, Asma Allababdeh, Jose Gonzalez Garcia, Kyle Duke, Kyle Preusser, and Victoria Messuri, for their constant support and encouragement, which kept me motivated throughout this journey. Their belief in my abilities has been an essential driving force in achieving my academic goals.

I am extremely proud of my father, Ramesh Dhungana, who always inspired me to aim higher and my mother, Rama Dhungana, who has always been encouraging me for the success. I

am equally grateful to my brother Basanta and sister Deepa who have never let me fail through their constant support in everything. Thank you, my family!!

Lastly, I would like to thank all the participants who generously gave their time and shared their experiences. Without them, this research work would not have been possible. This project was supported by the University Research Council Grants from the Office of Research at YSU. Once again, thank you to everyone who has contributed to this work in any way, directly or indirectly.

## Table of Contents

Abstract.....	i
Acknowledgment.....	iii
List of Figures.....	viii
List of tables.....	xi
List of Abbreviations.....	xii
1. Introduction.....	1
1.1. Background.....	1
1.1.1. Wound healing and wound care.....	1
1.1.2. Hydrogels.....	5
1.2. Objectives.....	10
1.3. Organization.....	11
1.4. Scope of work.....	12
2. Literature review.....	13
2.1. Polyelectrolyte complex hydrogels in biomedical applications.....	13
2.2. Controlled release.....	14
2.2.1. pH stimulated drug release.....	14
2.2.2. Electric field responsive hydrogel.....	20
2.2.3. Temperature sensitive hydrogel.....	27
2.2.4. Photo responsive hydrogel.....	32
2.2.5. Enzymatic responsive hydrogel.....	37
2.2.6. External magnetic field responsive hydrogel.....	42
3. Methodology.....	47

3.1.	Materials .....	47
3.2.	Synthesis of (Fc-CHI) and formation of PEC hydrogel.....	48
3.3.	Characterization of PEC hydrogels.....	50
3.3.1.	Ninhydrin assay .....	50
3.3.2.	Turbidity .....	51
3.3.3.	Viscosity .....	51
3.3.4.	Fourier-transform infrared spectroscopy (FTIR) .....	52
3.3.6.	SEM/EDS imaging.....	52
3.3.6.	Swelling behavior .....	53
3.3.7.	Gel content.....	54
3.4.	Drug release kinetics.....	54
3.4.1.	Electrical stimulus: Continuous mode .....	56
3.4.2.	Electrical stimulus: Switching mode (On/Off) .....	57
3.5.	In-vitro drug release.....	57
3.6.	Statistics .....	59
4.	Results and discussion .....	61
4.1.	Characteristics of PEC hydrogels .....	62
4.1.1.	Degree of conjugation of Fc in CHI .....	62
4.1.2.	Stoichiometric ratio.....	63
4.1.3.	Mechanical property .....	65
4.1.4.	FTIR.....	66
4.1.5.	Morphology and elemental analysis .....	68
4.1.6.	Swelling ratio .....	70



4.1.7. Gel content.....	72
4.2. Drug release on the phantom skin (agarose).....	73
4.2.1. Drug release: Passive vs. active .....	75
4.2.2. Dynamic release.....	81
4.3. In-vitro biofilm assay: Antimicrobial effect .....	83
5. Conclusions and recommendations.....	88
References.....	91

## List of Figures

<b>Figure 1.1.</b> Wound healing process and major cellular components. [4].....	1
<b>Figure 1.2.</b> Difference between normal and chronic wound. [9].....	4
<b>Figure 1.3.</b> Formation of PEC.....	7
<b>Figure 1.4.</b> Chemical structure of (a) CHI, (b) ALG. [21].....	9
<b>Figure 2.1. (a)</b> the preparation and the release process of drug-loaded hydrogels. <b>(b)</b> gentamicin sulphate and lysosome release process from gelatin meth acryloyl and hyaluronic acid-aldehyde hydrogel at different pH. [43].....	15
<b>Figure 2.2. (a)</b> graphical abstract of formation of hydrogel and <b>(b)</b> release of drug with and without electric field. [49].....	20
<b>Figure 2.3.</b> Drug release study of (a) dexamethasone at the different electric potential. <b>(b)</b> dexamethasone electric potential of 3V for 3 min, repeated every 30 min. [50].....	21
<b>Figure 2.4. (a)</b> swelling and de-swelling mechanism of hydrogel in different temperature <b>(b)</b> schematic representation of drug loading and <b>(c)</b> pH and temperature-responsive release behavior from PNIPAM-co-PAAM hydrogel system. [57].....	28
<b>Figure 2.5.(a)</b> schematic of the go hybrid hydrogel scaffold fabrication <b>(b)</b> preparation and nir-induced stiffness change of the go hybrid hydrogel scaffold. [65].....	32
<b>Figure 2.6 .(a)</b> the scheme demonstrating the NIR responsive controlled drugs delivery. <b>(b)</b> switchable release of Rhodamine.B <b>(c)</b> controllable FITC-BSA. [65].....	33
<b>Figure 2.7. (a)</b> preparation of gelatin microspheres containing celecoxib. <b>(b)</b> preparation of the hydrogel and the characteristics of temperature sensitive shape self-adaptive. [69].....	38
<b>Figure 2.8.</b> Cumulative release of the hydrogels <b>(a)</b> insulin and <b>(b)</b> celecoxib. [69].....	38

<b>Figure 2.9.</b> (a) proposed mechanism for the formation of magnetic hydrogel, (b) loading guaifenesin into hydrogel, and (c) <i>in-vivo</i> release of guaifenesin with and without the magnetic field. [76].....	43
<b>Figure 3.1.</b> UV-vis spectroscopy of wash methanol solution to detect amount of free Fc present after each wash.....	49
<b>Figure 3.2.</b> PEC hydrogels loaded on aluminum stumps, attached by the carbon tapes and conductivity is supplied through the copper tape. ....	53
<b>Figure 3.3.</b> Hydrogel loaded with fite placed next to the agarose structure to observe the passage of drug from hydrogel to agarose gel. (1) agarose gel, (2) area under microscope, (3) anode/cathode, (4) anode/cathode, and (5) drug loaded PEC.....	56
<b>Figure 3.4.</b> Biofilm growth after dropping liquid culture over the membrane (a) 0 min (b) after 24 hours incubation (c) 48 hours incubation.....	58
<b>Figure 3.5.</b> Experimental setup for <i>in-vitro</i> drug release. 1. PEC loaded with CIP- encapsulated inside the electric device, 2. Biofilm. ....	59
<b>Figure 4.1.</b> Schematic formation of pec hydrogels with ionic interaction. (a) CHI/ALG (b) Fc- CHI/ALG. ....	61
<b>Figure 4.2.</b> Degree of conjugation of different Fc-CHI at 1.5 weight% concentration. (n=5) ....	62
<b>Figure 4.3.</b> Turbidity value of different pec with their respective stoichiometric point, with standard deviation (n=3). ....	64
<b>Figure 4.4.</b> Viscosity of different PEC samples (n=3).....	66
<b>Figure 4.5.</b> Ftir of different PEC.....	67
<b>Figure 4.6.</b> Sem images (a) pure ALG, (b) pure CHI, (c) pure CHI/ALG, (d) pure Fc-CHI and (e) Fc-CHI/ALG.....	68

<b>Figure 4.7.</b> EDS spectra of (a) pure CHI, (b) EDS image of Fc-CHI. ....	70
<b>Figure 4.8.</b> Swelling ratio of different PEC with standard deviation (n=3).....	71
<b>Figure 4.9.</b> Gel content of different PEC (n=3). ....	73
<b>Figure 4.10.</b> Schematic representation of the release of the drug from PEC.....	74
<b>Figure 4.11.</b> FITC release from different pec with (a) 0V electric supply, (b) 2V electric supply. .....	75
<b>Figure 4.12.</b> FITC-Dextran release intensity profile with (a) 0V electric supply, (b) 2V electric supply.....	77
<b>Figure 4.13.</b> FITC-BSA release intensity profile (a) with 0V cathode-anode-agar (b) with 2V cathode- anode- agar. ....	79
<b>Figure 4.14.</b> FITC release from different PEC with cyclic voltage application. (a) 1.5V cathode- anode-agar, (b) 1.5V anode-cathode-agar, (c) 2V cathode-anode-agar and (d) 2 V anode- cathode-agar.....	81
<b>Figure 4.15.</b> FITC-Dextran release from different PEC with cathode-anode-agar configuration (a) 1.5V cyclic voltage application (b) 2V cyclic voltage application. ....	82
<b>Figure 4.16.</b> CFU count of <i>S. aureus</i> . (n=3).....	84
<b>Figure 4.17.</b> CFU counts of <i>P. aeruginosa</i> . (n=3) .....	85

## List of Tables

<b>Table 2.1.</b> Summary of pH-responsive hydrogel systems.....	18
<b>Table 2.2.</b> Summary of electric field responsive hydrogel systems. ....	25
<b>Table 2.3.</b> Summary of thermo-responsive hydrogel systems. ....	31
<b>Table 2.4.</b> Summary of photo-responsive hydrogel systems. ....	36
<b>Table 2.5.</b> Summary of enzymatic-responsive hydrogel systems. ....	41
<b>Table 2.6.</b> Summary of magnetic field- responsive hydrogel systems.....	46
<b>Table 3.1.</b> Concentration of the drug uptake by different PEC.....	55
<b>Table 4.1.</b> Weight % of different element in pure CHI and Fc-CHI.....	69

## List of Abbreviations

AgNPs: Silver Nanoparticles

ALG: Alginate

AMF: Alternating Magnetic Field

CAP: Cold Atmospheric Temperature

CHI: Chitosan

CIP: Ciprofloxacin

EGF: Epidermal Growth Factor

EMF: Electromagnetic Field

E-PEC: Electrochemically responsive Polyelectrolyte Complex

Fc: Ferrocene

Fc-CHI: Ferrocene Conjugated Chitosan

FITC: Ferrocene Isothiocyanate

FITC-BSA: Ferrocene Isothiocyanate Bovine Serum Albumin

FITC-Dextran: Ferrocene Isothiocyanate Dextran

GO: Graphene Oxide

LCST: Lower Critical Solution Temperature

MMP-9: Matric Metalloprotein

MNP: Magnetic Nanoparticles

NIR: Near Infrared

PAAm: poly-(Acrylamide)

PBS: Phosphate Buffer Saline

PDMAAp: ploy (di-methyl acrylamide)

PDMS: Polydimethylsiloxane

PEDOT: poly (3,4-ethylene di-oxythiophene)

PEC: Polyelectrolyte Complex

PNPAAm: poly- (N-isopropylacrylamide)

rhCol II: Recombinant Human type collagen II

ROS: Reactive Oxygen Species

USCT: Upper Critical Solution Temperature

VPTT: Vapor Phase Transition Temperature

# 1. Introduction

## 1.1. Background

### 1.1.1. Wound healing and wound care

Wounds are trauma that occurs when the skin is broken during an accident or during surgery. Wounds must be treated for recovery and prevention of infection. [1] There are two types of wounds: acute and chronic. [2] The healing process comprises of mainly four stages: hemostatic, inflammatory, proliferation and remodeling (Figure 1.1). [3]

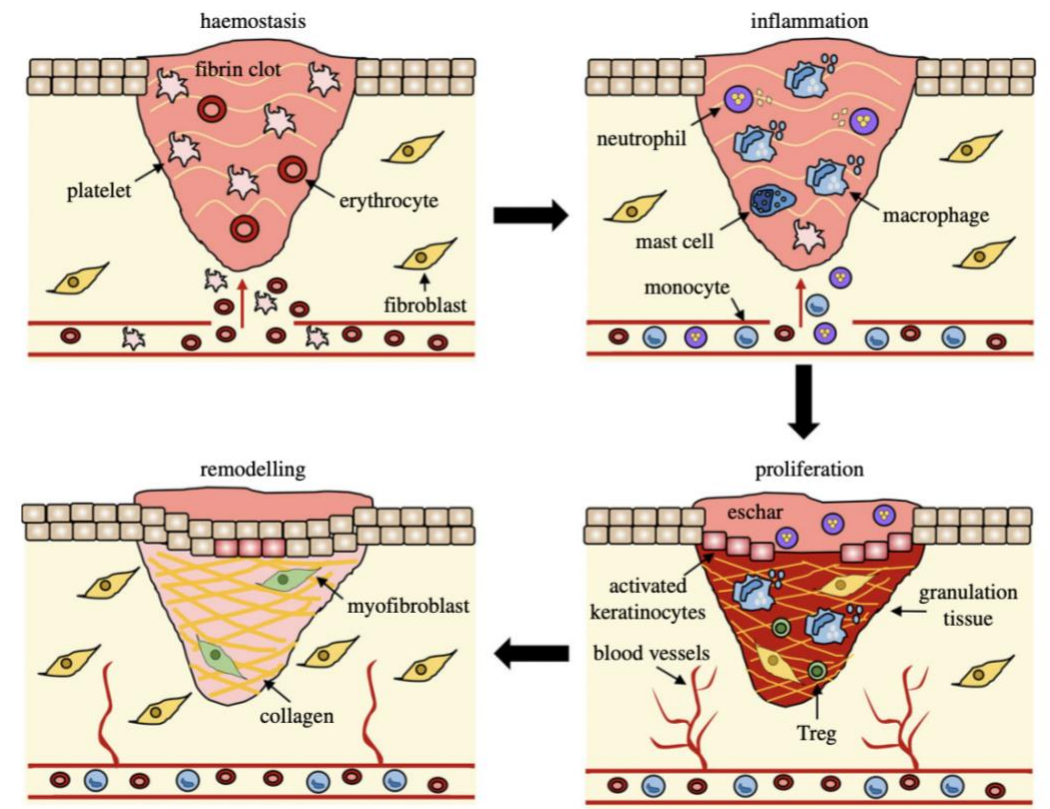


Figure 1.1. Wound healing process and major cellular components. [4]

Hemostasis is the initial phase of wound healing that occurs within 3-5 minutes. This step involves the constriction of blood vessels lying nearby smooth muscle cells. The constriction of



blood vessels reduces blood flow depending on the platelet concentration in the blood. [5] Then, platelets and coagulation factors maintain homeostasis by forming a fibrin material called a clot. The resulting fibrin material provides a durable scaffold that prevents the entry of microorganisms and helps organize cells during the healing process.

The inflammatory stage occurs within 24 hours after injury. This stage is different for chronic and acute wounds. In the case of acute wounds, platelets formed during hemostasis lead to the release of cytokines and growth factors that fight against foreign bodies and promote tissue repair.[6] This stage is initiated by neutrophils killing bacteria by phagocytosis and degrading matrix protein by forming cytokines. Monocytes then arrive at the wound site within 24 hours and convert to macrophages. Macrophages phagocytize microbes, remove tissue debris, and destroy remaining neutrophils and pave the way for angiogenesis and tissue granulation.[5] Macrophages also produce nitric acid early in the healing process. In addition to its antibacterial property, nitric acid stimulates collagen deposition and angiogenesis. Antibiotics prevent pathogen colonization and cornification lesions. Routine use of antibiotics in wound management favors cellular and vascular proliferation, thus accelerating the healing of cutaneous lesions.[7]

The proliferation stage follows by the inflammatory stage. This step occurs from 2-10 days after injury. This phase involves keratinocytes, fibroblasts, lymphocytes, myofibroblasts, and endothelial cells. Keratinocytes coverage of the wound restores the skin barrier.[8] Platelet-derived growth factor (PDGF) and epidermal growth factor (EGF) stimulate fibroblast formation during hemostasis. The formation of granulation tissue repairs the tissue and the growth of new blood vessels. An increased supply of water, nutrients, and oxygen assist in healing. Furthermore, keratinocytes, released by the interfollicular epidermis, proliferate, and migrate to cover the wound. They undergoes stratification and differentiation to the rebuilt epidermal barrier.[5] To

prevent fluid loss and infection, epithelial cells create a barrier. Fibroblasts secrete collagen which forms a scar that closes in the edges of the wound. [10]

The last step of wound healing is the remodeling stage. This starts from 2-3 weeks and can last up to 1 year. In re-epithelization, collagen is deposited in the skin, which determines the strength of the Scar. [6] Collagen remodeling also leads to matrix metalloproteinase (MMPS) and altered collagen synthesis that produces a scar. During this phase tensile strength increases, by ~40% in 1 month and ~70% in 1 year. Infection leads to irregular initiation, or termination in any stage of healing and can cause pyogenic granulomas (overgrowth of granulation tissue), hypertrophic scars (excessive fibrotic response), or chronic ulcers (prolonged inflammation and inability to re-epithelize). [5]

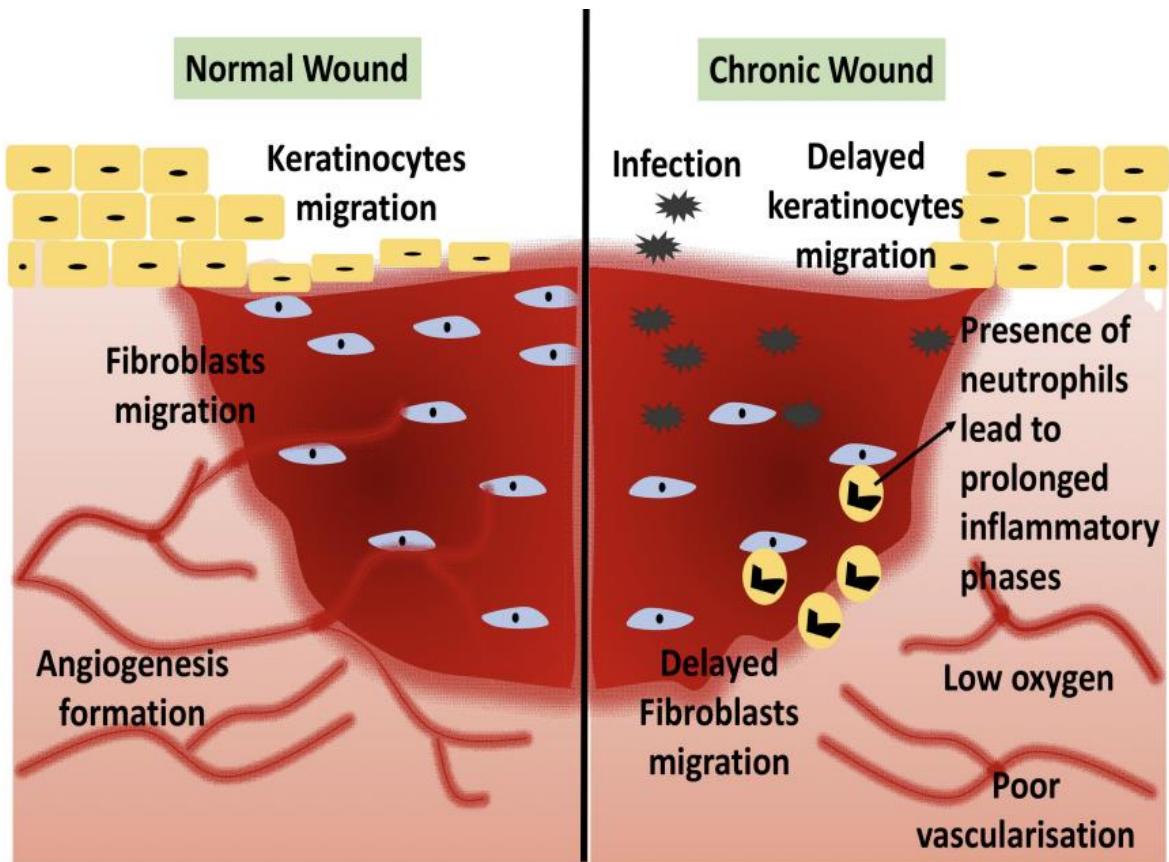


**Figure 1.2.** Difference between normal and chronic wound. [9]

The healing of chronic wounds differs from the healing of inflammatory wounds (**Figure 1.2**). Due to various reasons like peripheral arterial diseases, neuropathy, ischemia and diabetes, this stage is prolonged and the subsequent stages of healing do not proceed. [6, 10-13] Instead, an undiagnosed ulcer forms even after a minor trauma.[11] Controlling blood glucose levels can prevent further ulceration. Behavioral changes i.e., refraining from smoking, cholesterol management, and avoiding alcohol consumption can promote a better healing environment. [13] Vascular diseases and ischemia also cause delayed healing and can lead to amputation. [12] Infection also impairs repair mechanisms by preventing fibroblast migration and damaging in protective barriers.[13] A chronic wound has a slightly basic environment with a pH ranging from 7.15 to 8.90 due to the presence of a metalloprotein concentration that 10-25 times higher in

patients with diabetes.[6, 13] The lack of oxygen in the wound, the partial pressure of oxygen ( $pO_2$ ) is 5-20 mmHg for a diabetic wound whereas a healthy wound has 30-50 mmHg. Lack of oxygen can significantly impede wound healing by delaying inflammation, impairing angiogenesis, and inhibiting collagen synthesis. Therefore, it is crucial to maintain proper oxygenation in wound healing, and medical interventions such as supplemental oxygen or hyperbaric oxygen therapy may be necessary to improve outcomes in some cases. [6]

Proper care and frequent dressing replacement is required for proper healing, especially for the chronic wounds.[3] Before dressing a wound, it should be debrided. The dressing should provide a moist environment, gaseous exchange (water vapor and air), thermal insulation and low adherence. It should also be cost effective. [14] Hydrogels having the adhesive properties are used in the hemostasis stage while hydrogels with antioxidant properties are used in inflammatory stage of wound healing.[15]

### **1.1.2. Hydrogels**

The history of hydrogels can be traced back to the early 1900s, when scientists first observed the swelling behavior of certain polymers in water. [16] Additionally, hydrogels are well-suited for all stages of wound healing, and they do not irritate or react with biological tissues. Furthermore, they allow the passage of metabolites. [17] Modern wound dressings are effective in promoting wound healing by serving as a protective shield that prevents bacteria from entering the wound area. One such modern dressing is the hydrogel, which possesses several crucial characteristics. Hydrogels are hydrophilic and consist of more than 70% water. The significant water content of hydrogels helps in the formation of granulation tissue and re-epithelialization. There are mainly two types of hydrogels: physical and chemical hydrogels. Physical hydrogels are

made with hydrogel bonding, ionic forces, Van-der Waals interaction, polyelectrolyte complexation, stereo complex action, and hydrophobic forces. These hydrogels have the reversible response to environmental change. Generally, these are fragile, mechanically weak and dissolve in organic solvents. The other type of hydrogels are chemical hydrogels, these have covalent bonding and do not dissolve in the surrounding medium. [15]

In the 1940s, researchers began to synthesize and study polyelectrolytes, which led to the discovery of the polyelectrolyte effect – the observation that the solubility and properties of polyelectrolytes are strongly influenced by the presence of counterions in solution. [18] Polyelectrolyte hydrogels are formed by the complex formation of polycations with polyanions. These hydrogels have improved shear and tensile strength along with the swelling characteristics and mechanical stability. [19] Polyelectrolyte complex (PEC) hydrogels are a type of hydrogel that is formed from a polymer network composed of polyelectrolyte chains (**Figure 1.3**). Polyelectrolytes are polymers that contain ionizable groups along their backbone, which give them a net charge in solution. [20, 21] The charged groups can be either positive (cations) or negative (anions), and the net charge of the polymer depends on the balance between these groups. When these polyelectrolyte chains are cross-linked to form a hydrogel, the resulting material exhibits swelling behavior due to the absorption of water molecules into the network. [22, 23]

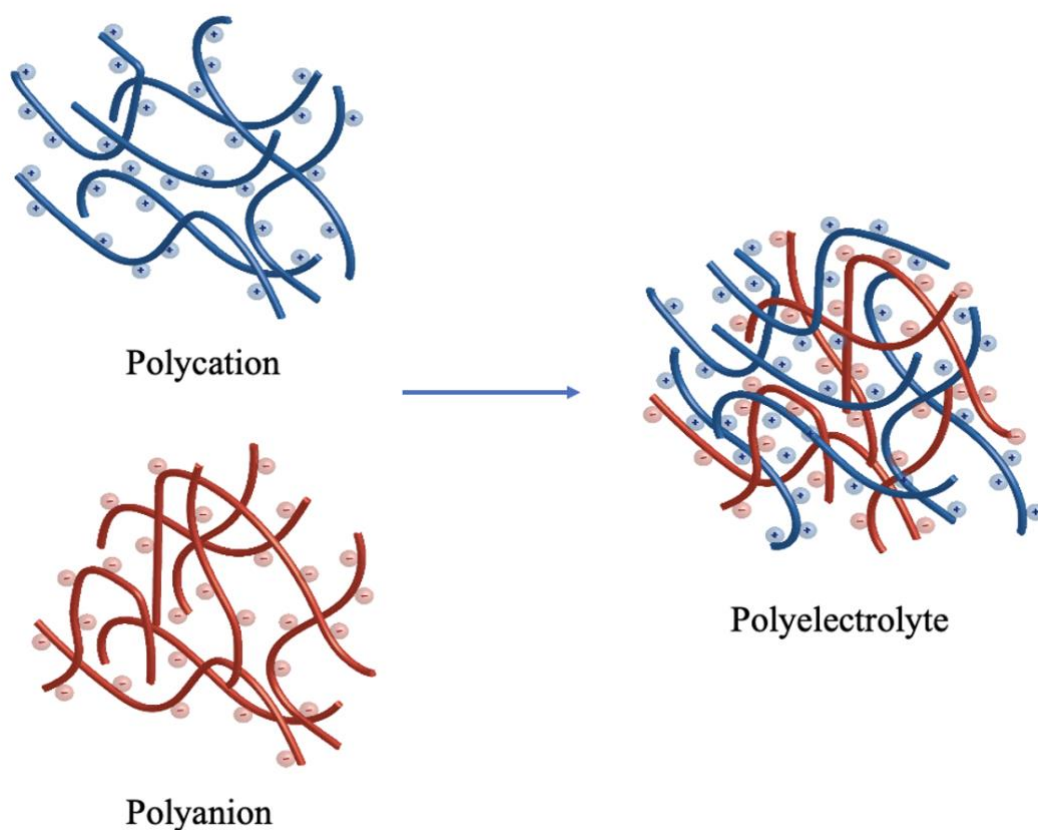


**Figure 1.3.** Formation of PEC.

These materials exhibited unique properties such as high swelling ratios, high water content, and the ability to respond to changes in pH and ion concentration. These properties made PEC hydrogels attractive for a range of applications, including drug delivery, tissue engineering, and sensors. [24-28] Since then, research in the field of PEC hydrogels have focused on improving the mechanical properties, biocompatibility, and functionality of these materials. Advances in polymer synthesis, cross-linking strategies, and characterization techniques have enabled the design of PEC hydrogels with precise control over their properties and performance. As a result, PEC hydrogels have become an important class of materials in the fields of biomaterials and soft matter. The major components of PEC are polyanions and polycations. [18, 20]

Polyanions are a type of polyelectrolyte that have negatively charged functional groups along their polymer chain. They can be used as building blocks for the formation of PEC hydrogels, which have a wide range of applications in biomedical and environmental engineering. [29] A hydrogel with a positive polarity can increase the binding to biological tissues by means of electrostatic interaction. In addition, the creation of in situ hydrogels through photo-cross-linking can also result in some level of tissue adhesion via covalent bonding induced by free radicals. [30] Some major polyanions that can be used for the formation of polyelectrolyte hydrogels include, sodium alginate, poly (acrylic acid), hyaluronic acid, carrageenan, chondroitin sulfate. Sodium alginate (ALG) is a polysaccharide derived from brown algae. It contains carboxylate groups that ionize in water, making it a negatively charged polyanion. ALG can be cross-linked with divalent cations such as calcium to form hydrogels. [31] ALGs are anionic block copolymers of  $\alpha$ -(1-4)-L-guluronic (g) and  $\beta$ -(1-4)-D-mannuronic acid (m) and are usually presented as the sodium salt. The pKa values of m- and g-residues are 3.38 and 3.65. [20]

Polycations are a type of polyelectrolyte that have positively charged functional groups along their polymer chain (**Figure 1.4**). They can be used as building blocks for the formation of polyelectrolyte hydrogels, which have a wide range of applications in biomedical and environmental engineering. [25] These cations are used as the anti-inflammatory responsive hydrogels because the positive charge among them easily attracts the bacteria with surface negative charge and kill it by damaging bacterial cell membrane.[32] Some major polycations that can be used for the formation of PEC hydrogels include, poly(ethyleneimine), chitosan (CHI), poly(allylamine), poly(ethyleneimine), poly (diallyl dimethylammonium chloride), poly-L-lysine. CHI is a polysaccharide derived from chitin; a natural polymer found in crustacean shells. It contains amine groups along its polymer chain, which ionize in water to produce positively

charged ammonium groups. CHI can be cross-linked with a variety of cross-linkers such as genipin or tripolyphosphate to form hydrogels. CHI is a polycationic polysaccharide consisting of  $\beta$ -(1-4)-2-acetamido-2-deoxy-glu-copyranose and 2-amino-2-deoxy-b-d-glucopyranose and has a macro pKa value in the range of 6.3–6.5. [20, 33]

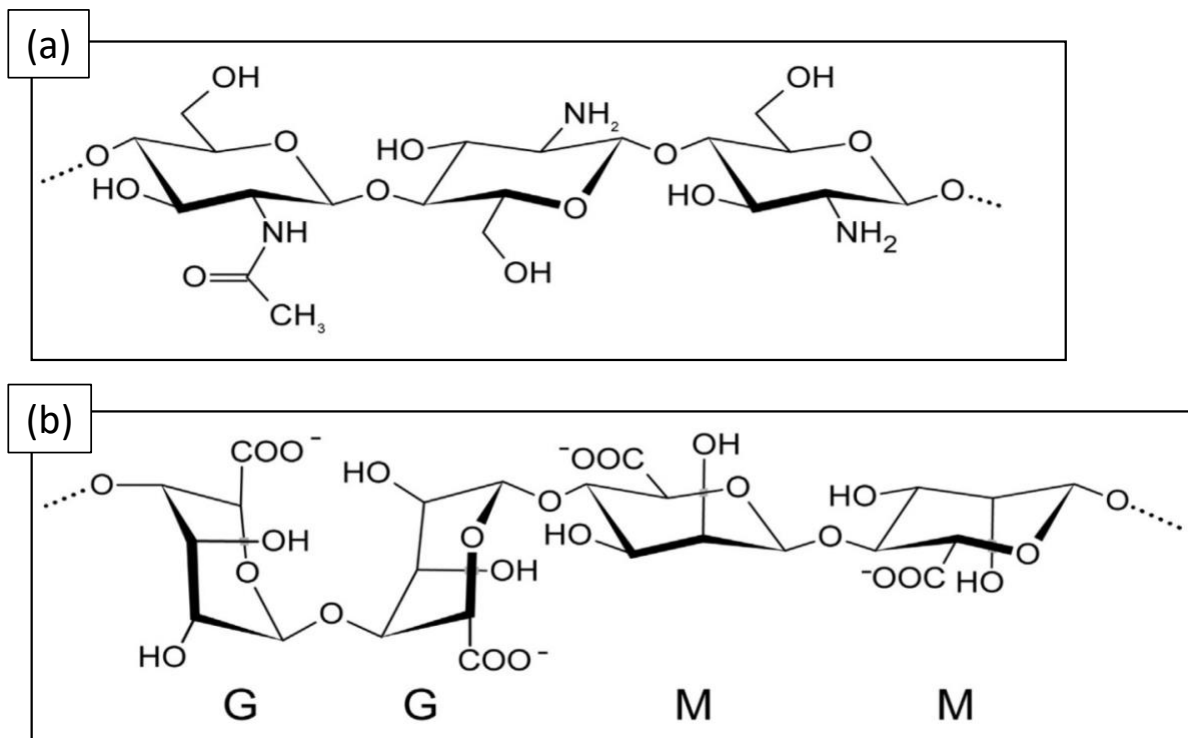


**Figure 1.4.** Chemical structure of (a) CHI, (b) ALG. [21]

Ferrocene (Fc) is an organometallic compound consisting of a cyclopentadienyl iron (II) center that has been extensively studied for its electrochemical and redox properties. It has been utilized in various applications, including as a redox mediator, electrocatalyst, and in drug delivery systems. One interesting application of ferrocene is in combination with chitosan-alginate hydrogel. [32] Fc is a redox mediator. When the drugs particles are exposed to a PEC environment, the Fc undergoes reduction, causing the release of drug encapsulated within the PEC. This allows



for targeted drug delivery and controlled drug release, which reduces the efficacy and reduces the side effect of drugs.

Chitosan-alginate (CHI/ALG) hydrogel is a type of biomaterial that has been widely investigated for its potential use in tissue engineering and drug delivery. [21] The incorporation of Fc into this hydrogel has been proposed as a means of enhancing its electrochemical properties. The resulting ferrocene-chitosan (Fc-CHI) hydrogel has been shown to exhibit enhanced conductivity and redox properties, which can be useful for applications such as biosensors and electrochemical energy storage devices. Additionally, the Fc component can also act as a redox mediator to facilitate the delivery of drugs or other bioactive molecules. [34, 35] The antioxidant properties provided by Fc makes the hydrogel preferable for the inflammatory stage of wound healing. Likewise, the hydrogel has the adhesive properties provided by the anionic group and the cationic group helps in defending the infection. Overall, the combination of Fc with CHI/ALG hydrogel represents a promising avenue for the development of new biomaterials with enhanced electrochemical properties for the healing of hemostasis and inflammatory stage of wound healing.

## **1.2. Objectives**

The purpose of this study is to create a PEC hydrogel using CHI, ALG, and Fc and to analyze its chemical, mechanical, and electrochemical properties. The hydrogel will then be used to release drugs such as FITC, FITC-Dextran, and FITC-BSA by applying an electric field. The objective of this release study is to determine whether the release can be controlled. An in-vitro drug release experiment will be conducted to verify the hydrogel's efficiency in releasing antibiotics in biofilm and test its eradication efficiency. The project was carried out in the following steps:

- Synthesizing Fc-CHI/ALG with varying amounts of Fc and a balanced stoichiometric proportion of each Fc-CHI/ALG.
- Characterizing the resulting PEC hydrogel using UV spectroscopy, Ninhydrin assay, turbidity measurement, viscosity measurement, gel content and swelling behavior study, SEM/EDS study, and FTIR spectroscopy.
- Testing the hydrogel's electrochemical properties by releasing FITC in agarose gel using the fluorescence technique.
- Studying the controllability of drug release by releasing FITC-Dextran and FITC-BSA in agarose gel with the same fluorescence technique.
- Finally, performing an in-vitro drug release with the hydrogel by loading CIP into it and releasing it over the biofilm of gram-positive and gram-negative bacteria at different time points.

### **1.3.Organization**

The thesis is divided into several chapters, including:

- Chapter 1 provides a brief introduction to the project, objective and scope of this project.
- Chapter 2 contains the similar research related to different approach in drug release with the help of different hydrogels and different stimulus.
- Chapter 3 discusses the materials and methods used.
- Chapter 4 presents the results obtained and the corresponding discussion.
- Chapter 5 summarizes the conclusion.

#### **1.4.Scope of work**

The aim of this project is to produce both PEC hydrogel and electrochemically active PEC (E-PEC) hydrogel and then compare their chemical, physical, mechanical, and electrochemical properties. Several tests were conducted to make comparisons, such as Ninhydrin assay, turbidity measurement, viscosity measurement, FTIR spectroscopy, Gel content/swelling ratio test, SEM/EDS imaging. The electrochemical properties were examined by releasing FITC on agarose gel and analyzing its profile with fluorescence technique. Furthermore, FITC-Dextran and FITC-BSA were released over the Agarose gel to observe the release pattern, which helped determine the controllability of drug release with E-PEC. The sustained release of CIP over the biofilm helped to eradicate both *Staphylococcus aureus* (*S. aureus*) and *Pseudomonas aeruginosa* (*P. aeruginosa*) biofilms. The efficiency of E-PEC hydrogel in releasing antibiotics over biofilm was also investigated, and the results suggest that this E-PEC has practical applications.

## 2. Literature review

### 2.1. Polyelectrolyte complex hydrogels in biomedical applications

Among various categories of hydrogels, based on their formation these are categorized into physical and chemical hydrogels. Physical hydrogels have low mechanical properties and are weak, whereas chemical hydrogels are generally stronger due to the presence of covalent bonds. [15] Natural polyelectrolytes, which include polysaccharide-based polymers such as alginate, chitosan, carrageenan, dextran sulfate, and hyaluronic acid. These are beneficial because they are biocompatible, biodegradable, and have low toxicity. Synthetic polymers, on the other hand, have controllable properties, tunable strength, and are reproducible, but they have lower biological activity. [36] The electrostatic interaction between oppositely charged polyelectrolytes can result in the formation of self-assembling polyelectrolyte complexes (PECs). As a result, the participating polymers must be ionized and have opposite charges to create a PEC. [37] These hydrogels possess a porous structure that permits water and small solute molecule transport, making them ionically conductive. They can be classified into three types, namely polyanions, polycations, and zwitterionic hydrogels. Among these, zwitterionic hydrogels have higher ionic conductivity compared to cationic and anionic hydrogels. Cationic and anionic hydrogels have mobile counterions that result in high conductivity in low salt solutions. [28] Synthetic hydrogels can remain water-resistant due to their crosslinked network structure, which ensures their physical stability. Additionally, their hydrophobicity and elasticity enable them to encase drugs for controlled release and maintain the hydrogel's durability over an extended period. The size of the pores in the hydrogel is a crucial aspect that can be adjusted based on environmental variations.

These changes in pore size affect the rate of drug diffusion through the hydrogel network, making it necessary to monitor. [33]

The properties of hydrogels created from PEC are influenced by various factors, including the charge density of each polymer, the amount and ratio of the polymers used, and their solubility environment. [38] Hydrogels with a high-water content can change their size and shape by swelling or deswelling, which can be controlled by external stimuli such as temperature, pH, light, salt, magnetic and electric fields. The swelling capacity is determined by factors such as electrostatic force, osmotic pressure, and crosslinking strength. [39] CHI is most commonly formed via electrostatic interaction between its positive amino group and opposite negative groups of numerous polyelectrolytes such as alginate, gelatin. [40]

## **2.2. Controlled release**

### **2.2.1. pH stimulated drug release**

Drug release with the stimulus of pH is guided by four main mechanisms: breaking of Schiff based bond, physiological change in hydrogel structure, swelling and de-swelling of the hydrogel, and the solubility of the drugs with the release solution. [41, 42] Du. M. et. al. conducted research to produce hydrogel using gelatin methacryloyl and hyaluronic acid-aldehyde. This hydrogel is used to release gentamicin sulphate or lysozyme under pH 7.4 and pH 5. The release of gentamicin sulphate was higher in acidic conditions due to the cleavage of Schiff base bonds and electrostatic interactions. (**Figure 2.1(a)**) The hydrogel loaded with both drugs showed pH-stimulus responsiveness, with gentamicin sulphate release increasing from 59% in pH 7.4 buffer to approximately 78% in pH 5.0 buffer within the first 6 hours (**Figure 2.1(b)**). These findings

demonstrate the potential for using this hydrogel as a controlled drug delivery system in acidic environments.

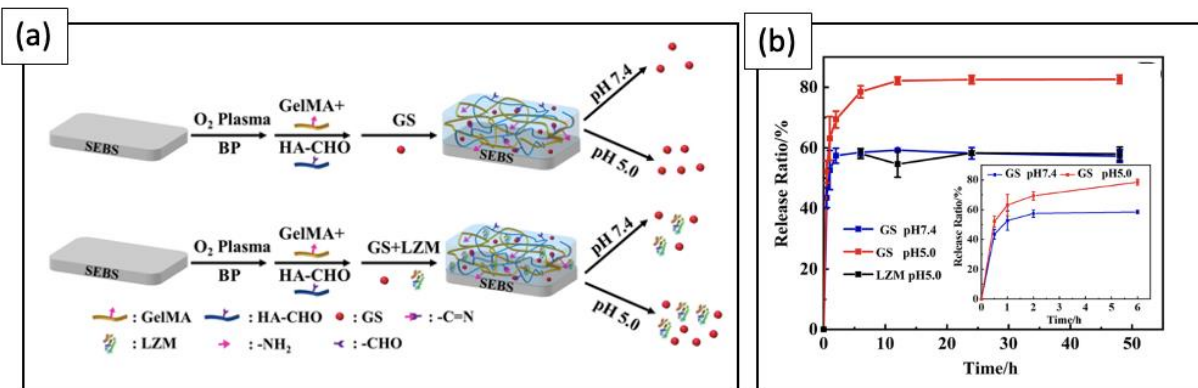


**Figure 2.1. (a)** The preparation and the release process of drug-loaded hydrogels. **(b)**

Gentamicin sulphate and lysosome release process from gelatin meth acryloyl and hyaluronic acid-aldehyde hydrogel at different pH. [43]

In an acidic environment, the electrostatic interaction Schiff base linkage between gentamicin sulphate and hydrogel breaks causing the release of this drug from the gel. The release amount of lysosome increases significantly when the concentration of hyaluronic acid- aldehyde in the hydrogels is increased. This is due to the microstructure and swelling behavior of hydrogels. With an increase in hyaluronic acid concentration, the hydrogels have more porous structure and possesses a higher swelling rate, makes it easier for the drug to diffuse. [43] There are several other hydrogel systems those work in releasing the drug from the hydrogel with pH stimulus. A hydrogel made of CHI and oxidized dextran can be stimulated with both electric and pH factors. Amoxicillin and ibuprofen were used in conjunction with this hydrogel. Breakage of the Schiff base bond was the reason for the faster release of the drugs in the lower pH.[44] The same stimulus i.e., pH is used to release the deferoxamine from the hydrogel made by CHI and poly ethylene glycol. This drug has been considered safe by world health organization (WHO). The mechanism of drug

release involves breaking of Schiff-based bonds. These hydrogels are most effective during the inflammatory stage of wound healing. [45] Another pH sensitive hydrogel was made in 2021, by Hu. C. et. al. When exposed to the lower pH the Schiff based bond breakage caused the release of silver nanoparticles (AgNPs) and deferoxamine. The hydrogel had no toxic side effects, made it vary suitable for application in wound healing application, mostly this system is used for healing angiogenesis stage of healing. [46]

Another mechanism for the release of drugs from the pH sensitive hydrogel is modification in swelling ration of the hydrogel. This modification makes the release sustained; thus, the release is slower than that of the normal pH. A hydrogel was made from CHI, arabinoxylan, and reduced graphene oxide crosslinked with tetraethyl ortho silicate. This hydrogel was encapsulated with silver sulfadiazine, the swelling ratio decreases in lower pH due to reduction in anion-anion repulsion between functional groups of hydrogels. This hydrogel is most effective during the proliferation stage of wound healing. [47] Another hydrogel was made, that was pH and ROS responsive, biocompatible, self-healing and injectable. This hydrogel was made with carboxy phenylboronic acid crosslinked with poly (vinyl alcohol). This hydrogel was used to release Vancomycin conjugated with silver nanoclusters or nimesulide. The mechanism of drug release involved the dissociation of pH sensitive phenylboronic acid-diol ester bond and hydrogel collapse in lower pH. This hydrogel is most effective during the inflammatory stage of wound healing. [48]

These hydrogels are designed to release drugs in response to specific pH conditions, with their mechanism of drug release involving breaking of Schiff-based bonds and swelling and deswelling mechanism. Hydrogels made of different materials like chitosan, oxidized dextran, quaternary ammonium salt, and carboxy phenylboronic acid are discussed, and their unique features and applications are explained. These hydrogels are most effective during specific stages

of wound healing and have the potential to offer targeted and controlled drug delivery for better patient outcomes.



**Table 2.1.** Summary of pH-responsive hydrogel systems.

Types of Stimuli	Material	Therapeutics	Advantages or limitations	Mechanism of Drug release	Target wound healing stage	References
pH	Gelatin methacryloyl hyaluronic acid-aldehyde	Gentamycin Sulphate and Lysosome	Excellent antibacterial effect	Breaking of Schiff based bond and electrostatic interaction between drug and hydrogel	Hemostatic	[43]
Electric/pH	Chitosan/ Oxidized Dextran	Amoxicillin Ibuprofen	Both stimuli could be used.	Breaking of Schiff based bond	Inflammatory	[44]
pH	Chitosan and polyethylene glycol	Deferoxamine	The model drug is considered safe by WHO.	Breaking of Schiff base bond	Inflammatory	[45]
pH	Chitosan, Quaternary ammonium salt	Silver nanoparticles/ deferoxamine	No toxic side effect	Breaking of Schiff base bond	Angiogenesis	[46]
pH	Chitosan, Arabinoxylan, Reduced graphene oxide, tetraethyl ortho silicate	Silver Sulfadiazine		Swelling ratio decreases in the lower pH due to reduction in anion-anion repulsion between functional groups of hydrogels.	Proliferation	[47]

pH/ ROS	Carboxy phenylboronic acid crosslinked with poly (vinyl alcohol)	Vancomycin conjugated with Silver Nanoclusters/ Nimesulide	Biocompatibility, self-healing, injectability	Dissociation of pH sensitive phenylboronic acid-diol ester bond-hydrogel collapse in lower pH	Inflammatory	[48]
---------	--	--	---	---	--------------	------

### 2.2.2. Electric field responsive hydrogel

There are two primary reasons for electric-field-driven drug release from conductive hydrogels. First, the charged drug molecules migrate due to the electric-field-driving force. Second, the net charge of the hydrogel polymeric network changes during the reduction or oxidation reaction. Negatively charged drugs are typically released by the reduction reaction of drug carriers, while positively charged drugs are released by the oxidation reaction. These drug molecules then move towards the electrode with an opposite charge due to the driving force of the electric field, allowing for smart drug release.

Qu J. et. al. synthesized a series of biocompatible hydrogels by combining dextran and electroactive aniline trimer with hexamethylene diisocyanate as a crosslinker to form a hydrogel network. In this study, the negatively charged drugs dexamethasone and indomethacin were released by the reduction of the positively charged aniline trimer, which expelled negative drug molecules from the hydrogel matrix (**Figure 2.2(a)**). Furthermore, when the Dextran incorporated hydrogels were applied with negative voltage, not only did the reduction reaction of conducting polymers affect the migration of negatively charged drug molecules, but the hydrogel bulk also contracted to expel loaded drug molecules from the hydrogel matrix (**Figure 2.2(b)**). [49]

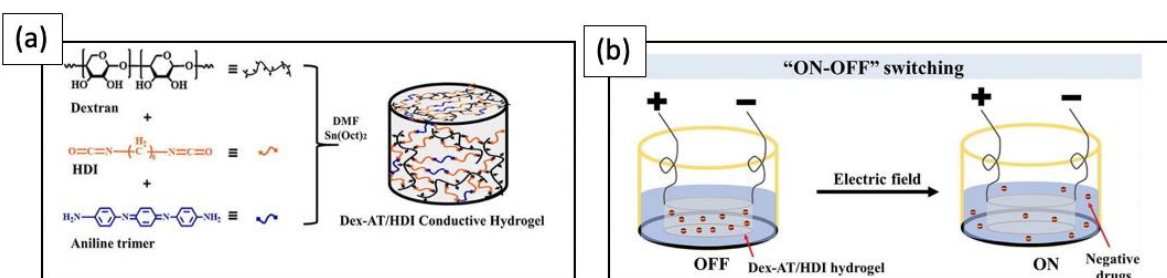


**Figure 2.2.** (a) Graphical abstract of formation of hydrogel and (b) release of drug with and without electric field. [49]

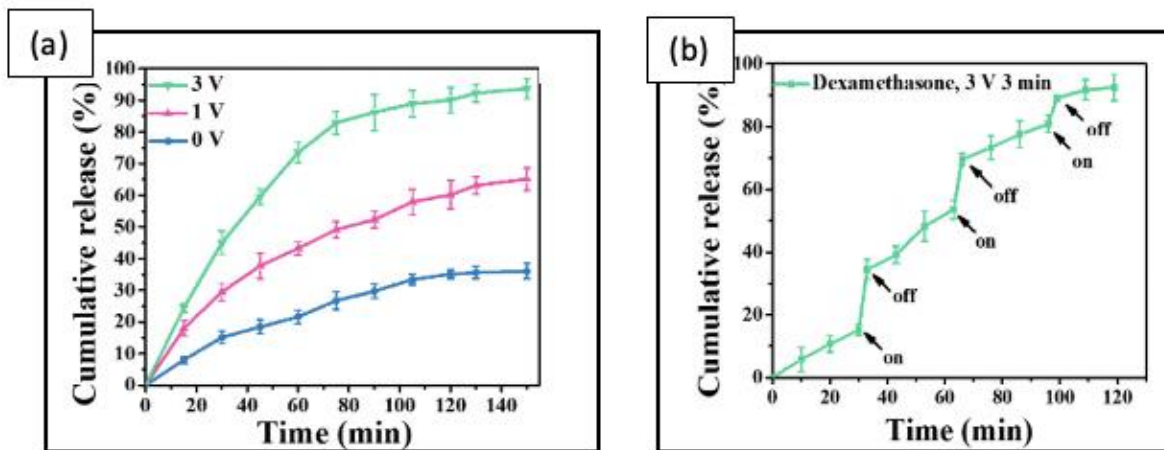


**Figure 2.3.** Drug release study of (a) dexamethasone at the different electric potential. (b) dexamethasone electric potential of 3 V for 3 min, repeated every 30 min. [50]

The release of dexamethasone from 0V, 1 V and 3 V after 120 minutes was 35%, 61% and 90%, respectively (**Figure 2.3(a)**). The concept of the external control over the release can be predicted (**Figure 2.3(b)**), the amount of release during the 3 minutes of electric field was significantly increasing while the release was slower while the voltage was turned off for next 30 minutes. [49]

Similarly, an electric field and temperature-sensitive hydrogel was made from poly (lactic acid-co-glycolic acid) and poly (ethylene glycol). This could be used to release dodecyl trimethyl ammonium bromide, encapsulated poly-pyrrole, and daunorubicin drug. The drug release process was driven by electrochemical reduction/oxidation and the movement of charged molecules under the influence of an electric field. A voltage of -1.5 V between two electrodes was applied for 60 seconds and repeated every 20 minutes. The release was significantly high while the electric field was supplied and the release was steady in the case of no-voltage supply condition. [50] Likewise, to predict the delivery of inflammatory drug: minocycline, triboelectric nanogenerators and magnesium-aluminum layered double hydroxide hydrogel were used. This hydrogel could inhibit

up to 100% of bacteria. The intake of minocycline is improved by increasing the permeability of the bacterial membrane with short-term electric stimulus. The cumulative release with 8V reached 100%, but the release at 2V reached only 70% within 24 hours, due to the inherent hydrophilicity of minocycline. The enhanced mobility of charged species under an electric field helps to explain this process. [51]

Acrylamides are majority components for making the electric responsive hydrogels. A hydrogel system is made with (dimethylacrylamide-co-4-methacryloyloxy benzophenone (5%)-co-4-styrenesulfonate (2.5%)) PDMAAp/ (poly (3,4-ethylenedioxythiophene)) PEDOT. This system was used to study release of the anti-inflammatory drug: dexamethasone. This system had the advantage of being used for up to 3 times with new drugs. The release of the model drug fluorescein from it suggested that the release of the fluorescein with 0.6V is 8-9 fold higher than that of the release from 0.1 V.[52] As compared to conventional PEDOT/ Polystyrene Sulfonate, the release from PDMAAp is up to 6 times faster, because of the coating limits the mechanical property that allows the delivery of smaller molecule. [53] Bagheri B. et. al., studied the hydrophobic feature of aniline oligomer with its electro responsive properties. Electro responsive nanofibers poly vinyl acetate/CHI-aniline oligomer was developed for the study of release of dexamethasone with the stimulus of electricity. Due to the hydrophilic feature of aniline oligomer the release drug from non-conductive polymer was higher. But in the case of simulated drug release, conductive polymer showed faster release due to hydrophobicity. After adding the aniline oligomer, the passive drug release rate reduced. However, the total cumulative passive release increased because of the change in the state of the aniline oligomer. The interaction between the hydrophobic aniline oligomer segment and dexamethasone was ruptured by applied electrical stimulation. Therefore, the conductive nanofiber showed a higher drug release rate in comparison

with non-conductive nanofiber. The on-demand drug release feature of the conductive web resulted in about a 40% increment in the drug release at 40 min in comparison with the non-stimulated web. [54]

Another platform has been developed for the controlled release of heparin using an electric field-based system. This system consists of microfabricated electrodes serving as the cathode and anode. The anode is coated with a pH-sensitive hydrogel layer made of poly (ethylene glycol)-diacrylate/laponite and containing drug-loaded chitosan nanoparticles. When a DC voltage is applied between the electrodes, it causes a local change in pH near the electrodes. In the basic environment near the anode, the chitosan nanoparticles released its drug due to the dehydration process; while in acidic environments, the release profile is negligible. The system is highly responsive, and when the DC voltage is turned off, the pH change is immediately reversed. [55]

An electromagnetic nanocomposite hydrogel encapsulating green-synthesized polypyrene was collided with gellan gum. The hydrogel had a porous, interconnected structure. Ibuprofen was used as the model drug and was released with electric stimulus. The potential of 5V increased the release up to 63%, while the passive release showed a release of only 10%. The conductive filler made from polypyrene nanoparticles enhances the effect of the electric field in the material, inducing variations in the association state of ionic groups within the hydrogel and thus affecting the diffusion of any chemical through the material and its release kinetics. [56]

In conclusion, various platforms and systems have been developed for the controlled release of drugs using electric field stimuli. These systems typically involve the use of microfabricated electrodes, pH-sensitive hydrogels, conductive fillers, and electroactive polymers. The release of the drugs can be enhanced by increasing the applied potential or by inducing changes in the association state of ionic groups within the hydrogel. The mechanisms of drug

release may involve the electric field driving the migration of charged molecules, or the overall net charge changes due to reduction or oxidation reactions in the hydrogel polymer network. The release of drugs may also be influenced by the inherent hydrophilicity or hydrophobicity of the drug molecules. These electric field-based systems have the potential to offer precise and controllable drug delivery for various applications.

**Table 2.2.** Summary of electric field responsive hydrogel systems.

<b>Stimulus</b>	<b>Material</b>	<b>Therapeutics</b>	<b>Advantages</b>	<b>Mechanism of release</b>	<b>Target wound healing stage</b>	<b>Reference</b>
Electric field	Dextran, electroactive aniline trimer, hexamethylene diisocyanate	dexamethasone and indomethacin	The controllability can be achieved because the hydrogel is highly responsive to the electric field.	The reduction of the positively charged aniline trimer expelled negative drug molecules from the hydrogel matrix.		[49]
Electric field	Poly (lactic acid-co-glycolic acid) and poly (ethylene glycol)	Daunorubicin		Electrochemical reduction/oxidation and electric field driven movement charge molecule		[50]
Electric field	Triboelectric nanogenerators	Minocycline	Up to 100% bacteria could be killed	The mobility of charge is influenced by the electric field.	Inflammatory	[51]
Electric field	PEDOT/PDMA	Fluorescein/Dexamethasone	Can be reused with new drugs. Presoaking causes the lower burst release.	External potential induces changes in charge and volume.	Inflammatory	[52]
Electric field	PVA/ CHI Aniline Oligomer	Dexamethasone	Applicable in the case of tissue engineering	The interaction between the hydrophobic aniline oligomer segment and dexamethasone was ruptured by applied electrical stimulation.		[54]
Electric field	Polyethylene glycol-diacrylate/Laponite with chitosan-nanoparticles	Heparin	The system is highly responsive to DC voltage thus electric field driven release is effective.	DC voltage near electrode causes local change in pH near electrode. In basic condition the dehydration causes the drug release.		[55]



Electric field	Poly-pyrrole and gellan gum (GG)	Ibuprofen	The release after electric stimulus is more than 5 times as compared to passive release.	Poly-pyrrole increases the electrochemical activity of the hydrogel. Variation in certain ionic group affects the diffusion channel.		[56]
Electric field	Dextran mixed with aniline trimer and hexamethylene diisocyanato	Dexamethasone and Indomethacin	Controllability can be achieved with external stimulus	Electric field causes the migration of charged molecules. Oxidation causes the release of positive drug and reduction causes the release of negative charge.		[49]

### 2.2.3. Temperature sensitive hydrogel

Encapsulated drug molecules can be released with the effect of the temperature by modifying the physiology of the hydrogel. Dynamic light scattering analysis showed micro-sized particles were formed above the lower critical solution temperature (LCST), indicating the copolymer undergoes phase transition at temperatures above that temperature, meaning it undergoes a phase transition from a linear hydrophilic polymer chain to a hydrophobic globule coil state at temperatures above LCST. This temperature-responsive behavior can be used for drug delivery by encapsulating hydrophobic drugs and releasing them selectively at target sites. The copolymer's high LCST means it can be injected into the body without quick micelle formation. The controlled release of drugs is achieved by dissolving them at a lower temperature and raising the temperature above the LCST to form micelles. In contrast, upper critical solution temperature (UCST) hydrogels become soluble and form a gel when the temperature drops below a certain threshold. Mixing copolymers and drugs at a low temperature protects the drug from denaturation or aggregation. The functional groups covalently crosslink with water, and the attached drug is encapsulated. Fine temperature control is necessary for drug delivery using this copolymer. [57, 58]

Dual responsive hydrogel system was made with poly (N-isopropylacrylamide-co-poly-(acrylamide)) (PNIPAm-co-PAAm) with N-isopropyl acrylamide (NIPAm) and acrylamide (AAm) as comonomers. Curcumin was used as the model drug to be released. The release was tested with different temperature and different pH. The release of curcumin from the system was caused by electrostatic repulsion due to the protonation of amine and amide groups and the Cur molecules at pH 5.5 (**Figure 2.4(a)**). Illustration of the phase transition of PNIPAAm-co-PAAm HG under the pH stimulus. Red color indicates the hydrophobic domain, and blue line indicates

the hydrophobic polymer segments in the presence of water. Additionally, **(Figure 2.4(c))** the release of Cur was significantly increased when both acidic pH (5.5) and elevated temperature (40°C) were present. This could be attributed to the acid-induced protonation and temperature-induced phase transition, which causes a shift from a chain structure to a globule structure and ultimately pushes out the encapsulated drug molecules. **(Figure 2.4(b))** [57]

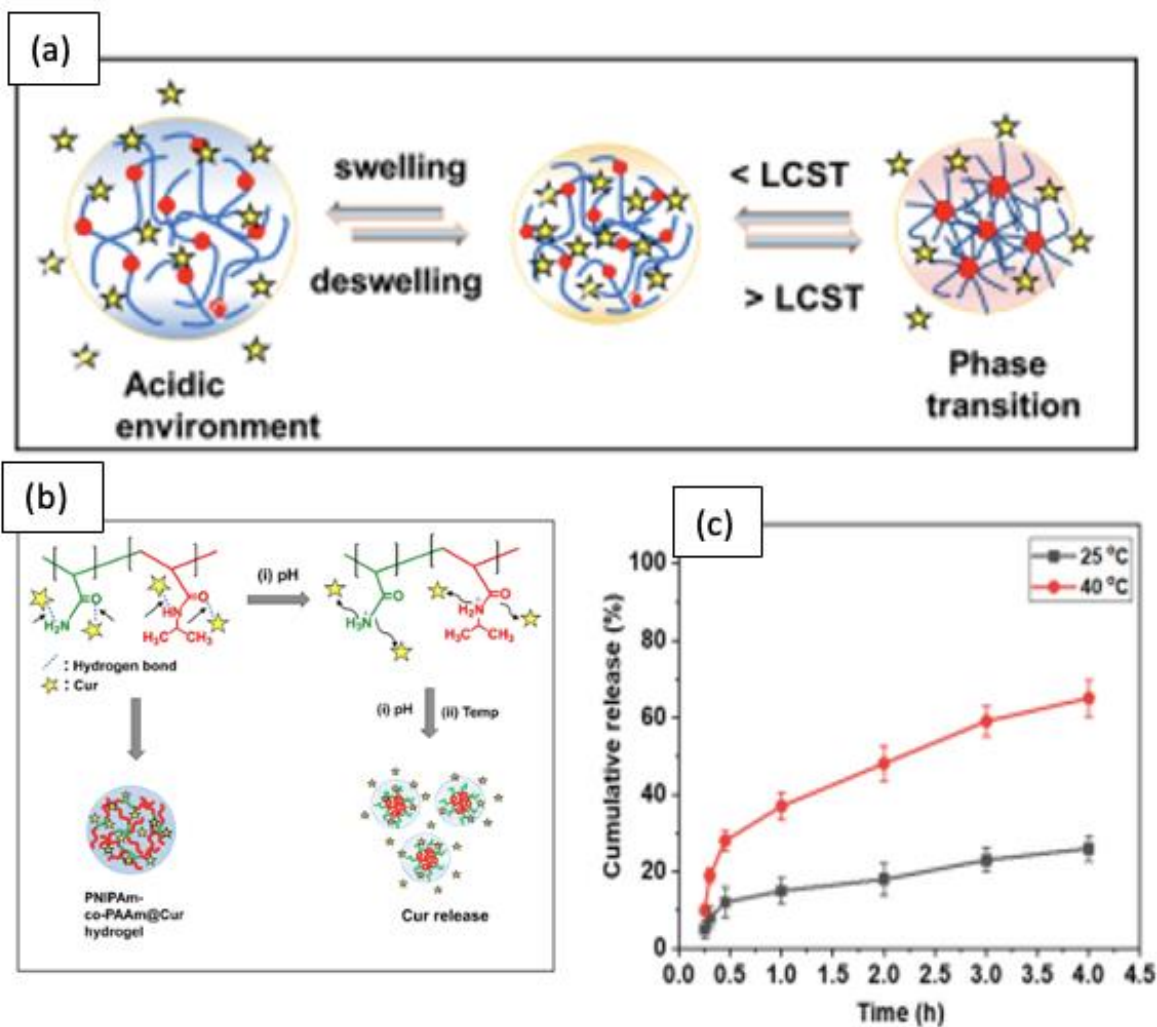


**Figure 2.4.** (a) Swelling and de-swelling mechanism of hydrogel in different temperature (b) Schematic representation of drug loading and (c) pH and temperature-responsive release behavior from PNIPAm-co-PAAm hydrogel system. [57]

The PNIPAm-co-PAAm hydrogel undergoes a pH-based phase transition due to attractive ionic interactions between its amide and carbonyl groups and H<sup>+</sup> ions. The copolymer ionizes at low pH, releasing the drug into the low pH microenvironment of tumors. [57] Several thermosensitive hydrogels have been manufactured with various materials that works on various release mechanisms. PNIPAAm hydrogels crosslinked with varying amounts of chitosan exhibit thermo-responsive behavior and are suitable for releasing azithromycin, a drug used to treat hemostatic and inflammatory stages of wound healing. The release of the drug is controlled by the relaxation of the polymer chain and followed by diffusion. The release rate of the drug decreases with an increase in the LCST of the hydrogel, which can be achieved by adding more chitosan. [59] Similarly, another hydrogel was made from quaternized CHI, polydopamine-coated reduced graphene oxide, and PNIPAAm exhibits excellent antioxidant and antibacterial properties and has biocompatibility and inherent photothermal properties. It is used as a drug carrier for tetracycline, a drug used for collagen deposition, vascularization, and thickening granulation tissue during the inflammatory stage of wound healing. The release of the drug from the hydrogel is influenced by the ratio of polydopamine coated graphene oxide in the hydrogel. As the ratio of polydopamine coated graphene oxide increases, the thermo-sensitive self-contraction property of the hydrogel also increases, leading to a decrease in the release of the drug. [60] Another research studied the release of lidocaine hydrochloride and ibuprofen with response of pH and temperature. The hydrogel was made from PNIPAAm hydrogel crosslinked with crotonic acid. The porosity of the hydrogel increased with an increase in the amount of crotonic acid. The rapid shrinkage of PNIPAAm when the temperature increases from 25 °C to 35 °C leads to the further squeezing out of the encapsulated drugs. To achieve a desired degree of swelling, an increase in temperature may be required. [61] The release of 5-fluorouracil from a hydroxyapatite gelatin polymer composite

is also influenced by temperature. The hydrogel, which is crosslinked with glutaraldehyde and encapsulated with 5-fluorouracil, exhibits the highest release rate at 42°C. Within 5 minutes, 55% of the drug is released due to the presence of non-encapsulated drug molecules on the surface of microparticles or drug molecules close to the surface. The remaining drug is released as the matrix density decreases due to the swelling of nanoparticles at higher temperatures, which facilitates the escape of the drugs. [62]

A hydroxypropyl chitosan and PNIPAAm hydrogel crosslinked with cyclodextrin and adamantly is used to release dipotassium glycyrrhizinate, a drug used to enhance collagen deposition and reduce inflammation. The hydrogel has injectable, thermo-sensitive, highly ductile, self-healing, and antibacterial properties, making it suitable for further applications. The volume phase transition temperature (VPTT) decreases with an increase in the adamantly content due to reversible hydrogen bonding between the polymeric side chains and water molecules and the hydrophilic/hydrophilic balance in the polymeric network. [63]

In conclusion, hydrogels possess the ability to undergo reversible changes in their physical properties due to variations in temperature, which alters the overall entropy of the system through changes in enthalpy and free energy. These changes enable the hydrogels to return to a solution state after the thermal stimulus responsible for their gelation is removed. These hydrogels possess various features, including high ductility, injectability, thermo-sensitivity, self-healing, and antibacterial activity, making them appropriate for a wide range of applications. Factors that can influence drug release from hydrogels include the physical structure of the hydrogel, chemical interactions between the drug and the hydrogel, and the presence of pores or other structural features that facilitate drug diffusion.

**Table 2.3.** Summary of thermo-responsive hydrogel systems.

Stimulus	Material	Therapeutics	Advantages	Mechanism of release	Target wound healing stage	Reference
Temperature	(PNIPAAm-co-PAAm) with (NIPAm) and (AAm)	Curcumin	This system is dual responsive, i.e., to pH and temperature	temperature-induced phase transition		[57]
Temperature	PNIPAAm crosslinked with Chitosan	Azithromycin	Is applicable in controlling drug release from hydrogel.	Relaxation of polymer chain followed by diffusion.	Inflammatory	[59]
Temperature	Quaternized chitosan, polydopamine coated graphene oxide and PNIPAAm	Tetracycline	Biocompatibility, antibacterial, antioxidant	Increasing concentration of graphene oxide causes the reduction in swelling ratio. Self-contraction in higher temperature squeezes the drug.	Collagen deposition, vascularization, and granulation	[60]
Temperature/pH	PNIPAAm with crotonic Acid	Lidocaine hydrochloride and Ibuprofen	Dual responsive, controlled release for different solubility	Increase in amount of crotonic acid causes increase in porosity, Rapid shrinkage of PNIPAAm with increasing temperature squeezes drug.		[61]
Temperature	Hydroxyapatite gelatin	5-fluorouracil	Biocompatible, biodegradable	Matrix density decreases as the swelling of nanoparticles increases at higher temperature, that causes easy escape.		[62]
Temperature	Hydroxypropyl CHI, PNIPAAm	Dipotassium glycyrrhizinate	Injectable, highly ductile, self-healing antibacterial	Phase transition behavior caused by reversible hydrogel bonding between hydrogel and water causes VPTT.	Inflammation	[63]

#### 2.2.4. Photo responsive hydrogel

Cold atmospheric plasma (CAP), along with polymerized pyrrole, crosslink hybrid polymer, hyaluronic acid, and gelatin, has been used in the storage and delivery of therapeutic platelet proteins in response to near-infrared (NIR)-driven photothermal-hyperthermic effects. The expression of heat shock protein with anti-inflammatory effects, induced by the photothermal-hyperthermic effects, helps to improve the healing of diabetic wounds. [64]

One of the hydrogels was created with graphene oxide (GO) and vascular endothelial growth factor (VEGF), (**Figure 2.5**). The GO hybrid hydrogel scaffold was created using a capillary microfluidic device. Under photothermal behavior C=C bond breaks thus enhances the antibacterial performance.

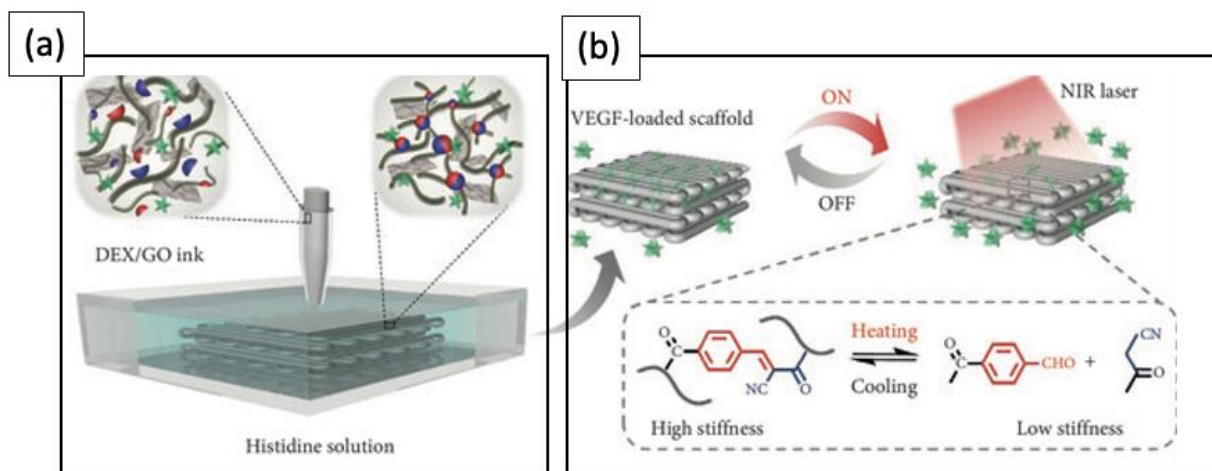


**Figure 2.5.** (a) Schematic of the GO hybrid hydrogel scaffold fabrication (b) Preparation and NIR-induced stiffness change of the GO hybrid hydrogel scaffold. [65]

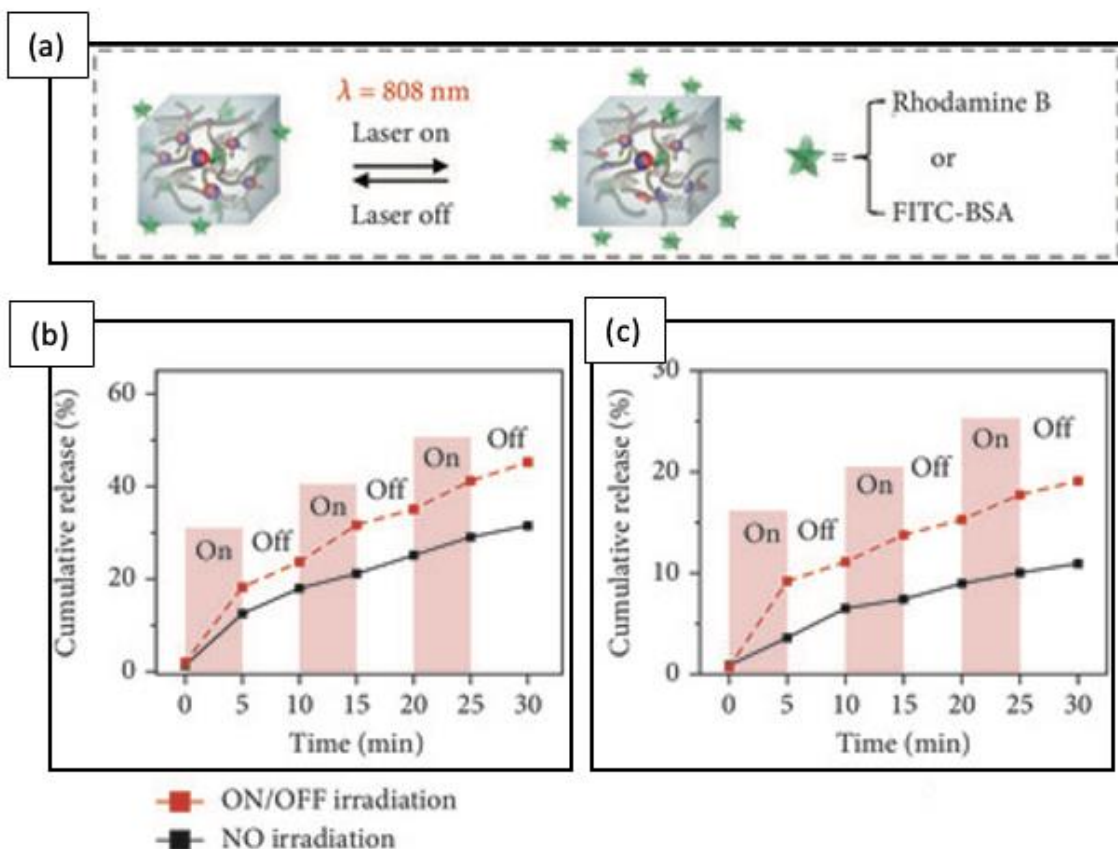


**Figure 2.6.** (a) The scheme demonstrating the NIR responsive controlled drugs delivery. (b) Switchable release of rhodamine B. (c) Controllable FITC-BSA. [65]

The controllable drug release of GO hybrid hydrogels was facilitated by thermo-induced stiffness changes using NIR, as shown in (**Figure 2.6(a)**). To demonstrate this, rhodamine B was loaded into the precursor during the formation of GO hybrid hydrogel. The irradiation of the hydrogel stimulated a fast drug release, which corresponded to a low-stiffness state under irradiation, while switching off the light showed a relatively slower release, which was attributed to the high stiffness without irradiation. Similarly, FITC-BSA was also incorporated into the GO hybrid hydrogel, and similar switchable drug release behavior could be demonstrated. Thus, as



shown in **(Figure 2.6(b))** it could be concluded that thermo-induced stiffness changes in GO hybrid hydrogels stimulated controlled drug release, and cyclic ON/OFF irradiation onto the hydrogel offered a promising strategy to control the released dose of loaded drugs. [65]

Following the same concept some hydrogels show the photo-responsive drug release. Zinc-aluminum layered double hydroxides has been used to release ibuprofen in response to NIR stimuli for the treatment of inflammatory stages of wound healing. The ibuprofen loaded hydrogel delivery system shows an initial burst release followed by a slower release of ibuprofen in phosphate buffer solution. With an initial burst release of 58.6% within the first hour, a total release of 68.37% was obtained in 6 hours. [66] Similarly, nitrox oxide was released from a hydrogel system formed by a palladium meal organic framework on poly-azobenzene and sodium nitroprusside. The release is accelerated by the application of UV/Vis light. The alkyl side chain length of poly-azobenzene in the system can be used to better control the switching of nitric oxide release and nanozyme activity. When UV light destroys the host-guest interaction between the poly-azobenzene and hydrogel, it leads to the release of nitric oxide and the recovery of Pd nanozyme activity. The Pd then catalyzes  $H_2O_2$  to produce reactive oxygen species (ROS), and the nitric oxide helps to reduce the bacterial effect. When the release is triggered with visible light, the release is slower by 10%. [67]

The release of epidermal growth factor (EGF) has been studied from photo-responsive supramolecular polysaccharide hydrogels formed through host-guest interactions between azobenzene and  $\alpha$ -cyclodextrin groups conjugated with hyaluronic acid chains. The addition of a photo-responsive gel hyaluronic acid and  $\alpha$ -cyclodextrin forms EGF photo-responsive hydrogel, which is more reactive to UV light. The release profile for EGF form photo-responsive is different from EGF supramolecular hydrogel, without photo-responsive hydrogel, as the release is

dependent on UV light. The burst release is higher, and the release is only seen when UV light is applied, with no release when UV light is not applied, demonstrating the photo-responsive behavior of photo-responsive gel. The reversible supramolecular interactions between the azobenzene and  $\alpha$ -cyclodextrin group in hyaluronic acid chains allow the supramolecular hydrogel to have a dynamic network crosslink density upon the application of photo stimuli. [68]

In summary, various photochemical, photoisomerization, and photothermal mechanisms have been used to trigger the structural disruption or disassembly of drug carriers in drug delivery systems. Photosensitizer molecules absorb incoming photons, leading to the excitation of an electron from a singlet ground state to an excited singlet state, which can then undergo a variety of energy loss processes. This excitation can also lead to vibrational relaxation, allowing excited molecules to relax to their lowest vibrational level of the excited electronic state through a non-radiative process. These processes can change the chemical structure of the hydrogel and allow the drug to diffuse through electron transfer energy and oxidation of the drug carrier. Various materials have been found to have properties such as initial burst releases, slow releases, and photo-responsive behavior, and have been used in a range of applications, including the treatment of inflammatory stages of wound healing and the release of NO and EGF.

**Table 2.4.** Summary of photo-responsive hydrogel systems.

Stimulus	Material	Therapeutics	Advantages	Mechanism of release	Target wound healing stage	Reference
NIR	Cold atmospheric plasma (CAP) made by polymerize pyrrole, Hyaluronic acid and gelatin	Therapeutic platelet proteins/ heat shock proteins	Anti-inflammatory properties boost the restoration of diabetic wound in-vitro	CAP treatment improves the mechanical properties thus increases the retention of the drug	Inflammatory	[64]
NIR	Dextran/Graphene oxide	Rhodamine B or FITC-BSA	Release can be controlled by turning on and off	thermo-induced stiffness changes in GO hybrid hydrogels stimulated controlled drug release		[65]
NIR	Zinc aluminum and layered double hydrogel	Ibuprofen		Chemical Structure of hydrogel is changed with the effect of vibrational relaxation.	Inflammatory	[66]
UV light	Palladium metal organic framework and poly-azobenzene with sodium nitroprusside	Nitric Oxide		When UV light destroys the host-guest interaction between the poly-azobenzene and hyaluronic acid, it leads to the release of nitric acid and the recovery of Pd nanozyme activity.	Inflammatory	[67]
UV light	Polysaccharide hydrogel azobenzene and $\beta$ -cyclodextrin and hyaluronic acid	Epidermal Growth factor	Has a great effect in tissue formation and growth factor	Destruction of host-guest interactions between azobenzene and $\alpha$ -cyclodextrin groups conjugated with hyaluronic acid chains	Angiogenesis	[68]

### 2.2.5. Enzymatic responsive hydrogel

Several drug delivery systems have been developed that are responsive to specific microenvironments, such as pH and ROS. The release of drugs from these hydrogels can be enhanced by the presence of enzymes such as glucose oxidase and phospholipase A2, and could be influenced by factors such as the microstructure of liposomes and the amount of boronated ester present. These hydrogels have potential applications in the treatment of diseases such as cancer and inflammation and can be used for the delivery of drugs such as doxorubicin, curcumin, and diclofenac sodium. These systems utilize hydrogels with self-healing properties and the ability to release drugs in a controlled manner in response to changes in the microenvironment. One such system uses animated gelatin and nano-zinc oxide to treat chronically infected diabetic wounds, while another uses collagen-based hydrogels and antibacterial nanoparticles to release Ag<sup>+</sup> in response to acidic environments and high levels of ROS. Another system utilizes a multifunctional hydrogel dressing that can release metformin in the presence of glucose. These systems have the potential to improve the treatment of chronic wounds and other medical conditions. [69-71] [72, 73]

Researchers developed a hydrogel that responds to glucose and matrix metalloproteinase 9 (MMP-9) and can change shape. The hydrogel contains insulin and celecoxib, and its release can be controlled by glucose and MMP-9. The hydrogel can quickly change from a fluid to a gel state and release its contents. The release of insulin and celecoxib increases with higher levels of glucose and MMP-9. The hydrogel disintegrates faster under the synergistic effect of glucose and MMP-9. [69]

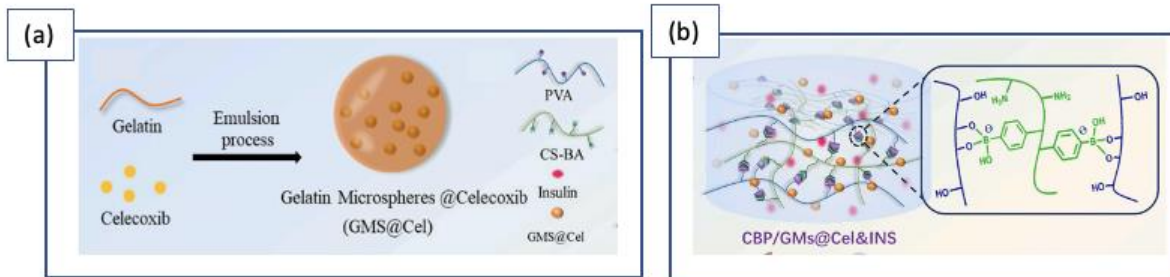


**Figure 2.7.** (a) Preparation of gelatin microspheres containing celecoxib. (b) Preparation of the hydrogel and the characteristics of temperature sensitive shape self-adaptive. [69]

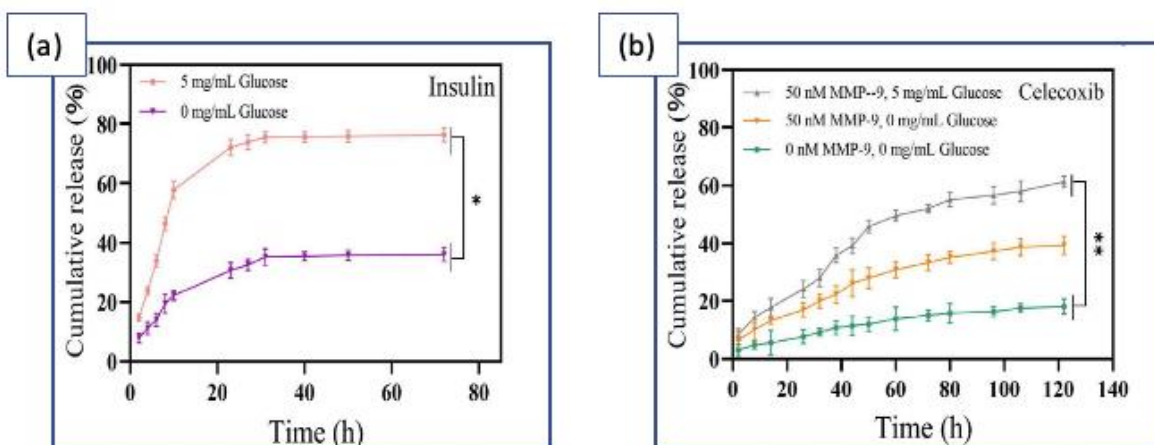


**Figure 2.8.** Cumulative release of the hydrogels (a) insulin and (b) celecoxib. [69]

Glucose reduces crosslinking density, causing insulin release by decomposing the hydrogel. High MMP-9 concentrations accelerate celecoxib release by degrading gelatin microspheres. The release of insulin and celecoxib increases with higher concentrations of glucose and MMP-9, respectively. The hydrogel disintegrates faster under the synergistic effect of glucose and MMP-9, with celecoxib release reaching 62.31% in 120 hours at 5 mg/mL glucose and 50 nM MMP-9. The hydrogel can release insulin and celecoxib on demand in response to high levels of glucose and MMP-9. [69]

Similarly, microenvironment-responsive hydrogel is made with animated gelatin reacted with oxidized dextran and encapsulated with nano-zinc oxide which can be used for curing refractory, chronically infected diabetic wounds. The addition of hydrochloric acid to the lower pH in the system resulted in pH-sensitive Schiff bond dissociation and collapse of hydrogel thus was dissolved rapidly in a higher ROS environment (1 mM H<sub>2</sub>O<sub>2</sub>). The hydrogel is made with innovative properties i.e., self-healing, and synergistically promotes angiogenesis by suppressing bacterial growth. The hydrogel can release the encapsulated drug in a smart manner in response to the reduced pH and high ROS present within chronically infected wound.[70] Hydrogel is made based on antibacterial nanoparticles polydopamine with silver nanoparticles and recombinant human type III collagen (rhCol III), rhCol III is used to decrease inflammatory response, increase proliferation and angiogenesis. The designed self-healing hydrogel was responsive to an acidic environment and a high level of reactive oxygen. In an acidic environment of pH 5 the release was 1.19 mg/ml at 48 hours. The difference between the release at 48 hours with 5 mM H<sub>2</sub>O<sub>2</sub> and 10 mM H<sub>2</sub>O<sub>2</sub> was 0.93 mL and 1.36 mL respectively. [71]

Alginate-based hydrogels have been used to study the delivery of BSA. These systems are responsive to the presence of ROS or H<sub>2</sub>O<sub>2</sub>, and are biocompatible, wearable, and implantable. They have the ability to fully operate under active conditions and prevent flow when there is no stimulus present. ROS can be produced due to inflammation, ischemia, or reperfusion, and materials that can detect and respond to ROS are a promising alternative for therapy. H<sub>2</sub>O<sub>2</sub> can be produced by oxidase enzymes such as glucose oxidase, lactate oxidase, and xanthine oxidase in the presence of their substrates (glucose, lactate, hypoxanthine), and can be used to "smartly" release model drugs (insulin, myoglobin, albumin) that are stimulated by endogenous biomarkers. Boronated esters are highly responsive to H<sub>2</sub>O<sub>2</sub>. [72] Zinc oxide and deferoxamine have been

loaded into metal-organic drug-loaded hydrogels, that are made responsive to glucose through the inclusion of glucose oxidase. The mechanical properties of these hydrogels, such as storage moduli and elastic behavior, are weaker in the presence of Glucose<sup>+</sup> ions in drug loaded hydrogel. As a result, the release of zinc ions from hydrogel is faster in the presence of Glucose<sup>+</sup> ions. Similarly, the release of deferoxamine is also faster when the hydrogel is made with glucose oxidase. 73% of the drug is released from the glucose oxidase-containing hydrogel, while only 30% is released from the hydrogel without glucose oxidase. [74]

Similarly, to study the enzymatic triggered release from the hydrogel, hydrogel micelles is formed with glycopeptide based on phenylboronic acid grafted oxidized dextran and caffeine acid grafted  $\epsilon$ -polyseme. The model drug used here are Mangifera and diclofenac sodium for angiogenesis and anti-inflammatory treatment. Due to the hydrolysis of the hydrogel network the Schiff base bond and boronic ester bond breaks under an acidic and oxidative condition. After the collapse of the network, diclofenac sodium and Mangifera are exposed to the external environment. The system is bio-degradable and has the good rheological property and self-healing ability. [73]

In summary, several different types of drug delivery systems have been developed that rely on various stimuli, including ROS/H<sub>2</sub>O<sub>2</sub>, magnetic fields, glucose, phospholipase A<sub>2</sub>, pH and temperature, and REDOX degradation, to release drugs in a controlled manner. These systems have shown promising results in terms of biocompatibility, drug release efficiency, and the ability to target specific cells or microenvironments. Additionally, some of these systems have self-healing properties and the ability to respond to multiple stimuli, making them suitable for various therapeutic applications.

**Table 2.5.** Summary of enzymatic-responsive hydrogel systems.

Stimulus	Material	Therapeutics	Advantages	Mechanism of release	Target wound healing stage	Reference
Glucose and MMP-9	Gelatin microsphere	insulin and celecoxib	The release of individual drug was possible to control	Glucose reduces the crosslinking density of the matrix and MMP-9 changes the structure of the hydrogel to irregular structure		[69]
pH/ ROS	Gelatin	Nano-ZnO	Self-healing, also has synergetic property	Dissociation of hydrogel in higher ROS environment.	Angiogenesis	[70]
ROS/H <sub>2</sub> O <sub>2</sub>	rhCol III	Antibacterial nanoparticles polydopamine with silver nanoparticles	Helps in multistage healing process and kills bacteria	The size of rchol III is larger thus the Ag particles are released faster and kills the bacteria and later release of rchol III helps is proliferation.	Proliferation, remodeling	[71]
Glucose oxidase	Alginate	BSA	Biocompatible, wearable	H <sub>2</sub> O <sub>2</sub> can be easily produced by oxidation of enzymes, which is read by highly responsive endogenous biomarkers and drug is rapidly released.	Inflammatory	[72]
Enzyme (Phospholipase A2)	Metal-organic drug loaded hydrogel	Zinc Oxide and Deferoxamine mesylate	Self-healing, good mechanical properties	The presence of glucose oxidase makes the hydrogel structure weaker, thus the release gets faster.	Reepithelization, collagen deposition, angiogenesis	[74]
pH /ROS	IA/Fe <sub>3</sub> O <sub>4</sub>	Mangifera, Diclofenac Sodium	self-healing, good rheological properties also	The hydrolysis of the hydrogel networks the Schiff base bond and boronic ester bond breaks under an acidic and oxidative condition	Angiogenesis, Inflammatory	[73]



### 2.2.6. External magnetic field responsive hydrogel

The drug release from magnetic hydrogels is triggered by the application of a magnetic field, which causes the magnetic nanoparticles to heat up through magnetic hyperthermia. This localized heating can cause the hydrogel matrix to swell, leading to the release of the drug molecules. The magnitude and duration of the magnetic field can be controlled to achieve a desired drug release profile. In wound healing applications, magnetic hydrogels can be used to deliver drugs such as growth factors, anti-inflammatory agents, and antibiotics to the wound site. The targeted drug release can enhance the efficacy of the treatment while minimizing systemic side effects.

The main mechanism of drug release is diffusion. The porous network of hydrogel entraps the small molecules inside gel matrix, which comes out into the environment. These drug molecules diffusion is facilitated by external stimuli. Either alternating magnetic field (AMF) is used or external magnetic field is used for release. When an external field is applied, the magnetic nanoparticles (MNP) form a barrier inside gel matrix, thus restricting the small molecules to come out from porous gel network. As the external field is switched off, the alignment is destroyed creating the path for drug release. This behavior is called magnetic pulsatile drug release behavior. It can be inferred that the magnetic field has the direct relationship with magnetic field strength.[75]

To verify this effect a hydrogel has been created with magnetic iron oxide ( $\text{Fe}_3\text{O}_4$ ), graphene sheets, itaconic acid, starch, and alginic acid. This was done through graft copolymerization, and the resulting material was used for delivering the drug guaifenesin to promoting wound healing. [76]

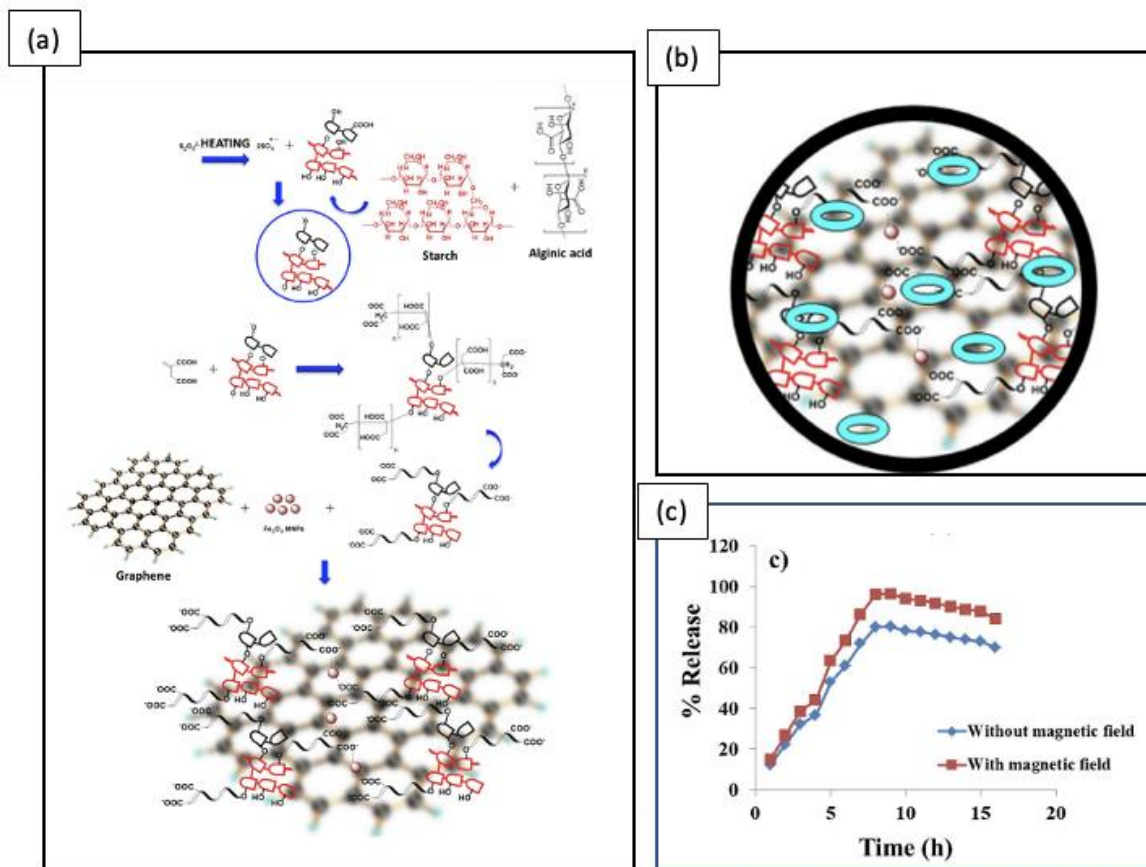


**Figure 2.9.** (a) Proposed mechanism for the formation of magnetic hydrogel, (b) loading guaifenesin into hydrogel, and (c) *in-vivo* release of guaifenesin with and without the magnetic field. [76]

The process for preparing the hydrogel involves the thermal mechanism (**Figure 2.9(a)**). Initially, thermal initiator generates sulfate free radicals at 68°C, which extracts hydrogen from the hydroxyl groups in starch and alginate acid. This creates active macro-radical centers on the main chains, allowing itaconic acid monomers to convert into acceptors of radicals during polymerization (**Figure 2.9(b)**).

When an external magnetic field was present, the drug release was increased due to the movement of ferrous oxide (Fe<sub>3</sub>O<sub>4</sub>). MNPs under the influence of the magnetic field, results in

more empty sites in the nanocomposite's porous structure. With the application of 1800G magnetic field for 5 hours the release of the guanfacine release was changed by 1.5 times. Where the passive release was 60.4% and magnetic field responsive release was 90% (**Figure 2.9(c)**). [76] Generally, similar effect in drug release is observed with the application of external magnetic field. [77] One system created to release guanfacine is also responsive to external magnetic field. The external magnetic field works as the stimulus to agitate magnetic nanoparticles,  $\text{Fe}_3\text{O}_4$ , this motion leads to relaxation of polymeric chain, loose network and finally accelerated drug release. For this reason, the release of guanfacine was released 66.4% in the absence of magnetic field and with magnetic field the release was 90.4%. [78]

A similar effect was observed when hydrogel was made from CHI and ALG encapsulated with Magnetic Gelatin Microsphere. The drug 5-Fluroucial is delivered with magnetic stimulus. Hydrogel is self-healing and can be used for soft-tissue engineering. The release of drugs from hydrogel was studied with and without magnetic field and it was observed that there was not much deference in the beginning but after 5 days the release under external magnetic field was seen higher. Almost 75% drug was released with external magnetic field whereas only 56.5% drug could be released without magnetic stimulus. [79]

Hydrogel with ALG and xanthan gum, crosslinked with  $\text{Ca}^{2+}$  ions with MNPs are prepared. The combination of dopamine and xanthan gum and MNP increases the material hydrophilicity, that favors the invitro cell adhesion and proliferation. The exposition of magnetic hydrogels to Electromagnetic field (EMF) might promote the orientation of MNP, causing hydrogel local mechanical vibrations and stimulating the hydrogel magnetic field sensitive. The release of dopamine from ALG and xanthan gum magnetic nanoparticles hydrogels without and with

magnetic stimulus is 45% and 64.6%, respectively. Drug release from without and with magnetic field was 38% and 48%. [80]

In conclusion, the use of nano composite hydrogels made from alginate incorporating graphene oxide and  $\text{Fe}_3\text{O}_4$  has been shown to be an effective means of delivering the drug Doxorubicin in a controlled manner using external stimuli such as near-infrared light, pH, and an external magnetic field. The transformation of energy from light and magnetic fields into heat causes an increase in the temperature of the hydrogel above its lower critical solution temperature, leading to shrinkage and accelerated drug release. The use of external magnetic fields has also been demonstrated to affect the characteristics of hydrogels made from methacrylate chondroitin sulfate and Irgacure, with a correlation being shown between growth factor release and degradation and the presence of an external magnetic field. These systems show promise as a means of controlled drug delivery using external stimuli.

**Table 2.6.** Summary of electromagnetic field- responsive hydrogel systems.

<b>Stimulus</b>	<b>Material</b>	<b>Therapeutics</b>	<b>Advantages</b>	<b>Mechanism of release</b>	<b>Target wound healing stage</b>	<b>Reference</b>
EMF	magnetic particles (Fe <sub>3</sub> O <sub>4</sub> ), graphene sheets, itaconic acid, starch, and alginic acid	Guanfacine	The release is 1.5 times faster with the help of stimulus.	External Magnetic field agitates the Fe <sub>3</sub> O <sub>4</sub> MNPs, causing them to move and relax the polymer chains, resulting in a looser network and increased drug release.		[76]
EMF/ pH	Magnetic nanoparticles, Fe <sub>3</sub> O <sub>4</sub>	Guanfacine	Non-cytotoxicity, biocompatibility of drug and hydrogel matrix	External magnetic field leads to relaxation of polymeric chain, loose network and finally accelerated drug release.	Inflammatory	[78]
EMF	CHI/ALG, magnetic gelatin microsphere	5-fluorouracil	Self-healing/ can be used for soft tissue engineering	External magnetic field provides the direction of drug delivery.	Cell adhesion and proliferation	[79]
EMF	ALG, Xanthan gum, MNP	Dopamine		The exposition of magnetic hydrogels to EMF promotes the orientation of MNP, causing hydrogel local mechanical vibrations and stimulating the hydrogel mechano-sensitive.	Proliferation	[80]

### 3. Methodology

#### 3.1. Materials

Sigma Aldrich was the supplier for various chemical substances used in this study, including low molecular weight chitosan (CHI) powder derived from deacetylated chitin, medium viscosity alginate (ALG), fluorescein isothiocyanate-dextran (FITC-Dextran) with a molecular weight range of 3000-5000, and albumin fluorescein isothiocyanate conjugate protein bovine (FITC-BSA) with a molecular weight of 66 kDa. The reducing agent used in the experiment, sodium cyanoborohydride ( $\text{NaBH}_3\text{CN}$ ), was also obtained from Sigma Aldrich. Ferrocene carboxaldehyde (Fc) was purchased from Alfa Aesar, while fluorescein (FITC) was obtained from ACROS organics. Ninhydrin (Monohydrate, Reagent) was purchased from spectrum chemicals. VWR supplied sodium hydroxide (NaOH) with a concentration of 50% w/w, and ninhydrin reagent was obtained from Spectrum Chemicals. Ciprofloxacin (CIP) was obtained from Enzo Life Sciences. In addition to these chemicals, Dow Chemicals provided elastomers for Polydimethylsiloxane (PDMS) preparation, and ATCC supplied both *Staphylococcus aureus* (*S. aureus*) (ATCC 29213) and *Pseudomonas aeruginosa* (*P. aeruginosa*) (ATCC 27853). Cellulose acetate filter membranes were purchased from Whatman, Sigma Aldrich, and Hardy Diagnostics offered 2 kgs lysogeny broth (LB) with combinations of tryptone 10 grams, sodium chloride 5 grams and yeast extract 5 grams for use in bacterial culture experiments. The supplier for LB agar for bacterial growth was VWR, while 500 grams 5X-M9 salt with disodium phosphate 33.9 grams, monopotassium phosphate 15 grams, sodium chloride 2.5 grams and ammonium chloride 5 grams for bacterial media preparation could be purchased from BD and BD chemicals. Agarose LE is obtained from EXCEL.

### **3.2. Synthesis of (Fc-CHI) and formation of PEC hydrogel**

To prepare the CHI solution, 1.5 weight percent (wt.%) of CHI was mixed with 0.1 M acetic acid solution. The ALG solution was prepared by mixing 1.5 wt.% of ALG with deionized water at 60 °C. The CHI/ALG PEC was then prepared by mixing the CHI and ALG solutions at different volumetric ratios, such as 1:9, 2:8, and so on. For example, a 1:9 CHI/ALG solution refers to; for every 1x volume of CHI solution, there are 9x volumes of ALG solution. This process results in the synthesis of the CHI/ALG PEC at different ratios.

For the synthesis of Fc-CHI solution, CHI solution was first prepared by dissolving 0.9 grams of CHI in 360 ml of 0.1 M acetic acid solution. Three different concentrations of Fc-CHI were then prepared by adding different concentrations of Fc solution to the CHI solution. The Fc solution was prepared in 340 ml methanol with three different concentrations. 0.06 mM, 0.12 mM, and 0.18 mM Fc were used to make low, medium, and high concentration Fc solutions, respectively. The volume of the Fc solution and CHI solution were kept the same for each concentration of Fc-CHI. [81, 82] This process will result in the synthesis of low, medium, and high concentrations of Fc-CHI.

After mixing Fc solution with CHI solution for one hour, a reducing reagent solution containing different amounts of sodium cyanoborohydride was added to the Fc-CHI solution. The reducing reagent solution was prepared in 20 ml methanol with 0.12 mM, 0.24 mM, and 0.36 mM of sodium cyanoborohydride for the low, medium, and high Fc-CHI solutions, respectively. The resulting solution was then mixed with Fc-CHI solution on a magnetic stirrer at 500 rpm for 24 hours at room temperature. After this, the solution was titrated with NaOH (5 vol%). The orange precipitate that forms was then filtered four times with methanol solutions of increasing

concentration (first with 70% methanol, second with 80% methanol, third with 90% methanol, and fourth with 100% methanol). The UV spectroscopy of the filtrate obtained at each step was used to confirm that there were no free Fc molecules present in the Fc-CHI residue. Finally, Fc-CHI granules were obtained after incubating the residue for 24 hours at 32 °C.

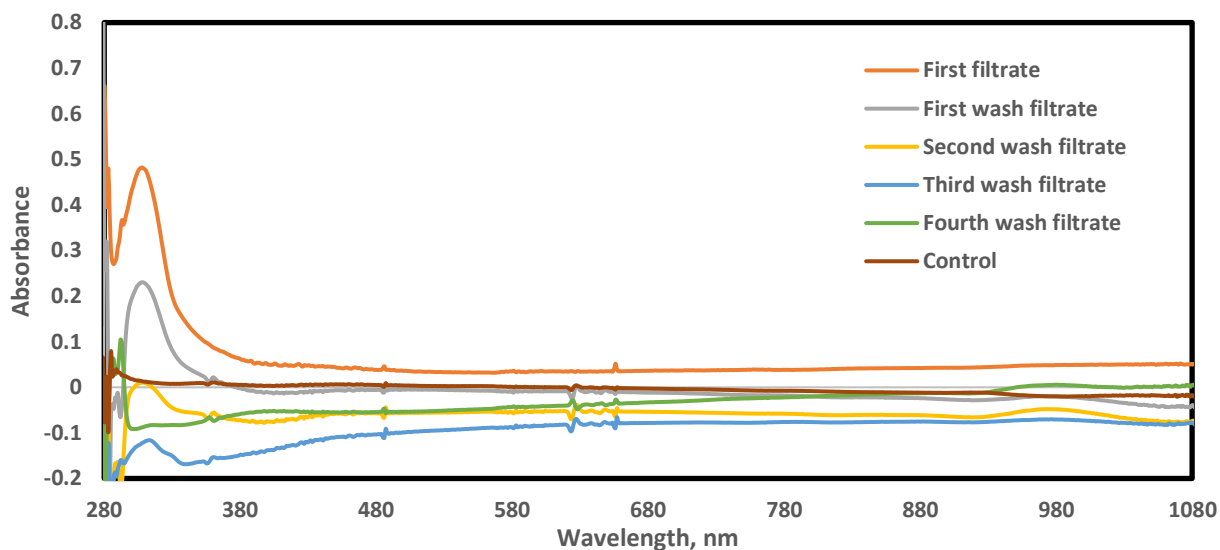


**Figure 3.1.** UV-Vis spectroscopy of wash methanol solution to detect amount of free Fc present after each wash.

To prepare the Fc-CHI solution, 1.5 wt.% (0.75 grams) of Fc-CHI was dissolved in 0.1 M acetic acid solution (50 ml). The ALG solution was prepared by mixing 1.5 wt.% (0.75 grams) of ALG with 50 ml of DI water at 60 °C. The Fc-CHI/ALG PEC was then prepared by mixing the Fc-CHI and ALG solutions at different ratios, such as 1:9, 2:8, and so on. The resulting Fc-CHI/ALG PEC solution was then lyophilized with Freeze dryer ‘Labconco Freezedryer’, Marshall Scientific, USA. The lyophilization is performed at -53 °C and 0.123 Torr for 24 hours.



### 3.3. Characterization of PEC hydrogels

#### 3.3.1. Ninhydrin assay

The degree of conjugation of CHI can be measured using ninhydrin. The number of amino groups present in the CHI and its conjugates can be quantified using this method. [83] Conjugation refers to the formation of chemical bonds between polymer chains, which can increase the strength and stability of the material. The amount of free amino groups in the test sample is proportional to the optical absorbance of the solution after heating with ninhydrin. This means that the higher the absorbance, the more amino groups are present in the sample.[84] By comparing the absorbance of the different samples, it is possible to estimate the degree of crosslinking in the Fc-CHI hydrogels.

To do this, a ninhydrin solution is made by mixing ninhydrin powder with Ethyl alcohol at a concentration of 20 mg/ml.[83] This solution is then mixed with CHI and CHI conjugates (such as Fc-CHI with low, medium, and high concentrations of Fc) in a 1:1 ratio. The mixture is then incubated at 50°C for 1 hour at 100 RPM. Since, ninhydrin is reactive to light, the incubation is done covering the mixture in aluminum foil. After that the mixture is cooled to the room temperature and the absorbance is read at 570 nm using Spectrophotometer (Bio TEK, USA) in 96 well plate.

The degree of conjugation is obtained by: [83]

$$\text{Degree of conjugation} = \frac{\text{NHN reactive amine}_{\text{fresh}} - \text{NHN reactive amine}_{\text{fixed}}}{\text{NHN reactive amine}_{\text{fresh}}} \times 100$$

Where, NHN reactive amine<sub>fresh</sub> is the absorbance of light by fresh amine i.e., pure CHI,

NHN reactive amine<sub>fixed</sub> is the absorbance of light by amine mixture i.e., Fc-CHI.

### **3.3.2. Turbidity**

Turbidity is an optical property that describes the amount of light that is scattered or absorbed by the suspended particles as it passes through a liquid. The maximum turbidity obtained helps to determine the stoichiometric proportion between the components.

PEC solution of pure CHI/ALG, low Fc-CHI/ALG, medium Fc-CHI/ALG and high Fc-CHI/ALG was prepared in different volumetric ratios of pure CHI or Fc-CHI to ALG. The Fc-CHI was made with 1.5 weight %. The ALG solution was also prepared 1.5 weight %. These individual solutions were mixed in the ratio of pure CHI or Fc-CHI: ALG in 0:1, 1:9, 2:8, 3:7, 4:6, 5:5, 6:4, 7:3, 8:2, 9:1 and 10:0. The turbidity of all PEC solution with all ratios was measured with Orion AQ4500 turbidity meter (Thermo Scientific). The PEC solutions were prepared for 3 times, and its turbidity was measured each time and the average is taken.

### **3.3.3. Viscosity**

Viscosity test is performed to determine the mechanical strength of the polymer solution. The viscosity of pure CHI/ALG, as well as low, medium, and high Fc-CHI/ALG solutions, was determined at their respective stoichiometric proportions. The stoichiometric proportions were established based on the results of the turbidity test and the measurements were taken at room temperature using a rotational viscometer (Fungilab Viscolead, Barcelona, Spain). The viscosity of PEC solutions was evaluated using an L2 spindle with a range of viscosity measurements from 300 cP to 100,000 cP at various rpm. The viscosity was determined at 12 rpm.

### **3.3.4. Fourier-transform infrared spectroscopy (FTIR)**

FTIR analysis was carried out using Attenuated Total Reflectance Fourier Transform Infrared Spectroscopy (ATR-FTIR) (PerkinElmer, Massachusetts, USA) with wavelength between 400-4000  $\text{cm}^{-1}$  and 16 scans. The peak of the absorbance obtained helps in predicting the functional groups present in the sample. All the PEC samples were lipolyzed before taking spectra. Pure CHI, pure ALG, pure Fc flakes, pure CHI/ALG with stoichiometric proportion and high Fc-CHI/ALG with stoichiometric proportion was studied.

### **3.3.6. SEM/EDS imaging**

The hydrogel samples of pure CHI, pure ALG, pure CHI/ALG, and high Fc-CHI/ALG were imaged with a JEM-2100F scanning/transmission electron microscope (JEOL, Tokyo, Japan) using acceleration voltage of 12 keV and 15 kV beam current. SEM images can reveal the microstructure of hydrogels, including their pore size, distribution, and interconnectivity, which can be correlated with the swelling behavior and mechanical properties of the hydrogel. EDS can also identify the elemental composition of the hydrogel, which can provide insights into its chemical properties and potential interactions with biological systems. To prepare samples for SEM/EDS, the samples were mounted on aluminum stub with the help of carbon tape. Adequate height was raised, and the sample was inserted inside the chamber of SEM microscope.

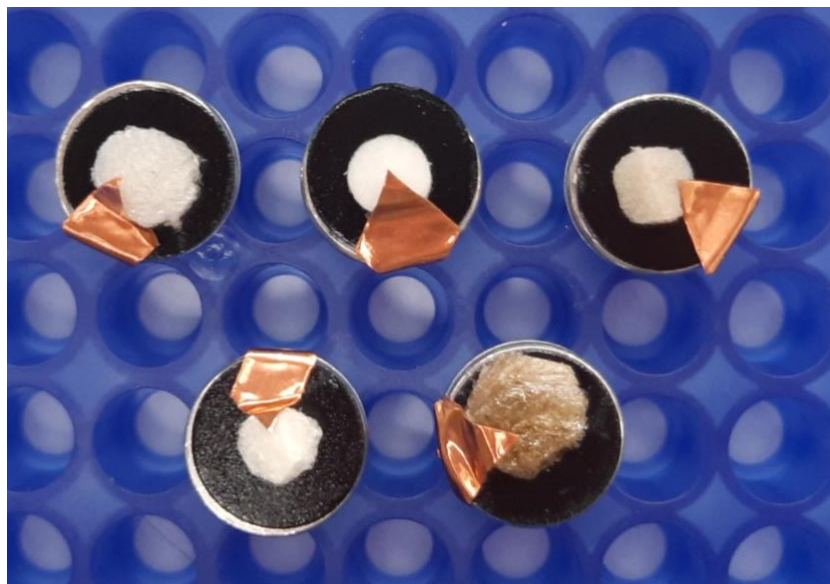


**Figure 3.2.** PEC hydrogels loaded on aluminum stumps, attached by the carbon tapes and conductivity is supplied through the copper tape.

### 3.3.6. Swelling behavior

A 5 mm<sup>3</sup> sponge of PEC was taken, weighed, and incubated in PBS to study the swelling behavior. Rate of swelling depend on the chemical and physical properties of the hydrogel, such as its crosslinking density, porosity, and charge density. Swelling can affect the drug release behavior by controlling the diffusion of the drug molecules through the hydrogel network.[85] The sponge of pure CHI, pure ALG and Fc-CHI dissolved in the PBS due to weak ionic bond. This ionic strength is increased by crosslinking CHI and ALG together. Swelling ratio test of the stoichiometric CHI/ALG, low Fc-CHI/ALG, medium Fc-CHI/ALG and high Fc-CHI/ALG was performed. After 24 hours of incubation, their weight was measured by drying in KimTECH tissue for 10 second. Swelling ratio was calculated as:

$$\text{Swelling ratio} = \frac{W_{\text{wet}} - W_{\text{initial}}}{W_{\text{initial}}} \times 100$$

$W_{\text{wet}}$  is the weight of the PEC after being soaked in PBS.  $W_{\text{initial}}$  is the weight of the PEC before soaking in PBS.[85]

### 3.3.7. Gel content

A 5 mm<sup>3</sup> PEC was taken, weighted, and incubated in PBS. After incubating for 24 hours, excess PBS was removed from the surface and lipolyzed in a fridge dryer at -50° C for another 24 hours.[86] Gel content was measured as:

$$\text{Gel Content} = \frac{W_{\text{dry}}}{W_{\text{initial}}} \times 100$$

Where,  $W_{\text{dry}}$  is the weight of the lipolyzed PEC.  $W_{\text{initial}}$  is the weight of the PEC before soaking in PBS.

### 3.4. Drug release kinetics

The release of different hydrophobic and hydrophilic drug gives the proper explanation for the overall release pattern from the specific material. The electrochemical properties and release kinetics of the PECs were evaluated using a fluorescent dye called FITC. FITC-Dextran and FITC- BSA were used as the model drugs.

The release platform was prepared with agarose LE, made by dissolving 2 weight % agarose LE in PBS solution. This mixture was boiled and kept at 60 °C for maintaining in liquid state. Once cooled to room temperature, it solidified within 2 minutes. Different PECs (pure CHI/ALG, low Fc-CHI/ALG, medium Fc-CHI/ALG and high Fc-CHI/ALG) were soaked in model drugs solution for 24 hours. FITC, FITC-Dextran and FITC-BSA solutions of 0.5 mg/ml, 1mg/ml and 1mg/ml concentration were selected to be the incubation solution, respectively. Before

releasing FITC into agarose structure excess solution and impurities from the surface of PEC was removed by washing the incubated PEC 2 times in the pure PBS solution for 1 minute each time.

**Table 3.1.** Concentration of the drug uptake by different PEC.

<b>FITC (0.5 mg/ml)</b>		<b>FITC-Dextran (1 mg/ml)</b>		<b>FITC-BSA (1 mg/ml)</b>	
Pure CHI/ALG	0.02	Pure CHI/ALG	0.052	Pure CHI/ALG	0.248
Low Fc-CHI/ALG	0.15	Low Fc-CHI/ALG	0.103	Low Fc-CHI/ALG	0.318
Medium Fc-CHI/ALG	0.22	Medium Fc-CHI/ALG	0.117	Medium Fc-CHI/ALG	0.401
High Fc-CHI/ALG	0.28	High Fc-CHI/ALG	0.158	High Fc-CHI/ALG	0.421

The concentration of FITC absorbed by the hydrogel was calculated by creating a calibration curve using solutions with varying concentrations of FITC. The absorbance intensity was measured at 495 nm. [87] The concentrations of the incubation and wash solutions was determined using the calibration curve. Finally, the exact concentration in the PEC was found by subtracting the concentrations of the incubation and wash solutions from the original solutions. This method was similar to the one used in a study by the team of Yu Wang in 2022. [88] The concentration of the FITC absorbed by pure CHI/ALG, low Fc-CHI/ALG, medium Fc-CHI/ALG and high Fc-CHI/ALG was 0.02, 0.15, 0.22 and 0.28, respectively. The concentration of FITC-Dextran up taken by pure CHI/ALG, low Fc-CHI/ALG, medium Fc-CHI/ALG and high Fc-CHI/ALG was 0.052, 0.103, 0.117 and 0.158 respectively. Similarly, the concentration of FITC-BSA loaded into pure CHI/ALG, low Fc-CHI/ALG, medium Fc-CHI/ALG and high Fc-CHI/ALG was found to be 0.248, 0.318, 0.410 and 0.421, respectively. The release of FITC from the PECs to the agarose structure was then observed using a fluorescent microscope and measured in terms of the intensity of the agarose material contacted to PECs. [89] The kinetics of release was measured with two approaches i.e., static voltage application and cyclic voltage application.

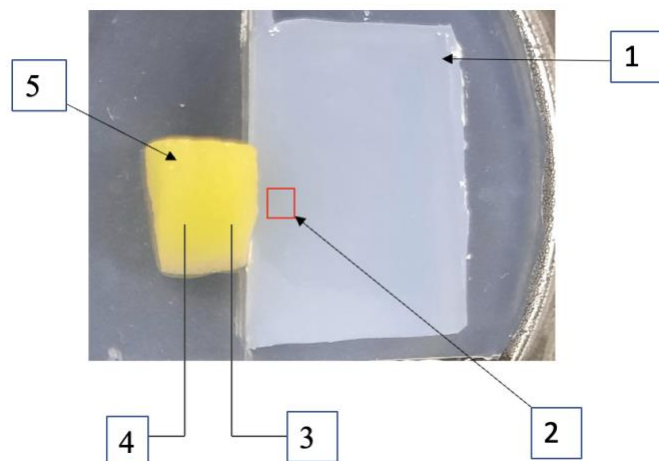


**Figure 3.3.** Hydrogel loaded with FITC placed next to the agarose structure to observe the passage of drug from hydrogel to agarose gel. (1) agarose gel, (2) area under microscope, (3) anode/cathode, (4) anode/cathode, and (5) drug loaded PEC.

### 3.4.1. Electrical stimulus: Continuous mode

When it comes to a type of electrochemical cells, there are two types: galvanic and electrolytic. Galvanic cells derive its current flow from redox reactions taking place on the electrodes, while electrolytic cells need an external electrical source like a DC power supply. In order to apply the electrical stimulus onto the E-PEC hydrogel, the anode was taken to be positive while the cathode was negative.[90] The drug was loaded into a PEC, which was prepared by soaking it in a 0.5 wt.% drug solution for 24 hours. PECs with varying concentrations of Fc were loaded with the drugs and washed twice with PBS. The drug-loaded PEC was then placed next to the agarose gel, and the passage of the drug was observed under a fluorescence microscope with specific settings. The particular configuration consists of the

choice of 20x magnification lens, 15 seconds of exposure of 50% intensity FITC light, and 10 second interval between each data point. A constant electric stimulus was applied at different voltages and currents to release the drug. The time taken for the release of FITC, FITC-Dextran, and FITC-BSA were 5, 10, and 15 minutes, respectively. The initial intensity of each datapoint was recorded to create an intensity profile plot.

#### **3.4.2. Electrical stimulus: Switching mode (On/Off)**

This experiment is performed to study the release of FITC-D, and FITC-BSA from PECs from PEC hydrogels in response of electric field. The PECs are incubated in solutions containing different concentrations of the drugs (1 mg/ml FITC-D, and 1 mg/ml FITC-BSA). The PECs are then placed next to a 2 wt.% agarose structure and the diffusion of the drugs from the PECs is observed through the intensity change. [91] Intensity was recorded using a ZEISS AxioVert A1 microscope with 20x lens, at interval of 10s. The electric stimulus is turned on and off at every 30s. A curve is generated from the recorded intensity values over time, and the average rate of release is calculated from the slope of the individual points on the curve. The obtained intensity profile helps to predict the responsiveness of the respective PEC with the electric field.

#### **3.5. *In-vitro* drug release**

This experiment was performed to study the interactions between the hydrogel and other substances, such as drugs.[92] Once the hydrogel with maximum electric responsivity is declared, this *in-vitro* experiment is carried out to see the effectiveness of the PEC in releasing the drug to the biological environment.



The release was carried out on *S. aureus* biofilm and *P. aeruginosa* biofilm. Biofilm was prepared with liquid bacterial culture of 0.05 OD. 100µl of liquid bacterial culture was dropped over the acetate filter membrane, kept over LB agar and incubated at 37°C for 48 hours. The growth of biofilm is seen over the period of 48 hours, (**Figure 3.4**).

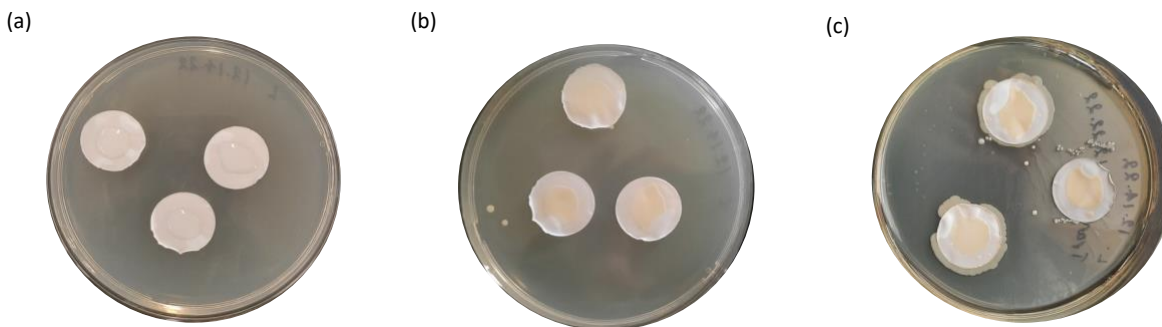


**Figure 3.4.** Biofilm growth after dropping liquid culture over the membrane (a) 0 min (b) after 24 hours incubation (c) 48 hours incubation.

Antibiotics were applied to the biofilm for different durations: 0 minutes, 30 minutes, 1 hour, 3 hours, and 6 hours, encapsulating 200 µg/ml, which was the minimum concentration required to eradicate the *S. aureus*. [93] To synthesize the CIP-loaded electrochemically active polyelectrolyte hydrogel (CIP-E-PEC), Fc-CHI/ALG was incubated in a 1000 µg/ml CIP solution for 24 hours and 195 µg/ml CIP was loaded into the hydrogel. This method was followed in the reference of task performed by Demiana where drug release rate was studied with incorporation of different amount of CIP. [94] The CIP/E-PEC was then placed over the biofilm for a fixed duration and removed. The biofilm was diluted with M-9 salts by adding it to a 15 ml Falcon tube containing 10 ml of 1x M-9 salts. The biofilm was dislodged from the filter with a glass rod using aseptic technique and vortexed for homogenization. This bacterial solution was diluted to  $10^{-7}$  dilutions with 1x M-9 salt. A 100 µl bacterial solution was then plated on an LB agar plate, and

the CFUs were counted after 24 hours of incubation. To compare the effectiveness of hydrogel, antibiotics, and electrical field in inhibiting bacterial growth, the activity of the bacteria was observed using E-PEC with PBS, E-PEC with electric field only (E-PEC+ Stimulus), E-PEC with CIP (CIP/E-PEC), and CIP loaded E-PEC with electrical stimulus (CIP/E-PEC + Stimulus). Sayeed Hasan and his team also used a similar approach to inhibit *S. aureus* by applying Chitosan hydrogel. [92] Here, the electric stimulus at 2V was supplied through the electric device. The hydrogel was encapsulated inside the device and was placed on top of the biofilm formed on the LB agar plate (**Figure 3.5**).

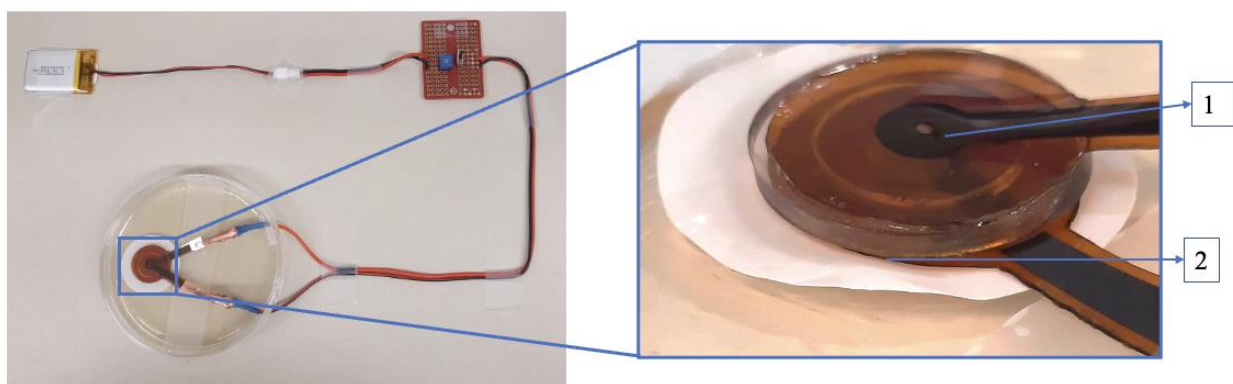


**Figure 3.5.** Experimental setup for *in-vitro* drug release. (1) PEC loaded with CIP- encapsulated inside the electric device, (2) biofilm.

### 3.6. Statistics

The characterization method involved ninhydrin test, turbidity test, viscosity measurement, FTIR measurement, SEM/EDS analysis, gel content and swelling ratio test. Ninhydrin test, turbidity test, viscosity measurement, gel content and swelling ratio tests were performed three times. The collected data was then used to determine the average and standard deviation using

Microsoft Excel. The drug release kinetics were analyzed using the same process, taking the average of ten data points, and calculating the standard deviation. The *in-vitro* drug release experiment was conducted three times and the average and standard deviation were calculated from the combined data using the same method.

## 4. Results and discussion

The properties of the hydrogel to be used for the wound healing mainly should have the certain polarity to help in migration of the drugs, proper porosity, structural integrity, high water retention and responsivity towards the external stimulus [17]. Here, CHI/ALG PEC is formed by the attraction between positively charged free amines ( $-\text{NH}_2$ ) of CHI and negatively charged free carboxylic group ( $-\text{COOH}$ ) of ALG (**Figure 4.1(a)**). This attraction results in the formation of a stoichiometric ionic bond between CHI and ALG. [95, 96] When Fc is added, a covalent bond is formed between Fc and CHI to produce Fc-CHI. Once the covalent bond is formed, the ionic bond is formed with the free carboxylic groups of ALG and Fc-CHI (**Figure 4.1(b)**).

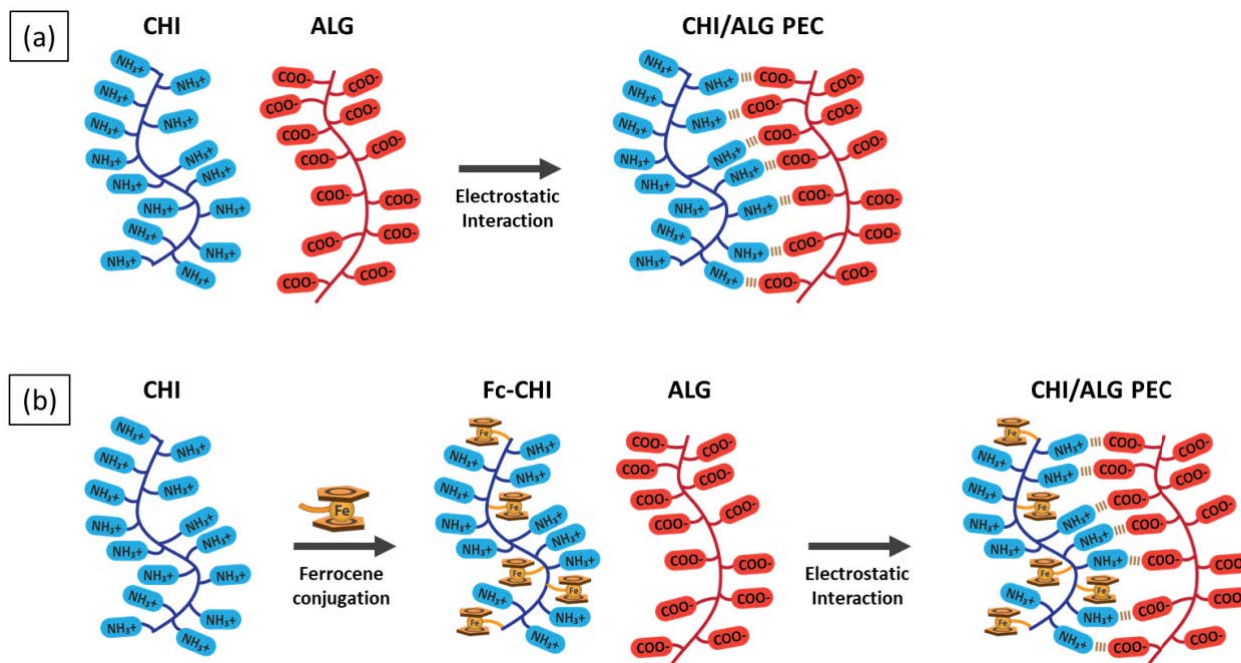


**Figure 4.1.** Schematic formation of PEC hydrogels with ionic interaction. (a) CHI/ALG (b) Fc-CHI/ALG.

#### 4.1. Characteristics of PEC hydrogels

Several characteristics of the manufactured PEC has been studied. Ninhydrin test, turbidity test, viscosity test, FTIR, swelling ratio, gel content study, SEM/EDS imaging was performed to evaluate the different properties the hydrogel.

##### 4.1.1. Degree of conjugation of Fc in CHI

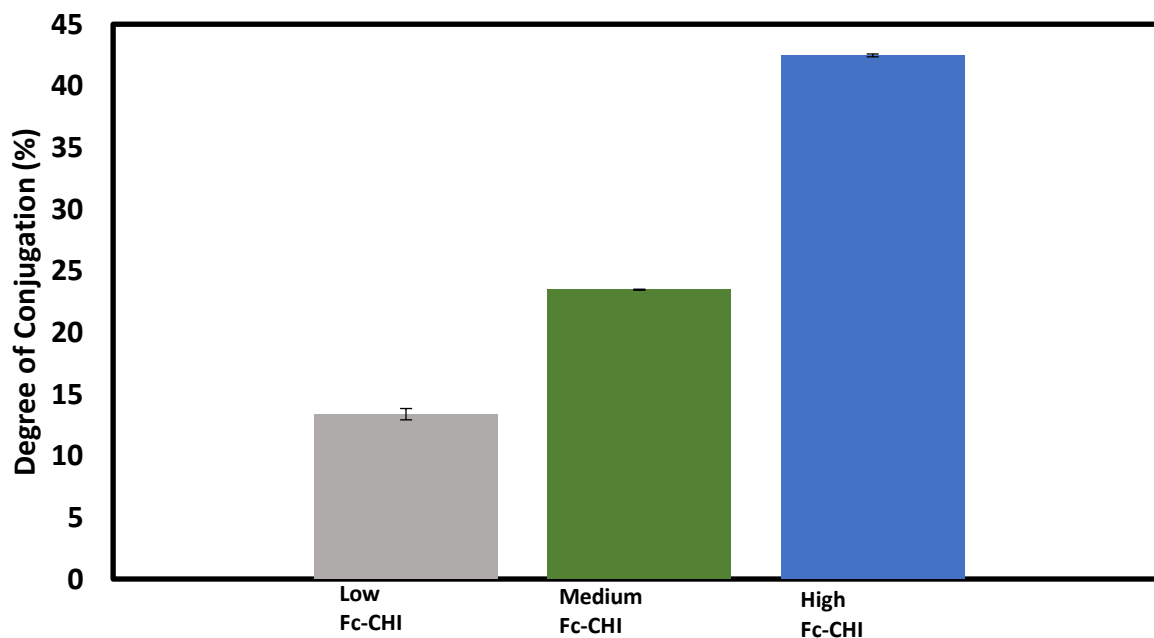


**Figure 4.2.** Degree of Conjugation of different Fc-CHI at 1.5 weight% concentration. (n=5)

Ninhydrin assay was used to determine the degree of conjugation. The degree of conjugation of low Fc-CHI, medium Fc-CHI and high Fc-CHI was studied with the reference of pure CHI. The degree of conjugation increases with increase in concentration of Fc in Fc-CHI (**Figure 4.2**). The degree of conjugation in low Fc-CHI is 13.37 %, medium Fc-CHI is 23.47 % and for high Fc-CHI is 42.47 %, respectively. This signifies that there is less amount of amino group in the high Fc-CHI. [83] As the degree of polymer conjugation increases, the density of the

polymer network also increases. Consequently, as the available free space for drug diffusion decreases, the rate of drug release also decreases.[95, 97, 98] The properties of a (CHI/ALG) material depend on the degree of conjugation between the CHI and ALG. When Fc is added to the CHI, there is an increased degree of conjugation between the Fc-CHI. This results in fewer amino groups available to react with the ALG, leading to a lower overall degree of conjugation in the resulting Fc-CHI/ALG material compared to the pure CHI/ALG material. As a result, the Fc-CHI/ALG material has a higher swelling ratio and higher drug release compared to the pure CHI/ALG material.

#### **4.1.2. Stoichiometric ratio**

The stoichiometric ratio of polycations and polyanions in a PEC solution is determined by measuring the turbidity of the solution. The turbidity of the solution is expected to increase up to a certain point and then decrease, with the peak point indicating the stoichiometric ratio of the polymers. [96] The increase in turbidity is thought to be due to the phase separation of oppositely charged polyelectrolytes into colloidal particles. [99] The turbidity is also expected to be directly proportional to the polymer concentration, with higher concentrations resulting in higher turbidity. [100] The turbidity curves obtained were different for different PEC concentration (**Figure 4.3**).

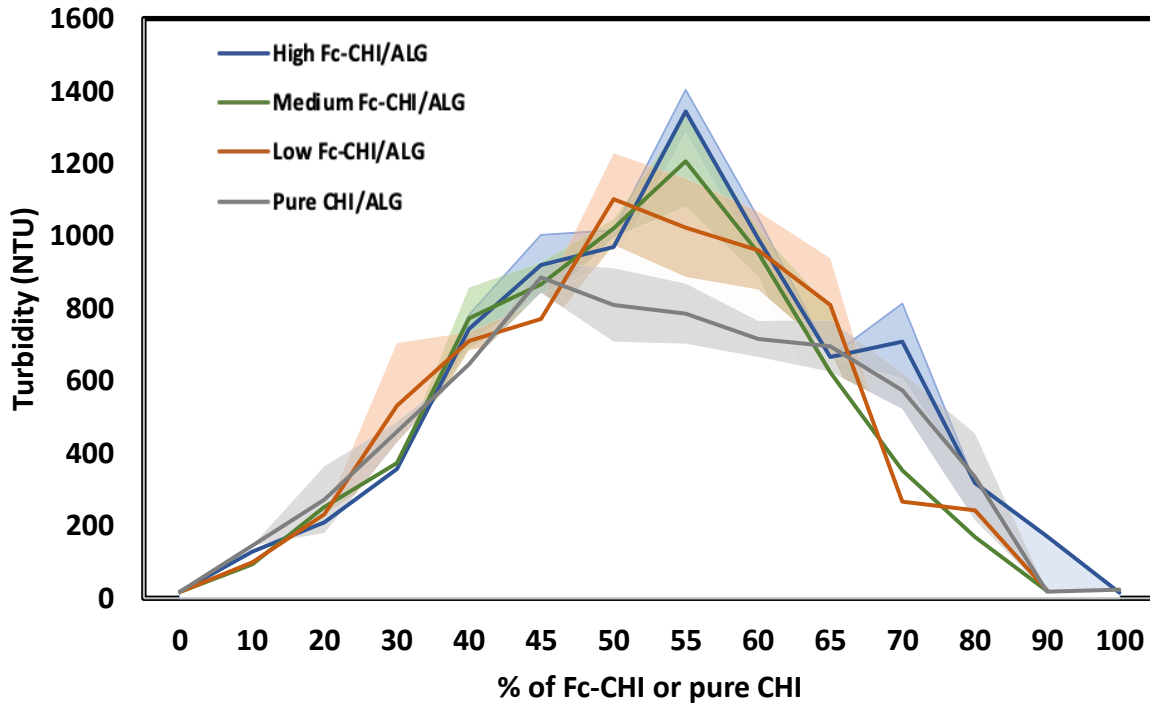


**Figure 4.3.** Turbidity value of different PEC with their respective stoichiometric point, with standard deviation (n=3).

The stoichiometric point was different for pure CHI/ALG, low Fc-CHI/ALG, medium Fc-CHI/ALG and high Fc-CHI/ALG. Turbidity value of 886, 1102, 1206, and 1344 was obtained in 40% CHI in pure CHI/ALG PEC, 50% Fc-CHI in low Fc-CHI/ALG, 55% Fc-CHI in medium Fc-CHI/ALG and 55% Fc-CHI in high Fc-CHI/ALG. This can be inferred a higher charge density of the polyanions in a PEC solution shifts the theoretical point of neutralization, or the point at which the positive and negative charges in the solution are balanced, towards a higher ratio of polycations. This means that a larger amount of polycations would be required to neutralize the anionic charge, as the charge density of the anions is higher. [96] The turbidity of a PEC solution decreases after reaching the stoichiometric point, or the point at which the positive and negative charges in the solution are balanced, because excess positive charge can cause destabilization of

the PEC and reduce its light scattering affinity.[95] Overall, the stoichiometric ratio of the PEC forms a ionically stable hydrogel, thus the hydrogel doesn't dissolve in the solvent. Also, ionically stable hydrogel helps in controlling the release by preventing the electro-osmotic release and enhancing the electrochemical drug release. [96]

#### **4.1.3. Mechanical property**

The highest viscosity of a cellulose chain-based hydrogel is achieved at a specific concentration ratio where the strongest intermolecular interactions occur among the cellulose chains, and that this high viscosity leads to a high compressive strength in the hydrogel. [101] Viscosity of combined CHI/ALG rises to 10-fold higher than that of the pure CHI or ALG when mixed in the ratio of 1:1. [102] The viscosity measurement of the stoichiometric proportion of each PEC was performed and concluded that the addition of the Fc in the solution reduces the viscosity. The viscosity decreases due to disruption of the dynamic crosslinking in the hydrogel network. [103] The highest viscosity of 2021.19 cP was obtained for CHI/ALG hydrogel solution, then it successively reduces in each sample according to the amount of Fc content i.e., 1472.53, 1286.27 and 1171.2 for low, medium, and high Fc-Chi/ALG, respectively(**Figure 4.4**). The compressive strength of the polymer is affected by the addition of crosslinker.[98] It can be inferred that the compressive strength of pure CHI/ALG PEC is highest and the strength of high Fc-Chi/ALG is lowest. The highest compressive CHI/ALG PEC signifies that this PEC is less affected by the external stimulus. Thus, the degradation of the hydrogel is very difficult. [103] This stiffness can be the reason for retardation in drug delivery. For this reason, the high Fc conjugated hydrogel is effective in the application of drug release.



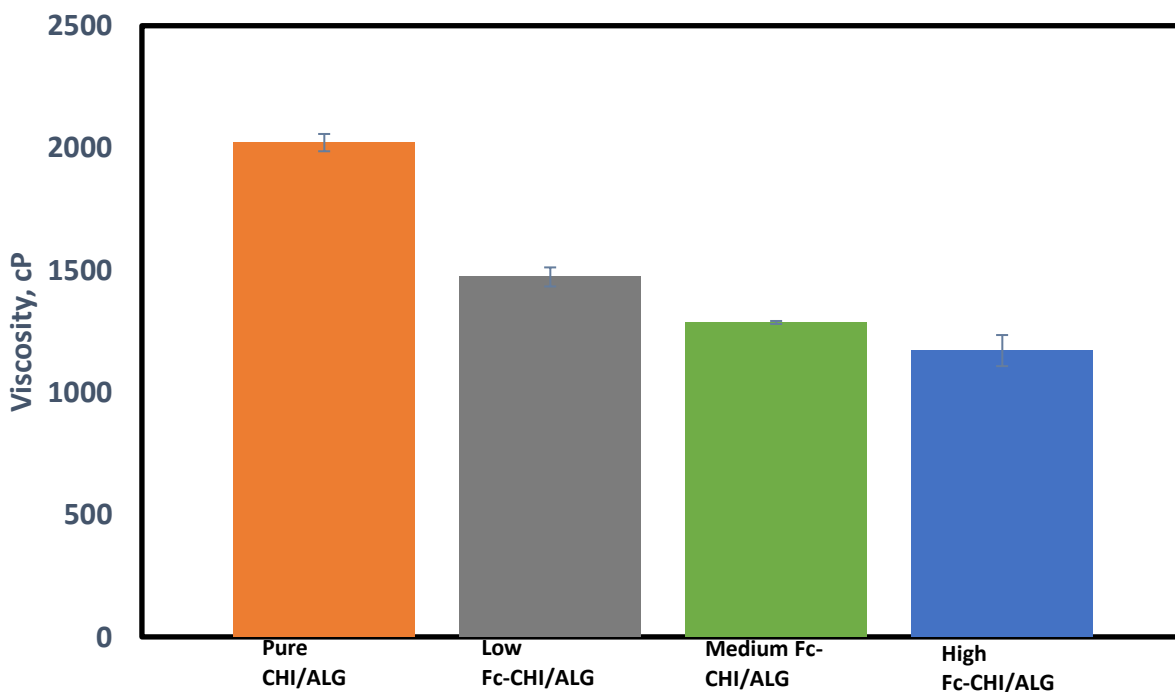


**Figure 4.4.** Viscosity of different PEC samples (n=3).

#### 4.1.4. FTIR

A FTIR spectrum of a sample is used to identify the types of bonds present in the sample and the functional groups that contain those bonds. [104] The characteristic peak of CHI is between 1649 and 1652  $\text{cm}^{-1}$ . [104] Similarly, the peaks for alginate were around 3250  $\text{cm}^{-1}$ , 1580  $\text{cm}^{-1}$ , and 1398  $\text{cm}^{-1}$ [104]. The peak of CHI is obtained at 1638 and 1541  $\text{cm}^{-1}$ . Similarly, the peak of ALG is obtained at 1591 and 1417  $\text{cm}^{-1}$ (**Figure 4.5**). The peak of CHI/ALG PEC is seen at 1587 and 1414  $\text{cm}^{-1}$ . Dai M. et. al. has obtained the spectra of the CHI/ALG sponge at 1567 and 1422  $\text{cm}^{-1}$ . [85]

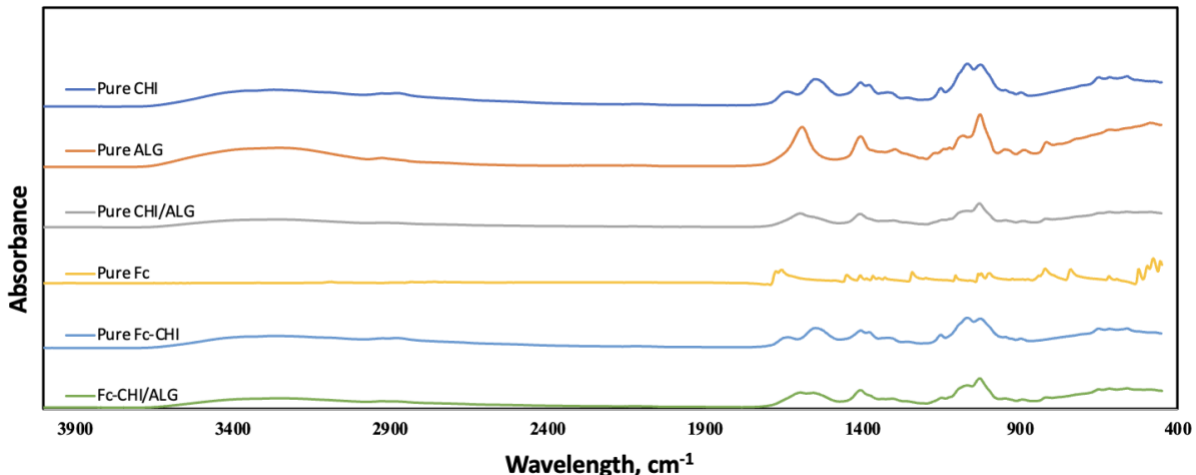


**Figure 4.5.** FTIR of different PEC.

The presence of the Fc in the hydrogel is proved through the FTIR spectra. The functional group of the Fc, organometallic ring around  $1500\text{ cm}^{-1}$ . The peak around  $540\text{ cm}^{-1}$  denotes the Fe-C bond and the peak of Fc-CHI is around  $1654\text{ cm}^{-1}$ ,  $1596\text{ cm}^{-1}$ , and  $814\text{ cm}^{-1}$ . [81] The peak observed in this experiment is  $1655$ ,  $1535$ , and  $832\text{ cm}^{-1}$ . The presence of peaks at  $1592$ ,  $1420$ , and  $826\text{ cm}^{-1}$  is proof of the formation of PEC between Fc, CHI, and ALG. The absorbance peak of CHI around  $1638\text{ cm}^{-1}$  decreases in Fc-CHI as seen in  $1655\text{ cm}^{-1}$  because of a reduction in primary amine N-H bending. [104] The reduction of peak absorbance in Fc-CHI/ALG than in CHI/ALG is due to the reduction of the degree of ionic interaction between the negatively charged carboxylic ion group of ALG and the positively charged amino group of CHI due to the introduction of Fc. [105] The reduction in the degree of ionic interaction helps in showing the faster response to the electric response, thus the release is responsive and faster with the Fc-CHI/ALG PEC.

#### 4.1.5. Morphology and elemental analysis

Scanning electron microscopy (SEM) is a widely used technique for imaging the surface morphology and structure of materials at high resolution. [106] The information obtained from SEM is also used to understand the physical properties of the material. Stability of a PEC under different environmental factor such as PBS can be determined with SEM as SEM could be used to visualize the network structure of the sponge. [85] The SEM images of the PECs at 100x magnification is taken (**Figure 4.6**). When the Fc is added, the structure looks much rougher and flakier. The reduction in crosslinking could leads to a more open, flexible structure for the polymer, which affects its physical properties such as pore size and drug release rate, for this reason the drug release is much faster from Fc-CHI/ALG. [34] Fc-CHI/ALG has larger pore size which enables it to hold a greater quantity of drugs. The network's uneven geometry traps the drugs within its pores and this structure prevents the occurrence of burst release.

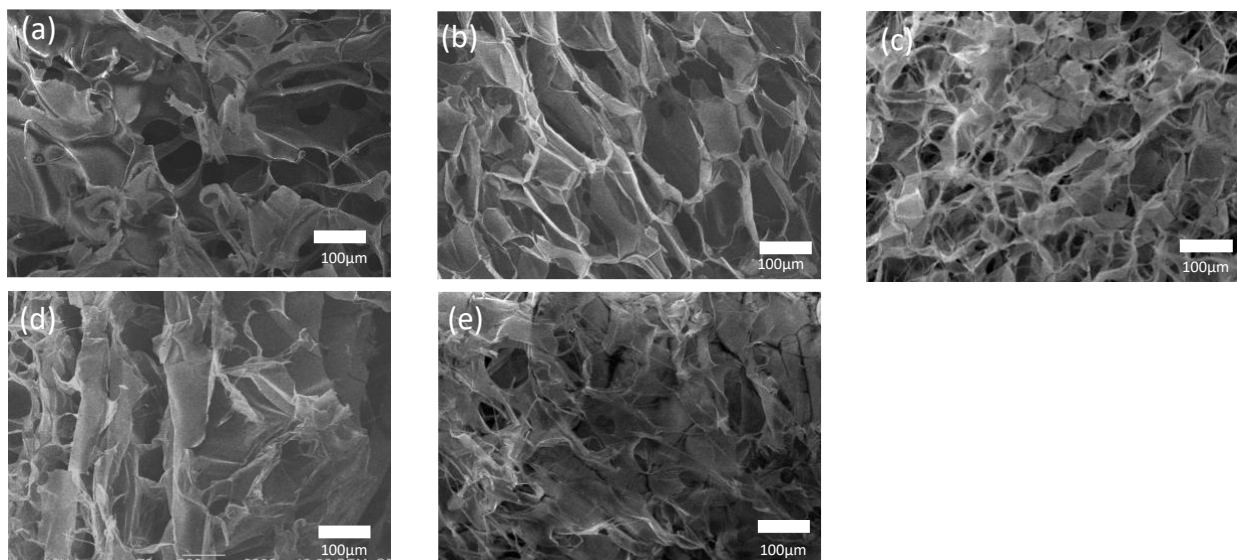


**Figure 4.6.** SEM images (a) Pure ALG, (b) Pure CHI, (c) Pure CHI/ALG, (d) Pure Fc-CHI and (e) Fc-CHI/ALG.

Energy dispersive spectroscopy (EDS) is a technique that has application in identifying the elemental composition of a material. EDS works by bombarding the surface of the sample with a beam of high-energy electrons and measuring the energy of the x-rays that are emitted from the surface as a result of the electron interactions with the atoms in the sample. [34] Elemental composition of Fc-CHI is analyzed with EDS. The EDS of pure CHI (**Figure 4.7(a)**) and Fc-CHI (**Figure 4.7(b)**) show the different result. CHI is a biopolymer that is derived from chitin, a natural polymer found in the shells of crustaceans such as shrimp, crabs, and lobsters. CHI is typically obtained by deacetylating chitin, which removes the acetyl groups from the polymer chain. CHI itself does not contain silicon or chlorine; it is possible that impurities from the source material (like, shrimp shells) could be present in the final product. [107] A small hump of Fe at 0.7 keV is seen in Fc-CHI spectra which conforms the presence of iron in Fc-CHI. [108] This small hump of Fe conforms that the Fc-CHI has the presence of Fc in the PEC. As the Fc contains functional group that enhance the solubility or permeability of the drug molecules, leading to more efficient drug release, and the property to inhibit the bacterial growth.

**Table 4.1.** Weight % of different element in pure CHI and Fc-CHI.

<b>Pure CHI</b>		<b>Fc-CHI</b>	
<b>Element</b>	<b>Weight %</b>	<b>Element</b>	<b>Weight %</b>
Carbon	52.64	Carbon	51.15
Nitrogen	12.37	Nitrogen	15.08
Oxygen	34.99	Oxygen	33.69
Iron	0.00	Iron	0.08

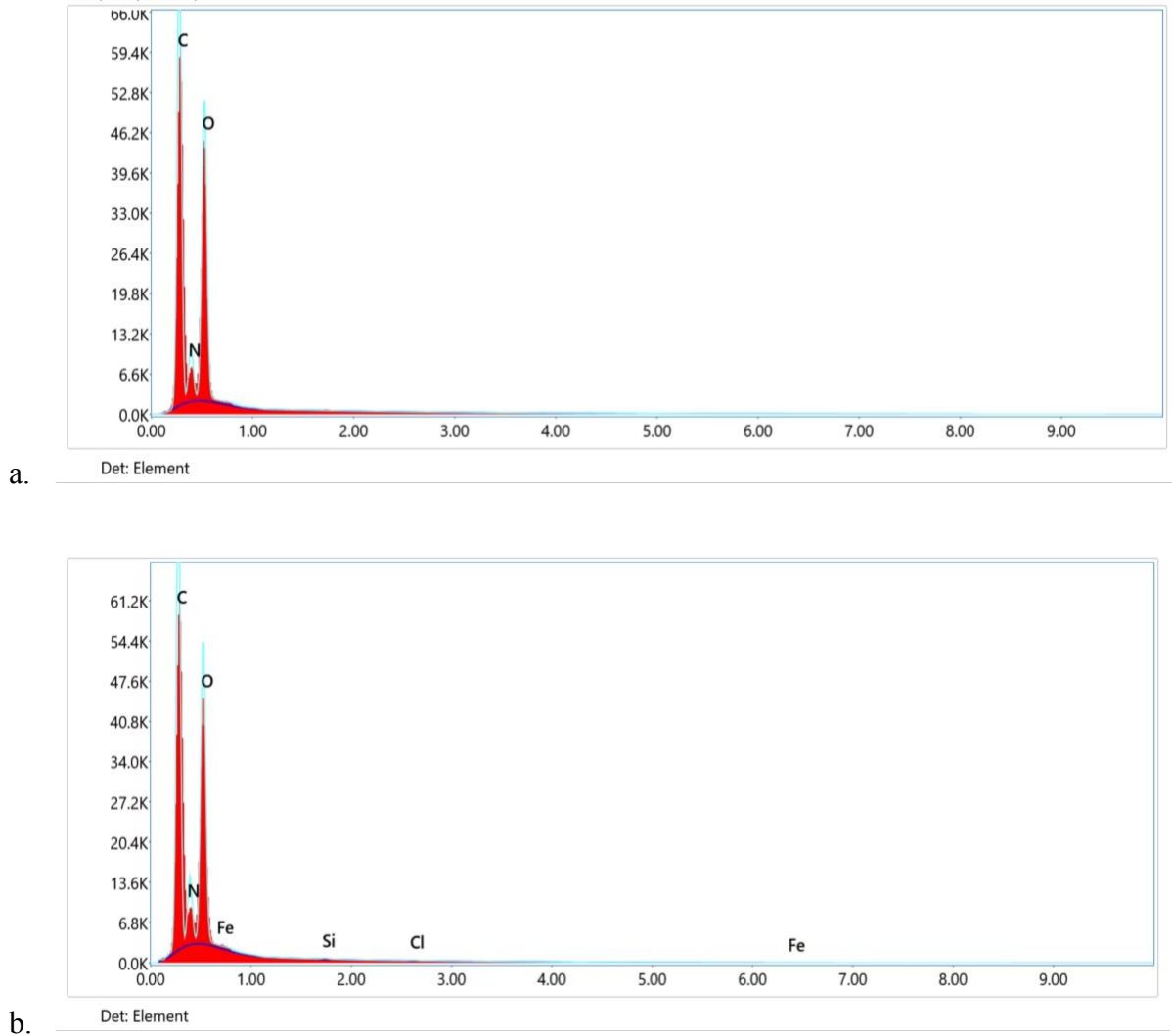


**Figure 4.7.** EDS spectra of (a) pure CHI, (b) Fc-CHI.

#### 4.1.6. Swelling ratio

The swelling ratio of a PEC can be used to determine the drug release profile of the PEC. [95, 109] The ionized amino groups in the PEC can contribute to the relaxation of the matrix and increase the uptake of the medium by repulsing each other. [109]

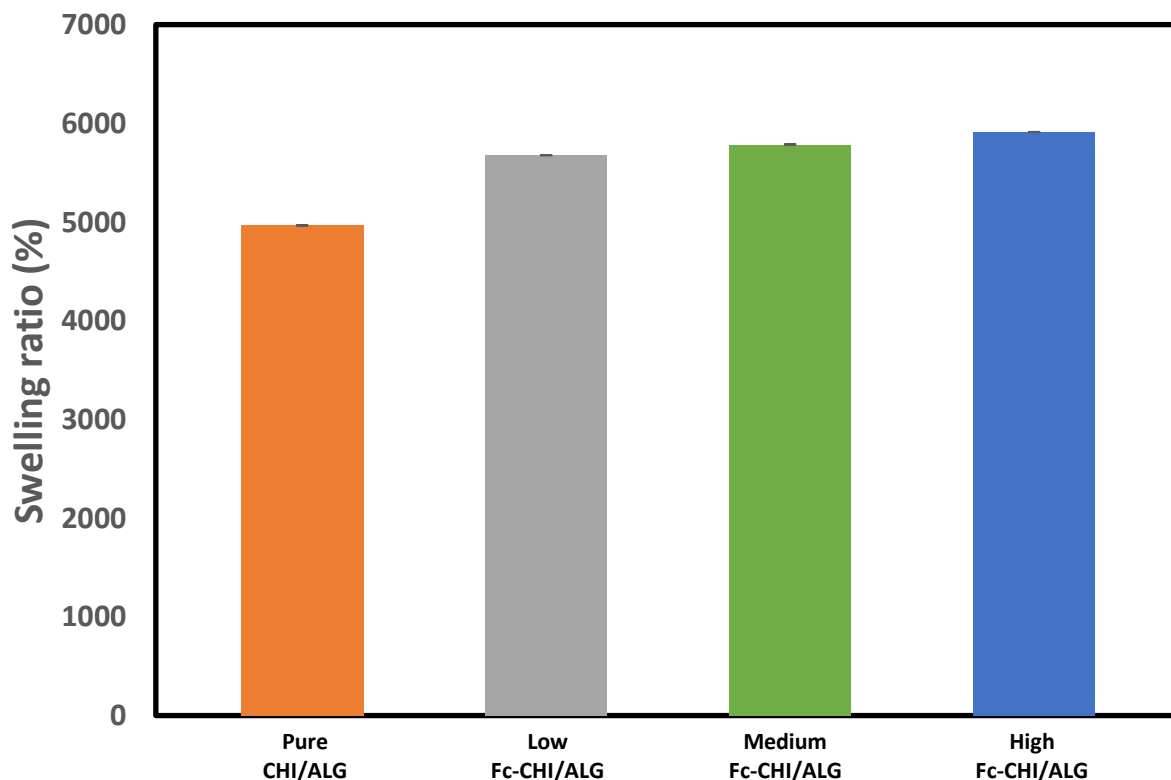


**Figure 4.8.** Swelling ratio of different PEC with standard deviation (n=3).

The swelling ratio of for CHI/ALG PEC, low Fc-CHI/ALG PEC, medium Fc-CHI/ALG PEC, and high Fc-CHI/ALG PEC were 4965.47%, 5676.88%, 5785.38%, and 5912.66%, respectively (**Figure 4.8**). When carboxylic group (-COOH) is ionized to (-COO<sup>-</sup>), it increased the internal electrostatic repulsion among the polymer chains which consequently swells the polymeric network. [110] The electrostatic repulsion force decreases as the -COO<sup>-</sup> combines with H<sup>+</sup> ions to the form (-COOH-), reducing the electrostatic repulsion force and thus receiving in a shrunken configuration at low pH. [95, 111] The addition of more positively charged cation causes the PEC to be non-stoichiometric, thus there is excessive swelling. [85, 111] The degree of crosslinking can affect the rate uptake of medium for the hydrogel, as the degree of crosslinking is higher the swelling is higher. As the uptake of the drug is enhanced with the high Fc-CHI/ALG PEC, there

is effective release of the drug from this PEC to the bacterial environment and can promote the healing of the wound.

#### **4.1.7. Gel content**

Gel content experiment gives the information for the stability of PEC. [112] The gel contents for pure CHI/ALG, low, medium, and high Fc-CHI/ALG, are 93.82%, 93.99%, 94.01%, and 94.48%, respectively(**Figure 4.9**). [86] The gel content of a polymer is related to the amount of free volume or pores present in the material. Polymers with a more dense, rigid structure will tend to have less free volume and therefore a lower gel content. This is because the gel content is a measure of the amount of polymer that is able to move and flow within the material, and a more densely packed structure will have less space for the polymer chains to move around. Conversely, polymers with a more open, flexible structure will tend to have more free volume and a higher gel content. [113] As the overall degree of conjugation of the high Fc-CHI/ALG is lower, the overall gel content percentage of the high Fc-CHI/ALG is higher. This property is also useful because the lower gel content signifies that there is more space for the polymer chains to move, which helps is migration of the drug inside the PEC. An enhanced release can be achieved with the external stimulus.

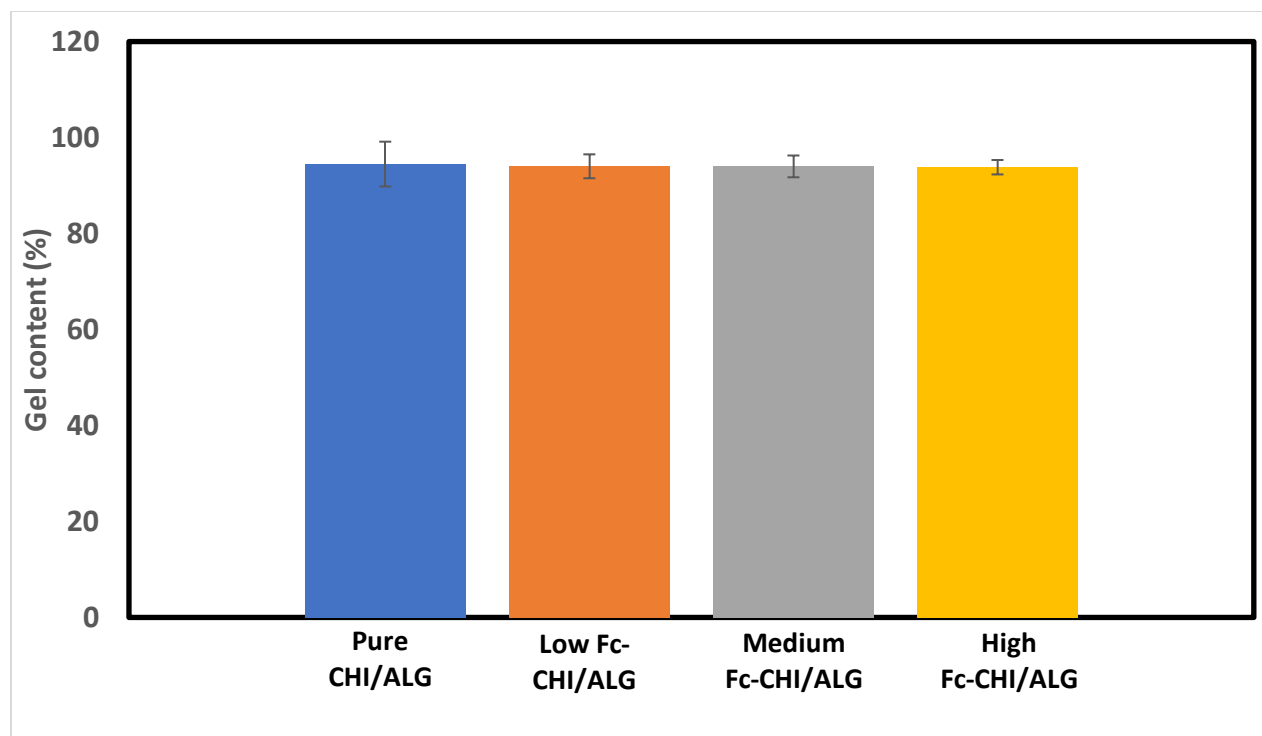


**Figure 4.9.** Gel Content of different PEC (n=3).

#### 4.2. Drug release on the phantom skin (agarose)

The movement of drugs within hydrogels is mainly influenced by diffusion and electrostatic interaction. As the hydrogel containing the drug is exposed to the surrounding environment, the drug can diffuse out of the hydrogel through its pores. [114] Additionally, electrostatic interactions between the hydrogel matrix and the drug can affect its migration. CHI and ALG are polyelectrolytes that contain charged groups, allowing them to interact with oppositely charged molecules such as FITC. FITC is an anionic molecule that can interact with the positively charged CHI component of the hydrogel, slowing down its release and affecting its migration within the hydrogel. [115]

In the case of Fc-CHI/ALG PEC hydrogel, the Fc component serves as a redox-active unit that interacts with an applied electric field, generating a concentration gradient within the hydrogel.



This gradient can affect the migration of FITC and other charged species within the hydrogel. [115] When an electric field is applied, the Fc-component undergoes an electrochemical oxidation on the anode side, producing protonated ferrocene ( $\text{Fc}^+$ ). The protonated ferrocene moieties provide the hydrophilic molecular environment, which increases a wettability on the anode side. The water molecules along with drug migrate towards the anode. Since the CHI component of the hydrogel is conjugated to Fc, it also undergoes an electrochemical reaction, generating a concentration gradient that can affect the migration of FITC and other charged species within the hydrogel. [116] Overall, the Fc component plays a crucial role in generating a concentration gradient within the hydrogel that can affect the migration of FITC and other charged species, which is important for the controlled release of drugs from hydrogels. The schematic representation of the release of drug from the hydrogel is shown in (Figure 4.10).

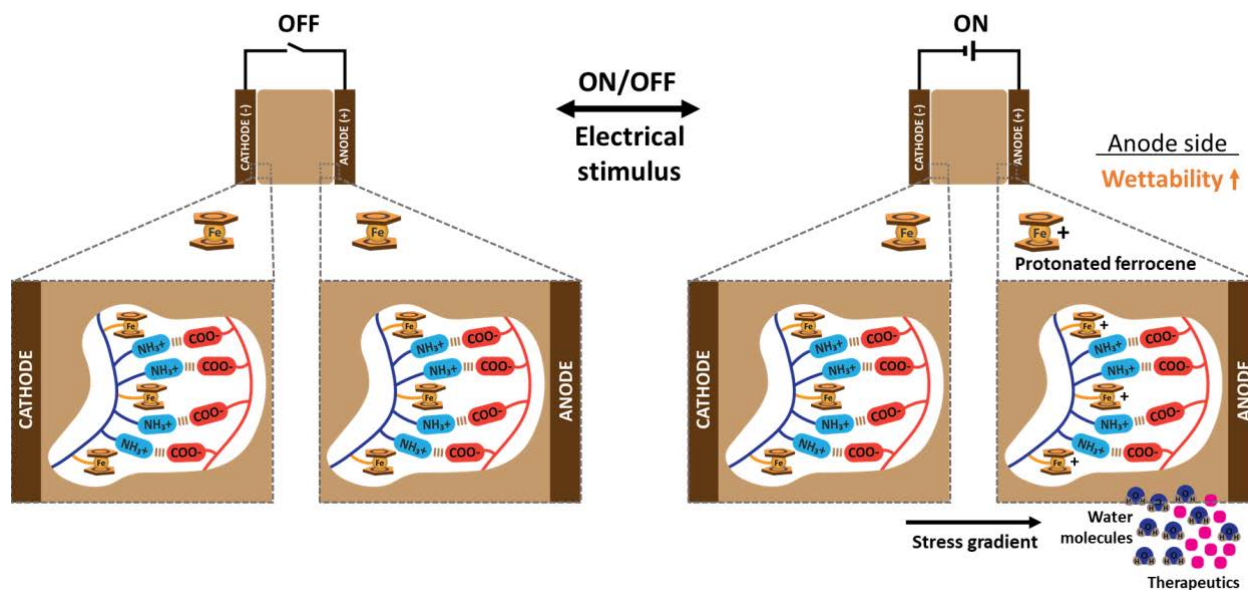


**Figure 4.10.** Schematic representation of the release of the drug from PEC.

#### 4.2.1. Drug release: Passive vs. active

The concentration of drug uptake in a hydrogel is related to the intensity of light collected from the hydrogel through a process called fluorescence. Fluorescence occurs when light is absorbed by the hydrogel and causes the release of energy in the form of light. [117] The intensity of the light emitted from the agarose gel is directly proportional to the concentration of the drug in the agarose gel. Thus, by measuring the intensity of the light emitted from the agarose, it is possible to determine the concentration of the drug within the agarose. [89, 118, 119]

The concentration of FITC absorbed by the hydrogel was found to be 0.02, 0.15, 0.22, and 0.28 mg/ml for pure CHI/ALG, low Fc-CHI/ALG, medium Fc-CHI/ALG, and high Fc-CHI/ALG, respectively. The increasing trend of the drug uptake is directly proportional to the swelling ratio because drug uptake and release is affected by the structural changes due to the degree of crosslinking. [120] The increase in ionic strength causes the decrease in swelling ratio. As the ionic strength of the Fc content hydrogel is lower than that of the pure CHI/ALG. [120] The swelling ratio became lower thus there was more possible area of the ionic drug uptake.

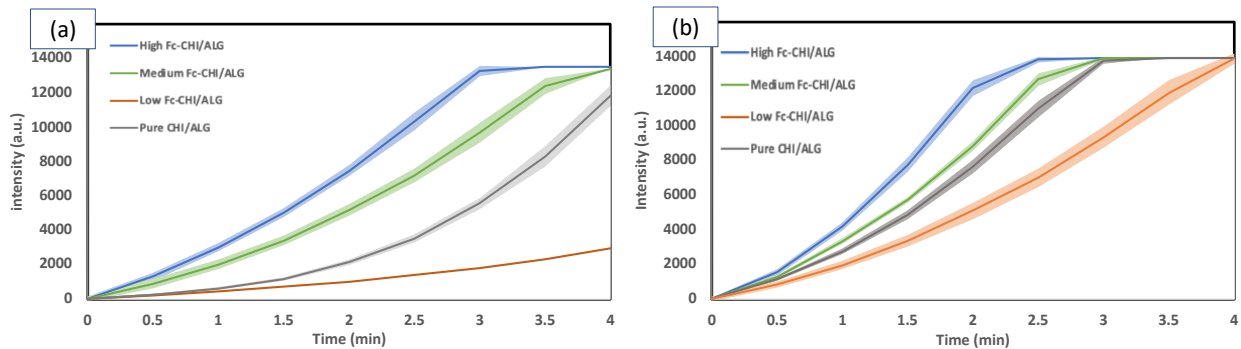


**Figure 4.11.** FITC release from different PEC with (a) 0V electric supply, (b) 2V electric supply.

In the intensity profile, the slope of the intensity is increasing successively with the increase amount of Fc in the PEC (**Figure. 4.11**). The intensity raises with passage of FITC form pure

CHI/ALG, low Fc-CHI/ALG, medium Fc-CHI/ALG and high Fc-CHI/ALG PECs without voltage supply was 2962.2, 11829.6, 13424.6, and 13424.6 a.u., respectively.

The release of FITC is very less from pure CHI/ALG compared to that of the Fc-CHI/ALG. When the hydrogel is made from stoichiometric ratio of chitosan (CHI) and alginate (ALG) only, the FITC would not migrate towards either the anode or cathode because chitosan and alginate do not have any electroactive groups that can interact with the FITC and drive its migration through electrostatic attraction. Therefore, the FITC would be relatively immobile within the hydrogel, unless it is driven by other physical means such as diffusion or convection. [114]

Addition of Fc in the hydrogel accelerated the change of intensity profile of FITC release. FITC migrate towards the anode (positive electrode) when it is conjugated to a hydrogel containing ferrocene. This is because FITC is a negatively charged molecule and it is being drawn towards the positively charged electrode by electrostatic attraction. The ferrocene in the hydrogel is also contributing to the migration of FITC by electrostatic attraction. [115]

Along with the application of voltage the release of FITC is highly increased. The release reached its saturation at 4 min from all hydrogels. The saturation is predicted with the plateau at 14000 a.u., which indicates that the intensity has reached the maximum limit for given material. The time to reach saturation from low Fc-CHI/ALG, medium Fc-CHI/ALG and high Fc-CHI/ALG is 2.5 min, and from the pure CHI/ALG is 4 min. The release trend with increasing amount of Fc is similar. It is observed that the intensity increases sharply while FITC is being released from pure CHI/ALG as compared to that of the passive release. This can be explained because when the hydrogel is made from chitosan (CHI) and alginate (ALG) only and an electric field is supplied, the FITC would migrate towards the anode (positive electrode) under the influence of the electric field. The FITC is a negatively charged molecule and it will be drawn towards the positively

charged electrode by the electric field. [116] Although chitosan and alginate do not have any electroactive groups that can interact with the FITC, the electric field will provide the necessary force to drive the FITC migration through electrostatic attraction.

When incubated in 1 mg/ml FITC-Dextran, the concentration of drug uptake by pure CHI/ALG, low Fc-CHI/ALG, medium Fc-CHI/ALG and high Fc-CHI/ALG was 0.052, 0.103, 0.117 and 0.158 mg/ml, respectively. The comparative release of FITC-Dextran is slower than that of the pure FITC. FITC Dextran has the molecular weight of 66 kDa which is the main reason behind the slow passage from the PEC to the agarose gel because the higher the molecular weight slower the drug migrates through the hydrogel. [121]

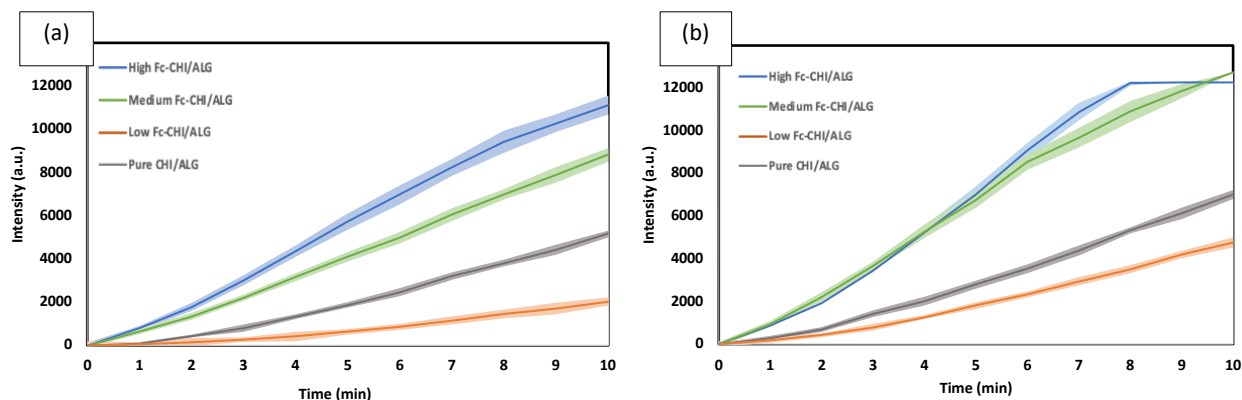


**Figure 4.12.** FITC-Dextran release intensity profile with (a) 0V electric supply, (b) 2V electric supply.

As like that of the FITC release FITC-Dextran has also been released from different PEC along with the different voltage application. From the intensity change observance, the release of FITC-Dextran from no electric current supplied were 2053.2, 5176.2, 8826.8, and 11135.8 a.u. from pure CHI/ALG, low Fc-CHI/ALG, medium Fc-CHI/ALG and high Fc-Chi/ALG, respectively.

It is seen that the release of FITC-Dextran from Fc-CHI/ALG is higher than that of pure Chi/ALG PEC. This is because the release is favored with only diffusion. As the pore size of the Fc-

CHI/ALG PEC is higher than that of pure CHI/ALG there is more diffusion channel for passage of more drug. [122] The study performed by Andreas Bertz and his team found that the increasing polymer concentration causes the increase in network density, which resulted in slower diffusion of dextran. Larger pore size in loose network density causes the fast diffusion due to burst release. [123]

The release of incorporated FITC-Dextran with 2V, 1.5A electric stimulus from pure CHI/ALG, low Fc-CHI/ALG, medium Fc-CHI/ALG and high Fc-CHI/ALG was found to be 4779, 7021.6, 11848.6, and 12276.4 a.u., respectively. It is observed that the FITC-Dextran started to migrate towards the anode much faster than as compared to that of the not applied with electric stimulus. The FITC-Dextran is a negatively charged molecule because of the presence of isothiocyanate group in FITC and the dextran is also negatively charged because it is a polysaccharide. [116] From the study performed by Jenson and his team it was found that there is direct relation of electrostatic force driving the negatively charged drug sulfosalicylic acid towards oppositely charged electrode, thus diffusion coefficient is higher even for the material having same crosslinking ratio or mesh size. [97, 124] Due to same effect when an electric field is applied, the negatively charged FITC-Dextran will be drawn towards the positively charged anode. Fc can act as a reducing agent, which can break the cross-links in the hydrogel and increase its degradation, leading to a faster release of the FITC-Dextran. [125] Additionally, Fc can alter the surface charge and hydrophilicity of the hydrogel, which can facilitate the diffusion of FITC-dextran and enhance its release. [126]

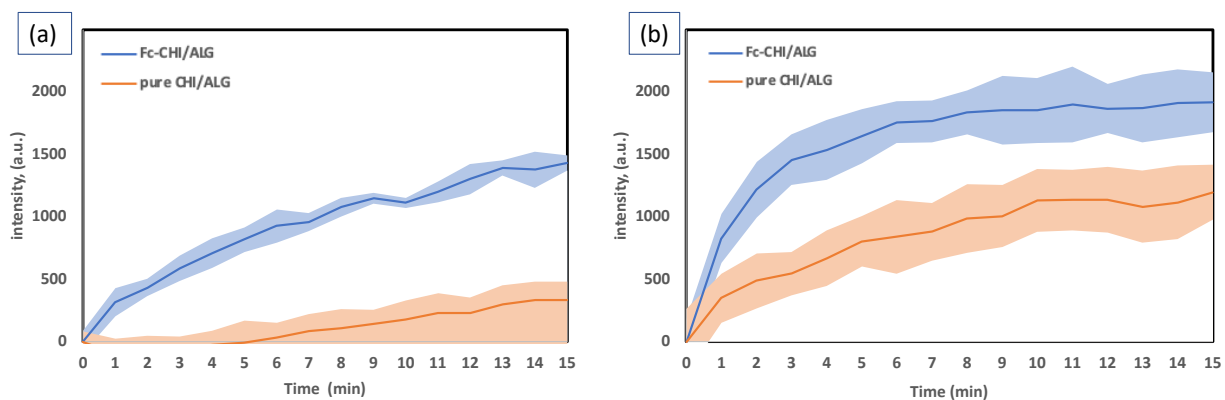


**Figure 4.13.** FITC-BSA release intensity profile (a) with 0V cathode-anode-agar (b) with 2V cathode- anode- agar.

The amount of FITC-BSA absorbed was 0.248 and 0.401 mg/ml for pure CHI/ALG and high-Fc-CHI/ALG, respectively. The release of predicted FITC-BSA from the rise of intensity pure CHI/ALG and Fc-CHI/ALG is 335.4 a.u. and 1433.8 a.u., respectively. When a hydrogel is made from only CHI and alginate ALG and fluorescein isothiocyanate-bovine serum albumin (FITC-BSA) is released, it is observed that, very less amount of FITC-BSA is released as compared to FITC this is due to the molecular size of FITC-BSA is larger than that of pure FITC. As similar to that of FITC, FITC-BSA also travels towards the anode.[127] This is due to the fact that chitosan is positively charged, and alginate is negatively charged, creating an electric potential gradient in the gel that drives the negatively charged FITC-BSA towards the positively charged anode. The study performed by Ju Young found that the negatively charged FITC-BSA migrated towards anode due to electrophoresis. They studied the diffusivity of the FITC-BSA on 2wt% agarose gel. Their comparative study of diffusivity of Rhodamine and FITC-BSA showed that FITC-BSA is negatively charged since its migration is towards anode while the migration of Rhodamine towards cathode proves that this is positively charged. [127] The addition of ferrocene to a hydrogel can increase the release of an encapsulated molecule, such as FITC-BSA, due to the redox (reduction-

oxidation) properties of ferrocene.[115] Ferrocene can transfer electrons from one molecule to another and can therefore cause changes in the local pH and redox potential of the hydrogel. These changes can in turn lead to changes in the structure and properties of the hydrogel, such as increased porosity or altered charge distribution, which can enhance the release of the encapsulated molecule.[128] Additionally, the presence of ferrocene in the hydrogel can also influence the diffusion of the encapsulated molecule through the hydrogel, contributing to the increased release rate.

Along with the application of 1.5 V electric stimulus, we observed a little change in release of FITC-BSA. The intensity of Agarose gel obtained from pure CHI/ALG and Fc-CHI/ALG was 1198.6 a.u. and 1922.8 a.u., respectively. When an electric field is supplied to a chitosan-alginate hydrogel, the release of an encapsulated molecule can be faster. This is due to the electrical stimulation of the hydrogel, which creates an electro-osmotic flow that helps to drive the release of the encapsulated molecule. The electric field can also cause the hydrogel to deform and change its structure, further increasing the release rate. Additionally, the application of an electric field can also enhance the diffusion of the. [129] Increasing the amount of ferrocene in the hydrogel will increase the overall charge distribution within the hydrogel, which can lead to a stronger electro-osmotic flow and an increased release of FITC-BSA in response to an electric field. The amount of ferrocene present in the hydrogel is related to the release of FITC-BSA in response to an electric field. [130]

## 4.2.2. Dynamic release

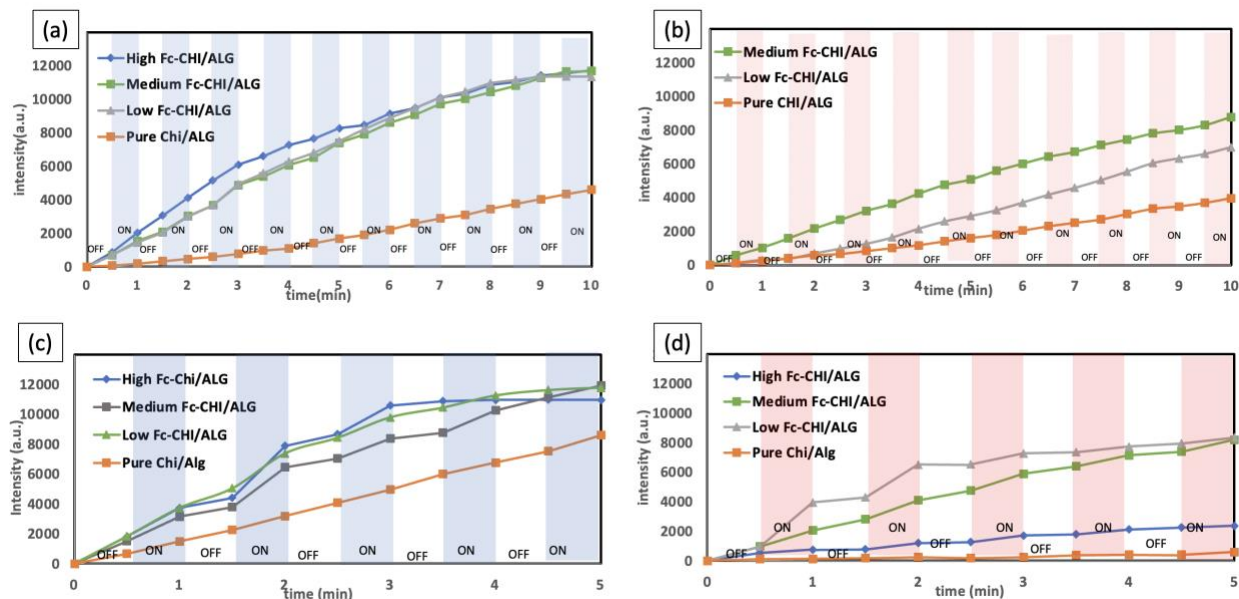


**Figure 4.14.** FITC release from different PEC with cyclic voltage application. (a) 1.5 V cathode-anode-agar, (b) 1.5 V anode-cathode-agar, (c) 2 V cathode-anode-agar and (d) 2 V anode-cathode-agar.

The cyclic voltage was applied in both directions, i.e., from cathode-anode-agar and from anode-cathode-agar. Since the migration of the drug in the incorporation of the  $Fc^-$  is driven towards the anode, the release through the cathode-anode-agar is faster than in the opposite direction. [116] The release of FITC is dependent on the presence of the  $Fc$  (**Figure 4.14.a**). The intensity profile with a 1.5V electric field shows that the drug migrates towards the anode with Fc-CHI/ALG PECs, and from pure CHI/ALG, the migration of drugs is slower. After 10 minutes of release, the intensity reaches 4600 and 11355  $\mu\text{m}$  from pure CHI/ALG and Fc-CHI/ALG hydrogels, respectively. The release of FITC in the opposite direction, i.e., anode-cathode-agar is much slower (**Figure 4.14.b**). At the end of 10 minutes, the release was 3971 a.u., 6991 a.u., and



8773 a.u. from pure CHI/ALG, low Fc-CHI/ALG, and medium Fc-CHI/ALG hydrogel, respectively. As shown in **(Figure 4.14.c)**, the release is accelerated while the voltage is ON (cathode-anode-agar), and the release is steady comparatively while the voltage is OFF. The intensity at the end of 5 minutes of 3V application of the release was 8610 a.u. and 11787 a.u. from pure CHI/ALG and all Fc-CHI/ALG, respectively. The release from the opposite direction, i.e., anode-cathode-agar **(Figure 4.14.d)**, is unclear as the intensity reaches 595 a.u. from pure CHI/ALG, and it is only 8344 a.u. from Fc-CHI/ALG at the end of 5 minutes. The migration of drugs towards the anode was faster, resulting in a higher release rate through cathode-anode-agar. The presence of Fc-CHI/ALG PECs also influenced the release rate of FITC, and the application of an electric field accelerated the release.

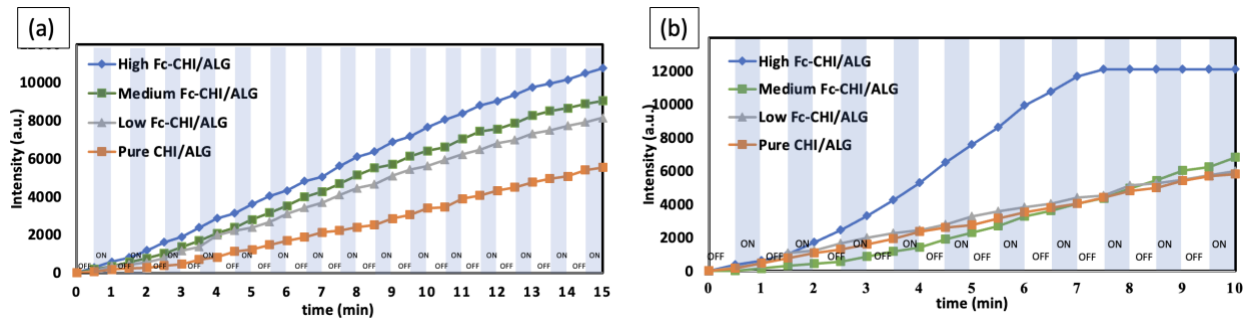


**Figure 4.15.** FITC-Dextran release from different PEC with cathode-anode-agar configuration (a) 1.5V cyclic voltage application (b) 2 V cyclic voltage application.

The release of FITC-Dextran in a dynamic environment is similar to that in a static environment. The application of voltage in a cyclic manner shows the slight change in slope while transitioning from the off state to the on state **(Figure. 4.15)**. After 15 minutes of cyclic release of FITC-Dextran with 1.5V, the intensity was found to be 5545 a.u., 8150 a.u., 9045 a.u. and 11076 a.u. from pure CHI/ALG, low Fc-CHI/ALG, medium Fc-CHI/ALG, and high Fc-CHI/ALG respectively. Following the same process, after 10 minutes of release of FITC-Dextran with 2 V,

the intensity was found to be 5815 a.u., 6830 a.u., 6830 a.u. and 12086 a.u. from pure CHI/ALG, low Fc-CHI/ALG, medium Fc-CHI/ALG and high Fc-CHI/ALG respectively. The results indicate that the release of FITC is highly controllable, with clear and distinct slopes in the on and off conditions, however the release of FITC-Dextran shows only a slight change in slope. The release time of FITC is faster with a 2V voltage compared to 1.5V, as it reaches saturation in half the time. Similarly, FITC-Dextran shows faster release after 10 minutes with a 2V voltage compared to 15 minutes with a 1.5V voltage. The results also suggest that the presence of Fc in the hydrogel makes it more electrochemically active PEC (E-PEC), as the release was greatly affected by the application of voltage in the high Fc-CHI/ALG.

It can be concluded that E-PEC hydrogel, specifically high Fc-CHI/ALG, is the best choice for use in wound healing purposes due to its controllable release of drugs and faster release time with the application of voltage. Its electrochemical activity and ability to enhance the release of drugs make it a promising candidate for wound healing applications.

#### **4.3. *In-vitro* biofilm assay: Antimicrobial effect**

The purpose of this experiment was to observe effectiveness of drug release on bacterial biofilms through the hydrogel. The selected hydrogel for this observation was E-PEC because of its enhanced properties like larger pore with irregular polymeric geometry, increased swelling ratio and electro-responsivity. This hydrogel is best for the release of the FITC and FITC release. The elimination of both gram-positive and gram-negative bacteria was observed using CIP antibiotics. It was noted that *S. aureus* is susceptible to certain types of antibiotics due to its thick cell wall as a gram-positive bacterium, while *P. aeruginosa*, a gram-negative bacterium with a thinner cell wall and outer membrane, is typically resistant to antibiotics.

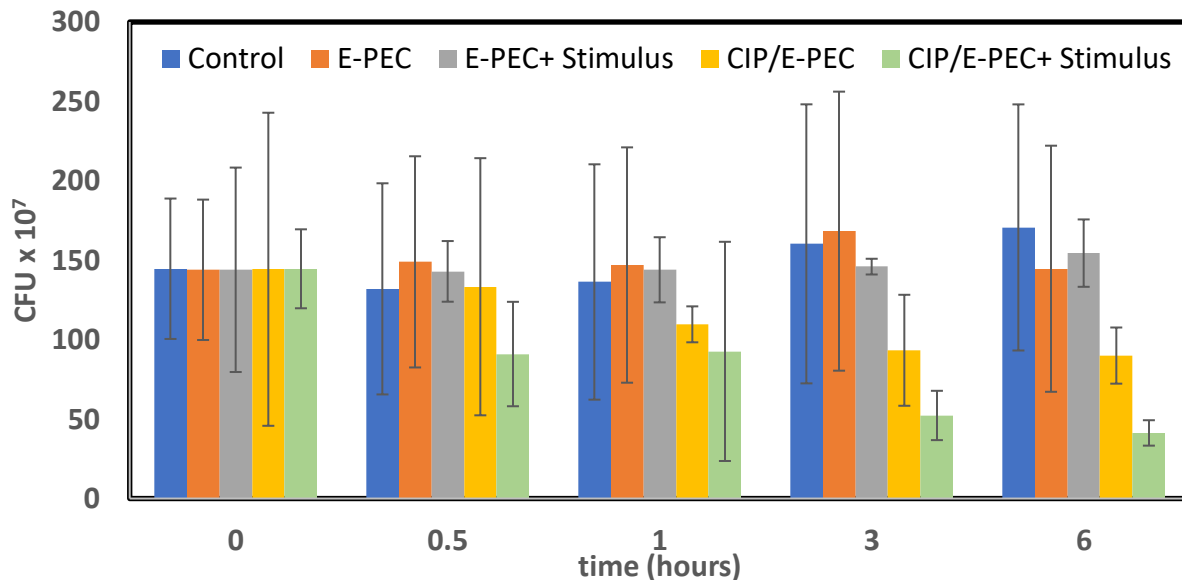


**Figure 4.16.** CFU count of *S. aureus* biofilm. (n=3)

The effectiveness of the release of CIP over *S. aureus* was compared with the release of the control, PBS, in an experiment. The hydrogel E-PEC was loaded with either PBS or CIP, and the release was performed in three ways: CIP/E-PEC, E-PEC loaded with PBS, and a control group treated with PBS only. The CIP/E-PEC group was also subjected to an electric voltage of 2 V.

CFU (colony-forming unit) counts were taken at specific time points. The control group showed a slight increase in CFU count over time, from  $144 \times 10^7/\text{ml}$  to  $165 \times 10^7/\text{ml}$ . The electric device was designed to show the effectiveness of the encapsulated hydrogel under electric stimulus, as demonstrated by the result of the E-PEC + stimulus, where the CFU count increased from 144 to  $150 \times 10^7/\text{ml}$ . The E-PEC group showed a slight increase in CFU count in the third hour, but by the end of the experiment, the CFU count was the same, indicating that the E-PEC does not inhibit but prevents the bacterial growth. The release of CIP without stimulus (CIP/E-PEC) resulted in a reduction in CFU count to  $90 \times 10^7/\text{ml}$ , while the release of CIP with electric

stimulus was highly effective, reducing the CFU count to  $50 \times 10^7/\text{ml}$  (**Figure 4.16**). In summary, the control group showed slight increase in CFU counts over time. The release of CIP with electric stimulus was highly effective in reducing CFU counts, while the hydrogel alone had no effect on the biofilm.

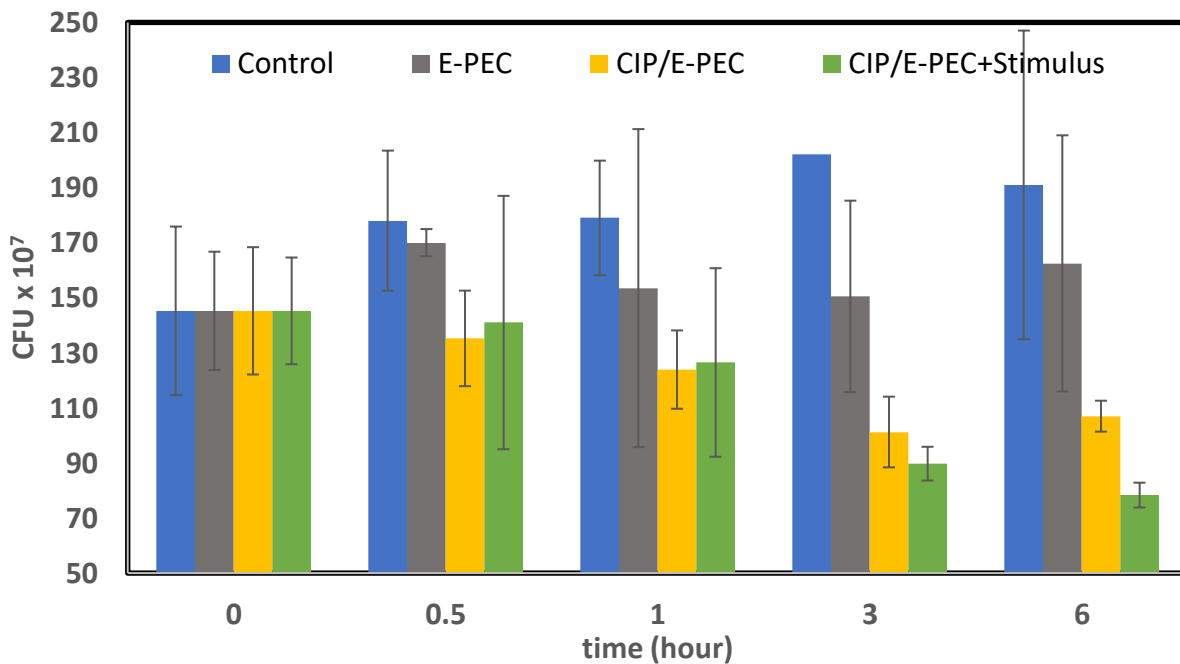


**Figure 4.17.** CFU counts for *P. aeruginosa* biofilm. (n=3)

The hydrogel E-PEC was also used to test its efficacy in reducing growth of gram-negative bacterial biofilms. The results showed that the combination of CIP and electric stimulus treatment led to a decrease in CFU count from  $145 \times 10^7/\text{ml}$  to  $78 \times 10^7/\text{ml}$  over six hours. In contrast, the CFU count of the biofilm treated with CIP alone was  $105 \times 10^7/\text{ml}$  after six hours. The biofilm treated with E-PEC alone had a higher CFU count of  $162 \times 10^7/\text{ml}$  after six hours, indicating that

it was ineffective in killing the bacteria. The control group treated with PBS showed an increase in CFU count from 144 to  $190 \times 10^7/\text{ml}$  after six hours (**Figure 4.17**).

The results indicate that the combination of CIP and electric stimulus treatment using the E-PEC hydrogel was effective in reducing bacterial growth in biofilms. The use of CIP alone showed some efficacy, but it was not as effective as the combination treatment. Treatment with the E-PEC hydrogel alone was found to be ineffective in killing the bacteria. The E-PEC hydrogel used in the experiment have acted as a controlled-release system. The electric stimulus has enhanced the release of the antibiotic from the hydrogel, allowing it to reach the bacterial cells more effectively within the biofilm. Controlled release of antibiotics from hydrogels was particularly effective. Biofilms are complex structures formed by bacteria that can provide a protective environment for the microorganisms, making them more resistant to traditional antibiotic treatments. [131] The controlled release of antibiotics through the different voltage supply from hydrogels can allow for a more gradual and prolonged exposure of the bacteria to the drug, which can increase the likelihood of eradicating the biofilm. [132]

Additionally, controlled release from hydrogels can also help reduce the frequency of dosing, which can be particularly beneficial for patients who require long-term antibiotic therapy. By reducing the need for frequent dosing, controlled-release hydrogels can improve patient compliance and reduce the risk of side effects associated with high-dose antibiotic therapy. [13, 15] In summary, controlled release of antibiotics from hydrogels can improve the effectiveness of antibiotics against bacterial biofilms by providing a continuous and controlled release of the drug over shorter or extended period of time. This controlled exposure can increase the likelihood of eradicating biofilm and reduce the frequency of dosing, which can improve patient compliance and reduce the risk of side effects.

The combination of the Fc, CHI and ALG hydrogel can be used in multiple stages of wound healing like, hemostasis due to adhesion property provided by ALG, inflammatory due to the anti-bacterial property provided by positive charges of CHI. Fc also helps in reducing the inflammation through the redox property. [7] The inhibition of the bacterial colony observed in the *in-vitro* experiment helps to clarify that this E-PEC hydrogel system can be used in the inflammatory stage of the wound healing. As well as the E-PEC also consists of the ALG, so it can be used for the hemostasis stage of wound healing.

## 5. Conclusions and recommendations

- PEC hydrogels are made from CHI/ALG, and E-PEC hydrogels are made with addition of varying amounts of Fc. The CHI was first conjugated with Fc to produce Fc-CHI and was then interacted with ALG to form the Fc-CHI/ALG. CHI/ALG was used as a control and the properties of Fc-CHI/ALG were studied in reference to it.
- The results from UV-Vis spectroscopy on unconjugated Fc proved that there was no free Fc present in the synthesized Fc-CHI flakes/granules.
- The degree of conjugation was measured by Ninhydrin assay, which indicated an increasing trend of free amines from low, medium, and high Fc-CHI. The percentage of free amines in low Fc-CHI, medium Fc-CHI and high Fc-CHI is 13.37%, 23.47% and 42.47%, respectively. This indicates that there are more amino groups that are not bound to ferrocene molecules in the high Fc-CHI sample than in the low Fc-CHI sample.
- The turbidity test revealed that adding Fc changed the stoichiometric proportion of polycation and polyanion. The stoichiometric proportion of the pure CHI/ALG, low Fc-CHI/ALG, medium Fc-CHI/ALG and high Fc-CHI/ALG is formed at 40% CHI, 50% Fc-CHI, 55% Fc-CHI and 55% Fc-CHI, respectively. The peak shifted towards higher proportions of Fc-CHI, indicating Fc-conjugation with CHI and a lower number of free amines, requiring reaction with ALG.
- Viscosity testing of the stoichiometric proportion demonstrated that the mechanical strength of PEC decreased with increasing amounts of Fc. The viscosity of pure CHI/ALG, low Fc-CHI/ALH, medium Fc-CHI/ALG and high Fc-CHI/ALG was 2021.9, 1472.52, 1286.27 and 1171.2 cP, respectively.

- Gel content and swelling ratio test results increased with an increase in Fc, as evidenced by SEM images showing larger pore size in PEC with more Fc. Gel content 94.48, 94.01, 93.99 and 93.82 % was obtained from pure CHI/ALG, low Fc-CHI/ALG, medium Fc-CHI/ALG and high Fc-CHI/ALG, respectively. Similarly, the swelling ratio of 4965.47%, 5676.88%, 5785.38 and 5912.66 %, respectively. The increasing concentration of the Fc in the PEC increased the pore size of PEC and changed the surface morphology, which can be used to hold larger amount of drugs within its pore.
- The continuous release of FITC from PEC resulted in increase in concentration of FITC inside agarose gel. The intensity changes after 4 minutes in agarose gel obtained with 0 V electric stimulus from pure CHI/ALG, low Fc-CHI/ALG, medium Fc-CHI/ALG and high Fc-CHI/ALG was 2962.2, 11829.6, 13424.8 and 13424.8 a.u., respectively. Similarly, with application of 2 V the intensity of the all Fc-CHI/ALG was 14000 at 3 minutes and after 4 minutes the intensity of pure CHI/ALG was 14000 form pure CHI/ALG.
- FITC-Dextran was released slowly as compared to that of the FITC. The release of FITC-Dextran with 0 V electric stimulus increased the intensity to 2053.2, 5176.2, 8826.6 and 12276.4 a.u., respectively, whereas with 2V the intensity was 4779, 7021.6, 11848.6 and 12276.4 a.u., respectively. FITC-BSA release with 0 V was 335.4 and 1433.8 a.u., respectively, whereas 2 V electric stimulus the release of the FITC-BSA increased the intensity in the agarose gel to 1198.6 and 1922.8 a.u., respectively.
- The high Fc-CHI/ALG upon electrical stimulus showed the highest amount of the released model drugs, whereas the lowest amount with CHI/ALG with no electrical stimulus.



- The drug release kinetics with the switching mode (On/Off) of the electrical stimulus showed a stair like release pattern with prompt responsiveness, which indicates the developed E-PEC hydrogel is controllable.
- The continuous release of the CIP from the E-PEC hydrogel upon electrical stimulus for up to 6 hours resulted in the number of colony forming units decreased from 144 to  $41 \times 10^7$ /ml for *S. aureus* biofilm and 145 to  $71 \times 10^7$ /ml for *P. aeruginosa* biofilm.
- Future work can be focused on use of the different antibiotics or mixed antibiotics of methicillin, vancomycin, ampicillin, tetracycline and ceftazidime, for the effective inhibition antibiotics on *S. aureus*, *P. aeruginosa*, and Methicillin-resistant *S. aureus* (MRSA) biofilms.
- Antimicrobial effect of the E-PEC hydrogel on biofilm demonstrated an enhanced effect on antibiotic release, as evidenced by the reduced CFU values on the treated biofilms. This eradication of the biofilm makes the E-PEC hydrogel suitable for inflammatory stage of the wound healing while the presence of ALG would be effective for hemostasis stage of the wound healing.

## References

1. Lei, J., et al., *The Wound Dressings and Their Applications in Wound Healing and Management*. Health science journal, 2019. **13**.
2. Schreml, S., et al., *Oxygen in acute and chronic wound healing*. Br J Dermatol, 2010. **163**(2): p. 257-68.
3. Koehler, J., F.P. Brandl, and A.M. Goepferich, *Hydrogel wound dressings for bioactive treatment of acute and chronic wounds*. European Polymer Journal, 2018. **100**: p. 1-11.
4. Wilkinson, H.N. and M.J. Hardman, *Wound healing: cellular mechanisms and pathological outcomes*. Open Biology, 2020. **10**(9): p. 200223.
5. Sun, B.K., Z. Siplashvili, and P.A. Khavari, *Advances in skin grafting and treatment of cutaneous wounds*. Science, 2014. **346**(6212): p. 941-945.
6. Brown, M.S., B. Ashley, and A. Koh, *Wearable Technology for Chronic Wound Monitoring: Current Dressings, Advancements, and Future Prospects*. Frontiers in Bioengineering and Biotechnology, 2018. **6**.
7. Altoé, L.S., et al., *Does antibiotic use accelerate or retard cutaneous repair? A systematic review in animal models*. PLOS ONE, 2019. **14**(10): p. e0223511.
8. Das, S. and A.B. Baker, *Biomaterials and Nanotherapeutics for Enhancing Skin Wound Healing*. Frontiers in Bioengineering and Biotechnology, 2016. **4**.
9. Masri, S., et al., *Cellular Interaction of Human Skin Cells towards Natural Bioink via 3D-Bioprinting Technologies for Chronic Wound: A Comprehensive Review*. Int J Mol Sci, 2022. **23**(1).
10. Davis, F.M., et al., *Dysfunctional Wound Healing in Diabetic Foot Ulcers: New Crossroads*. Current Diabetes Reports, 2018. **18**(1): p. 2.
11. Greene, D.A., M.J. Stevens, and E.L. Feldman, *Diabetic neuropathy: scope of the syndrome*. Am J Med, 1999. **107**(2b): p. 2s-8s.
12. Alavi, A., et al., *Diabetic foot ulcers: Part I. Pathophysiology and prevention*. J Am Acad Dermatol, 2014. **70**(1): p. 1.e1-18; quiz 19-20.
13. Gianino, E., C. Miller, and J. Gilmore, *Smart Wound Dressings for Diabetic Chronic Wounds*. Bioengineering (Basel), 2018. **5**(3).

14. Boateng, J.S., et al., *Wound healing dressings and drug delivery systems: a review*. Journal of pharmaceutical sciences, 2008. **97**(8): p. 2892-2923.
15. Bashir, S., et al., *Fundamental concepts of hydrogels: Synthesis, properties, and their applications*. Polymers, 2020. **12**(11): p. 2702.
16. Campbell, T.D. *Synthesis and physical characterization of biocompatible hydrogels*. 2007.
17. Dhivya, S., V.V. Padma, and E. Santhini, *Wound dressings - a review*. Biomedicine (Taipei), 2015. **5**(4): p. 22.
18. Thakur, S., V.K. Thakur, and O. Arotiba, *History, Classification, Properties and Application of Hydrogels: An Overview: Recent Advances*. 2018. p. 29-50.
19. Li, D., et al., *Polyelectrolyte Complex-Covalent Interpenetrating Polymer Network Hydrogels*. Macromolecules, 2022. **55**(11): p. 4481-4491.
20. Meka, V.S., et al., *A comprehensive review on polyelectrolyte complexes*. Drug Discov Today, 2017. **22**(11): p. 1697-1706.
21. Schoeller, J., et al., *pH-Responsive Chitosan/Alginate Polyelectrolyte Complexes on Electrospun PLGA Nanofibers for Controlled Drug Release*. Nanomaterials (Basel), 2021. **11**(7).
22. Kwon, I.C., Y.H. Bae, and S.W. Kim, *Heparin release from polymer complex*. Journal of Controlled Release, 1994. **30**(2): p. 155-159.
23. Phoeung, T., et al., *Alginate/chitosan compact polyelectrolyte complexes: a cell and bacterial repellent material*. Chemistry of Materials, 2017. **29**(24): p. 10418-10425.
24. Ganji, F., S. Vasheghani Farahani, and E. Vasheghani-Farahani, *Theoretical Description of Hydrogel Swelling: A Review*. Iranian Polymer Journal, 2010. **19**: p. 375-398.
25. Jones, D.S., G.P. Andrews, and S.P. Gorman, *Characterization of crosslinking effects on the physicochemical and drug diffusional properties of cationic hydrogels designed as bioactive urological biomaterials*. J Pharm Pharmacol, 2005. **57**(10): p. 1251-59.
26. Brannon-Peppas, L., *Preparation and Characterization of Crosslinked Hydrophilic Networks*, in *Studies in Polymer Science*, L. Brannon-Peppas and R.S. Harland, Editors. 1990, Elsevier. p. 45-66.
27. Choudhary, S., *Characterization of amorphous silica nanofiller effect on the structural, morphological, optical, thermal, dielectric and electrical properties of PVA–PVP blend*

- based polymer nanocomposites for their flexible nanodielectric applications*. Journal of Materials Science: Materials in Electronics, 2018. **29**(12): p. 10517-10534.
28. Lee, C.-J., et al., *Ionic conductivity of polyelectrolyte hydrogels*. ACS applied materials & interfaces, 2018. **10**(6): p. 5845-5852.
  29. Tian, Y., et al., *Polyanionic self-healing hydrogels for the controlled release of cisplatin*. European Polymer Journal, 2020. **133**: p. 109773.
  30. Liang, Y., J. He, and B. Guo, *Functional hydrogels as wound dressing to enhance wound healing*. ACS nano, 2021. **15**(8): p. 12687-12722.
  31. Xue, W., et al., *Controllable fabrication of alginate/poly-L-ornithine polyelectrolyte complex hydrogel networks as therapeutic drug and cell carriers*. Acta Biomaterialia, 2022. **138**: p. 182-192.
  32. Wang, H., et al., *Antibacterial Activity of Geminized Amphiphilic Cationic Homopolymers*. Langmuir, 2015. **31**(50): p. 13469-77.
  33. Nguyen, H.T.T., et al., *Synthesis, properties, and applications of chitosan hydrogels as anti-inflammatory drug delivery system*. Journal of Porous Materials, 2023. **30**(2): p. 655-670.
  34. Zhang, Y., et al., *Eco-friendly ferrocene-functionalized chitosan aerogel for efficient dye degradation and phosphate adsorption from wastewater*. Chemical Engineering Journal, 2022. **439**: p. 135605.
  35. Yang, W., H. Zhou, and C. Sun, *Synthesis of ferrocene-branched chitosan derivatives: redox polysaccharides and their application to reagentless enzyme-based biosensors*. Macromolecular rapid communications, 2007. **28**(3): p. 265-270.
  36. Wang, C.G., et al., *Polyelectrolyte Hydrogels for Tissue Engineering and Regenerative Medicine*. Chemistry—An Asian Journal, 2022. **17**(18): p. e202200604.
  37. Parhi, R., *Cross-linked hydrogel for pharmaceutical applications: a review*. Advanced pharmaceutical bulletin, 2017. **7**(4): p. 515-530.
  38. Hu, W., et al., *Advances in crosslinking strategies of biomedical hydrogels*. Biomaterials science, 2019. **7**(3): p. 843-855.
  39. Srivastava, N. and A.R. Choudhury, *Stimuli-Responsive Polysaccharide-Based Smart Hydrogels and Their Emerging Applications*. Industrial & Engineering Chemistry Research, 2022.

40. Srivastava, N. and A. Roy Choudhury, *Green Synthesis of pH-Responsive, Self-Assembled, Novel Polysaccharide Composite Hydrogel and Its Application in Selective Capture of Cationic/Anionic Dyes*. *Frontiers in Chemistry*, 2021. **9**: p. 761682.
41. Xu, J., Y. Liu, and S.-h. Hsu, *Hydrogels based on Schiff base linkages for biomedical applications*. *Molecules*, 2019. **24**(16): p. 3005.
42. Raczuk, E., et al., *Different Schiff Bases—Structure, Importance and Classification*. *Molecules*, 2022. **27**(3): p. 787.
43. Du, M., et al., *Dual drug-loaded hydrogels with pH-responsive and antibacterial activity for skin wound dressing*. *Colloids Surf B Biointerfaces*, 2023. **222**: p. 113063.
44. Qu, J., et al., *Injectable antibacterial conductive hydrogels with dual response to an electric field and pH for localized “smart” drug release*. *Acta Biomaterialia*, 2018. **72**: p. 55-69.
45. Wu, C., et al., *Injectable conductive and angiogenic hydrogels for chronic diabetic wound treatment*. *Journal of Controlled Release*, 2022. **344**: p. 249-260.
46. Hu, C., et al., *Dual-crosslinked mussel-inspired smart hydrogels with enhanced antibacterial and angiogenic properties for chronic infected diabetic wound treatment via pH-responsive quick cargo release*. *Chemical Engineering Journal*, 2021. **411**: p. 128564.
47. Khan, M.U.A., et al., *Smart and pH-sensitive rGO/Arabinoxylan/chitosan composite for wound dressing: In-vitro drug delivery, antibacterial activity, and biological activities*. *International Journal of Biological Macromolecules*, 2021. **192**: p. 820-831.
48. Wang, Y., et al., *Inflammation-Responsive Drug-Loaded Hydrogels with Sequential Hemostasis, Antibacterial, and Anti-Inflammatory Behavior for Chronically Infected Diabetic Wound Treatment*. *ACS Applied Materials & Interfaces*, 2021. **13**(28): p. 33584-33599.
49. Qu, J., et al., *Biocompatible conductive hydrogels based on dextran and aniline trimer as electro-responsive drug delivery system for localized drug release*. *Int J Biol Macromol*, 2019. **140**: p. 255-264.
50. Ge, J., et al., *Drug release from electric-field-responsive nanoparticles*. *ACS nano*, 2012. **6**(1): p. 227-233.

51. Du, S., et al., *Surface-engineered triboelectric nanogenerator patches with drug loading and electrical stimulation capabilities: Toward promoting infected wounds healing*. Nano Energy, 2021. **85**: p. 106004.
52. Kleber, C., et al., *Electrochemically Controlled Drug Release from a Conducting Polymer Hydrogel (PDMAAp/PEDOT) for Local Therapy and Bioelectronics*. Advanced Healthcare Materials, 2019. **8**(10): p. 1801488.
53. Adepu, S. and S. Ramakrishna, *Controlled Drug Delivery Systems: Current Status and Future Directions*. Molecules, 2021. **26**(19): p. 5905.
54. Bagheri, B., et al., *Tissue engineering with electrospun electro-responsive chitosan-aniline oligomer/polyvinyl alcohol*. International Journal of Biological Macromolecules, 2020. **147**: p. 160-169.
55. Kiaee, G., et al., *A pH-Mediated Electronic Wound Dressing for Controlled Drug Delivery*. Adv Healthc Mater, 2018. **7**(18): p. e1800396.
56. Salas, B.M.S., et al., *Nanocomposite hydrogels of gellan gum and polypyrrole for electro-stimulated ibuprofen release application*. Reactive and Functional Polymers, 2022: p. 105296.
57. Santhamoorthy, M., et al., *Thermo-Sensitive Poly (N-isopropylacrylamide-co-polyacrylamide) Hydrogel for pH-Responsive Therapeutic Delivery*. Polymers, 2022. **14**(19): p. 4128.
58. Klouda, L. and A.G. Mikos, *Thermoresponsive hydrogels in biomedical applications*. Eur J Pharm Biopharm, 2008. **68**(1): p. 34-45.
59. Pourjavadi, A., M. Bagherifard, and M. Doroudian, *Synthesis of micelles based on chitosan functionalized with gold nanorods as a light sensitive drug delivery vehicle*. International Journal of Biological Macromolecules, 2020. **149**: p. 809-818.
60. Li, M., et al., *Two-pronged strategy of biomechanically active and biochemically multifunctional hydrogel wound dressing to accelerate wound closure and wound healing*. Chemistry of Materials, 2020. **32**(23): p. 9937-9953.
61. Markovic, M.D., et al., *Biobased thermo/pH sensitive poly (N-isopropylacrylamide-co-crotonic acid) hydrogels for targeted drug delivery*. Microporous and Mesoporous Materials, 2022. **335**: p. 111817.

62. Aydin, N.E., *Effect of temperature on drug release: production of 5-FU-encapsulated hydroxyapatite-gelatin polymer composites via spray drying and analysis of in vitro kinetics*. International Journal of Polymer Science, 2020. **2020**.
63. Zhu, D.Y., et al., *Injectable thermo-sensitive and wide-crack self-healing hydrogel loaded with antibacterial anti-inflammatory dipotassium glycyrrhizate for full-thickness skin wound repair*. Acta Biomaterialia, 2022. **143**: p. 203-215.
64. Chen, Y.-H., et al., *Cold-atmospheric plasma augments functionalities of hybrid polymeric carriers regenerating chronic wounds: In vivo experiments*. Materials Science and Engineering: C, 2021. **131**: p. 112488.
65. Ding, X., et al., *Multifunctional GO hybrid hydrogel scaffolds for wound healing*. Research, 2022. **2022**.
66. Li, C., et al., *Near-infrared emission carrier, Er<sup>3+</sup>-doped ZnAl-LDH, for delivery and release of ibuprofen in vitro*. Journal of Sol-Gel Science and Technology, 2021. **99(2)**: p. 430-443.
67. Huang, T., et al., *Synergy of light-controlled Pd nanozymes with NO therapy for biofilm elimination and diabetic wound treatment acceleration*. Materials Today Chemistry, 2022. **24**: p. 100831.
68. Zhao, W., et al., *Photo-responsive supramolecular hyaluronic acid hydrogels for accelerated wound healing*. Journal of Controlled Release, 2020. **323**: p. 24-35.
69. Zhou, W., et al., *Glucose and MMP-9 dual-responsive hydrogel with temperature sensitive self-adaptive shape and controlled drug release accelerates diabetic wound healing*. Bioactive Materials, 2022. **17**: p. 1-17.
70. Guo, C., et al., *Development of a Microenvironment-Responsive Hydrogel Promoting Chronically Infected Diabetic Wound Healing through Sequential Hemostatic, Antibacterial, and Angiogenic Activities*. ACS Applied Materials & Interfaces, 2022. **14(27)**: p. 30480-30492.
71. Hu, C., et al., *Microenvironment-responsive multifunctional hydrogels with spatiotemporal sequential release of tailored recombinant human collagen type III for the rapid repair of infected chronic diabetic wounds*. Journal of Materials Chemistry B, 2021. **9(47)**: p. 9684-9699.

72. Roquero, D.M. and E. Katz, "Smart" alginate hydrogels in biosensing, bioactuation and biocomputing: State-of-the-art and perspectives. *Sensors and Actuators Reports*, 2022. **4**: p. 100095.
73. Wu, Y., et al., *A spatiotemporal release platform based on pH/ROS stimuli-responsive hydrogel in wound repairing*. *Journal of Controlled Release*, 2022. **341**: p. 147-165.
74. Yang, J., et al., *Glucose-responsive multifunctional metal–organic drug-loaded hydrogel for diabetic wound healing*. *Acta Biomaterialia*, 2022. **140**: p. 206-218.
75. Ganguly, S. and S. Margel, *Design of Magnetic Hydrogels for Hyperthermia and Drug Delivery*. *Polymers (Basel)*, 2021. **13**(23).
76. Forouzandehdel, S., S. Forouzandehdel, and M.R. Rami, *Synthesis of a novel magnetic starch-alginic acid-based biomaterial for drug delivery*. *Carbohydrate research*, 2020. **487**: p. 107889.
77. Shi, W., et al., *Imparting Functionality to the Hydrogel by Magnetic-Field-Induced Nano-assembly and Macro-response*. *ACS Applied Materials & Interfaces*, 2020. **12**(5): p. 5177-5194.
78. Nezami, S., M. Sadeghi, and H. Mohajerani, *A novel pH-sensitive and magnetic starch-based nanocomposite hydrogel as a controlled drug delivery system for wound healing*. *Polymer Degradation and Stability*, 2020. **179**: p. 109255.
79. Chen, X., et al., *Magnetic and self-healing chitosan-alginate hydrogel encapsulated gelatin microspheres via covalent cross-linking for drug delivery*. *Materials Science and Engineering: C*, 2019. **101**: p. 619-629.
80. Kondaveeti, S., D.R. Cornejo, and D.F.S. Petri, *Alginate/magnetite hybrid beads for magnetically stimulated release of dopamine*. *Colloids and Surfaces B: Biointerfaces*, 2016. **138**: p. 94-101.
81. Yang, W., H. Zhou, and C. Sun, *Synthesis of Ferrocene-Branched Chitosan Derivatives: Redox Polysaccharides and their Application to Reagentless Enzyme-Based Biosensors*. *Macromolecular Rapid Communications*, 2007. **28**(3): p. 265-270.
82. Yılmaz, Ö., et al., *Chitosan–ferrocene film as a platform for flow injection analysis applications of glucose oxidase and *Gluconobacter oxydans* biosensors*. *Colloids and Surfaces B: Biointerfaces*, 2012. **100**: p. 62-68.



83. Curotto, E. and F. Aros, *Quantitative Determination of Chitosan and the Percentage of Free Amino Groups*. Analytical Biochemistry, 1993. **211**(2): p. 240-241.
84. Butler, M.F., Y.F. Ng, and P.D. Pudney, *Mechanism and kinetics of the crosslinking reaction between biopolymers containing primary amine groups and genipin*. Journal of Polymer Science Part A: Polymer Chemistry, 2003. **41**(24): p. 3941-3953.
85. Dai, M., et al., *Chitosan-Alginate Sponge: Preparation and Application in Curcumin Delivery for Dermal Wound Healing in Rat*. Journal of Biomedicine and Biotechnology, 2009. **2009**: p. 595126.
86. Nagasawa, N., et al., *Radiation crosslinking of carboxymethyl starch*. Carbohydrate Polymers, 2004. **58**(2): p. 109-113.
87. Barbero, N., C. Barolo, and G. Viscardi, *Bovine serum albumin bioconjugation with FITC*. World Journal of Chemical Education, 2016. **4**(4): p. 80-85.
88. Wang, Y., et al., *Structural Color Ionic Hydrogel Patches for Wound Management*. ACS Nano, 2023. **17**(2): p. 1437-1447.
89. Krupa, I., et al., *Glucose diffusivity and porosity in silica hydrogel based on organofunctional silanes*. European Polymer Journal, 2011. **47**(7): p. 1477-1484.
90. Weppner, W. and R.A. Huggins, *Electrochemical methods for determining kinetic properties of solids*. Annual Review of Materials Science, 1978. **8**(1): p. 269-311.
91. Krupa, I., et al., *Glucose diffusivity and porosity in silica hydrogel based on organofunctional silanes*. European polymer journal, 2011. **47**(7): p. 1477-1484.
92. Hasan, S., et al., *Controlled and Localized Nitric Oxide Precursor Delivery From Chitosan Gels to Staphylococcus aureus Biofilms*. J Pharm Sci, 2017. **106**(12): p. 3556-3563.
93. Cruz, C.D., S. Shah, and P. Tammela, *Defining conditions for biofilm inhibition and eradication assays for Gram-positive clinical reference strains*. BMC Microbiology, 2018. **18**(1): p. 173.
94. Hanna, D.H. and G.R. Saad, *Encapsulation of ciprofloxacin within modified xanthan gum- chitosan based hydrogel for drug delivery*. Bioorg Chem, 2019. **84**: p. 115-124.
95. Potaś, J., et al., *Tragacanth Gum/Chitosan Polyelectrolyte Complexes-Based Hydrogels Enriched with Xanthan Gum as Promising Materials for Buccal Application*. Materials, 2021. **14**(1): p. 86.

96. Strand, A., et al., *In-situ analysis of polyelectrolyte complexes by flow cytometry*. Cellulose, 2018. **25**(7): p. 3781-3795.
97. Juntanon, K., et al., *Electrically controlled release of sulfosalicylic acid from crosslinked poly(vinyl alcohol) hydrogel*. Int J Pharm, 2008. **356**(1-2): p. 1-11.
98. Chavda, H. and C. Patel, *Effect of crosslinker concentration on characteristics of superporous hydrogel*. Int J Pharm Investig, 2011. **1**(1): p. 17-21.
99. Piculell, L. and B. Lindman, *Association and segregation in aqueous polymer/polymer, polymer/surfactant, and surfactant/surfactant mixtures: similarities and differences*. Advances in Colloid and Interface Science, 1992. **41**: p. 149-178.
100. Sato, H. and A. Nakajima, *Formation of a polyelectrolyte complex from carboxymethyl cellulose and poly (ethylenimine)*. Polymer Journal, 1975. **7**(2): p. 241-247.
101. Choe, D., et al., *Synthesis of high-strength microcrystalline cellulose hydrogel by viscosity adjustment*. Carbohydrate polymers, 2018. **180**: p. 231-237.
102. Rassu, G., et al., *Composite chitosan/alginate hydrogel for controlled release of deferoxamine: A system to potentially treat iron dysregulation diseases*. Carbohydrate polymers, 2016. **136**: p. 1338-1347.
103. Wong, J.H.M., et al., *Dynamic Grafting of Carboxylates onto Poly (Vinyl Alcohol) Polymers for Supramolecularly-Crosslinked Hydrogel Formation*. Chemistry–An Asian Journal, 2022: p. e202200628.
104. Kulig, D., et al., *Study on Alginate–Chitosan Complex Formed with Different Polymers Ratio*. Polymers, 2016. **8**(5): p. 167.
105. Wang, G., X. Wang, and L. Huang, *Feasibility of chitosan-alginate (Chi-Alg) hydrogel used as scaffold for neural tissue engineering: a pilot study in vitro*. Biotechnology & Biotechnological Equipment, 2017. **31**(4): p. 766-773.
106. Lee, Y.J., et al., *Quantitative image analysis of broadband CARS hyperspectral images of polymer blends*. Analytical chemistry, 2011. **83**(7): p. 2733-2739.
107. Pakizeh, M., A. Moradi, and T. Ghassemi, *Chemical extraction and modification of chitin and chitosan from shrimp shells*. European Polymer Journal, 2021. **159**: p. 110709.
108. Lin, K.-Y.A., J.-T. Lin, and H. Yang, *Ferrocene-modified chitosan as an efficient and green heterogeneous catalyst for sulfate-radical-based advanced oxidation process*. Carbohydrate Polymers, 2017. **173**: p. 412-421.

109. Spinks, G.M., et al., *Swelling Behavior of Chitosan Hydrogels in Ionic Liquid–Water Binary Systems*. Langmuir, 2006. **22**(22): p. 9375-9379.
110. Jiang, H., et al., *A pH-regulated drug delivery dermal patch for targeting infected regions in chronic wounds*. Lab on a Chip, 2019. **19**(13): p. 2265-2274.
111. Khare, A.R. and N.A. Peppas, *Swelling/deswelling of anionic copolymer gels*. Biomaterials, 1995. **16**(7): p. 559-567.
112. Dragan, E.S., M.V. Dinu, and C.A. Ghiorghita, *Chitosan-Based Polyelectrolyte Complex Cryogels with Elasticity, Toughness and Delivery of Curcumin Engineered by Polyions Pair and Cryostructuration Steps*. Gels, 2022. **8**(4): p. 240.
113. Chalitangkoon, J., M. Wongkittisin, and P. Monvisade, *Silver loaded hydroxyethylacryl chitosan/sodium alginate hydrogel films for controlled drug release wound dressings*. International Journal of Biological Macromolecules, 2020. **159**: p. 194-203.
114. Mikušová, V. and P. Mikuš, *Advances in chitosan-based nanoparticles for drug delivery*. International Journal of Molecular Sciences, 2021. **22**(17): p. 9652.
115. Pietschnig, R., *Polymers with pendant ferrocenes*. Chemical Society Reviews, 2016. **45**(19): p. 5216-5231.
116. Yi, Y., et al., *Programmable and on-demand drug release using electrical stimulation*. Biomicrofluidics, 2015. **9**(2): p. 022401.
117. Linsley, C.S. and B.M. Wu, *Recent advances in light-responsive on-demand drug-delivery systems*. Ther Deliv, 2017. **8**(2): p. 89-107.
118. Kang, H., et al., *Photoresponsive DNA-Cross-Linked Hydrogels for Controllable Release and Cancer Therapy*. Langmuir, 2011. **27**(1): p. 399-408.
119. Li, J. and D.J. Mooney, *Designing hydrogels for controlled drug delivery*. Nature Reviews Materials, 2016. **1**(12): p. 16071.
120. Gupta, N.V. and H.G. Shivakumar, *Investigation of Swelling Behavior and Mechanical Properties of a pH-Sensitive Superporous Hydrogel Composite*. Iran J Pharm Res, 2012. **11**(2): p. 481-93.
121. Brandl, F., et al., *Hydrogel-based drug delivery systems: Comparison of drug diffusivity and release kinetics*. Journal of Controlled Release, 2010. **142**(2): p. 221-228.

122. Simpliciano, C., et al., *Cross-Linked Alginate Film Pore Size Determination Using Atomic Force Microscopy and Validation Using Diffusivity Determinations*. Journal of Surface Engineered Materials and Advanced Technology, 2013. **3**: p. 1-12.
123. Bertz, A., et al., *Encapsulation of proteins in hydrogel carrier systems for controlled drug delivery: Influence of network structure and drug size on release rate*. Journal of Biotechnology, 2013. **163**(2): p. 243-249.
124. Massoumi, B. and A. Entezami, *Controlled release of sulfosalicylic acid during electrochemical switching of conducting polymer bilayers*. European Polymer Journal, 2001. **37**(5): p. 1015-1020.
125. Chang, X., et al., *Voltage-responsive reversible self-assembly and controlled drug release of ferrocene-containing polymeric superamphiphiles*. Soft Matter, 2015. **11**(38): p. 7494-7501.
126. Lee, Y. and D. Thompson, *Stimuli-responsive liposomes for drug delivery*. Wiley Interdisciplinary Reviews: Nanomedicine and Nanobiotechnology, 2017. **9**(5): p. e1450.
127. Jin, J., J. Shim, and J. Kim, *Study on Diffusion Coefficient of Fluorophores in 3D Hydrogel with Cationic Charge using Microchip*. 2019.
128. Moreno, S., et al., *Redox- and pH-Responsive Polymersomes with Ferrocene Moieties Exhibiting Peroxidase-like, Chemoenzymatic Activity and H<sub>2</sub>O<sub>2</sub>-Responsive Release Behavior*. Biomacromolecules, 2022. **23**(11): p. 4655-4667.
129. Kulkarni, R. and S. Biswanath, *Electrically responsive smart hydrogels in drug delivery: a review*. Journal of applied biomaterials and biomechanics, 2007. **5**(3): p. 125-139.
130. Ling, Q., et al., *ROMP Synthesis of Side-Chain Ferrocene-Containing Polyelectrolyte and Its Redox-Responsive Hydrogels Showing Dramatically Improved Swelling with  $\beta$ -Cyclodextrin*. Macromolecular Rapid Communications, 2021. **42**(11): p. 2100049.
131. Donlan, R.M. and J.W. Costerton, *Biofilms: survival mechanisms of clinically relevant microorganisms*. Clinical microbiology reviews, 2002. **15**(2): p. 167-193.
132. Ouyang, J., et al., *A facile and general method for synthesis of antibiotic-free protein-based hydrogel: Wound dressing for the eradication of drug-resistant bacteria and biofilms*. Bioact Mater, 2022. **18**: p. 446-458.